

**ALMA MATER STUDIORUM
UNIVERSITÀ DEGLI STUDI DI BOLOGNA**

**Facoltà di Scienze Matematiche Fisiche e Naturali
Scuola di Dottorato in Scienze Biologiche, Biomediche e Biotecnologiche
Dottorato di Ricerca in Biologia e Fisiologia Cellulare
Ciclo XXII
SSD: BIO/11**

**FUNCTIONAL GENOMICS AND CELL BIOLOGY OF
THE DOLPHIN (*Tursiops truncatus*):
ESTABLISHMENT OF NOVEL MOLECULAR TOOLS
TO STUDY MARINE MAMMALS
IN CHANGING ENVIRONMENTS**

Presentata da:

Dott.ssa ANNALaura MANCIA

Coordinatore Dottorato:

Prof.ssa Michela Rugolo

Relatore:

Prof.ssa Marialuisa Melli

**ALMA MATER STUDIORUM
UNIVERSITÀ DEGLI STUDI DI BOLOGNA**

**Faculty of Science
Physiology and Cellular Biology
XXII PhD Program
SSD: BIO/11**

**FUNCTIONAL GENOMICS AND CELL BIOLOGY OF
THE DOLPHIN (*Tursiops truncatus*):
ESTABLISHMENT OF NOVEL MOLECULAR TOOLS
TO STUDY MARINE MAMMALS
IN CHANGING ENVIRONMENTS**

PhD Student:

Dr ANNALAURA MANCIA

Program Coordinator:

Michela Rugolo, PhD

Supervisor:

Marialuisa Melli, PhD

*To my sister,
Roberta,
once again*

*“Dolphins are ‘non-human persons’
who qualify for moral standing as individuals”*

Thomas White

*“Research is what I'm doing when I don't know
what I'm doing”*

Wernher Von Braun

ABSTRACT

The dolphin (*Tursiops truncatus*) is a mammal that is adapted to life in a totally aquatic environment. Despite the popularity and even iconic status of the dolphin, our knowledge of its physiology, its unique adaptations and the effects on it of environmental stressors are limited. One approach to improve this limited understanding is the implementation of established cellular and molecular methods to provide sensitive and insightful information for dolphin biology.

We initiated our studies with the analysis of wild dolphin peripheral blood leukocytes, which have the potential to be informative of the animal's global immune status. Transcriptomic profiles from almost 200 individual samples were analyzed using a newly developed *species*-specific microarray to assess its value as a prognostic and diagnostic tool. Functional genomics analyses were informative of stress-induced gene expression profiles and also of geographical location specific transcriptomic signatures, determined by the interaction of genetic, disease and environmental factors.

We have developed quantitative metrics to unambiguously characterize the phenotypic properties of dolphin cells in culture. These quantitative metrics can provide identifiable characteristics and baseline data which will enable identification of changes in the cells due to time in culture. We have also developed a novel protocol to isolate primary cultures from cryopreserved tissue of stranded marine mammals, establishing a tissue (and cell) biorepository, a new approach that can provide a solution to the limited availability of samples.

The work presented represents the development and application of tools for the study of the biology, health and physiology of the dolphin, and establishes their relevance for future studies of the impact on the dolphin of environmental infection and stress.

INDEX

INDEX	I
SUMMARY	VII
<u>1. INTRODUCTION</u>	1
1.1 THE BOTTLENOSE DOLPHIN	3
1.1.1 DESCRIPTION AND TAXONOMY	3
1.1.2 PHYLOGENY AND EVOLUTION	6
1.1.3 ADAPTATION TO THE AQUATIC ENVIRONMENT	8
1.2 BOTTLENOSE DOLPHINS AND THE COASTAL ENVIRONMENT	13
1.2.1 EFFECTS OF ENVIRONMENTAL CONDITIONS	13
1.2.2 EMERGING DISEASE AND PATHOLOGY	16
1.2.3 THE BOTTLENOSE DOLPHIN, SENTINEL FOR THE COASTAL ECOSYSTEM	18
1.3 METHODS TO STUDY BOTTLENOSE DOLPHIN HEALTH	19
1.3.1 WILD DOLPHIN SAMPLE COLLECTION	19
1.3.2 TRADITIONAL APPROACHES TO STUDY DOLPHIN HEALTH	22
1.4 MOLECULAR BIOLOGY OF THE BOTTLENOSE DOLPHIN	24
1.4.1 DOLPHIN IMMUNITY: GENES AND PROTEINS	24
1.4.2 OVERVIEW OF MOLECULAR APPROACHES TO STUDY BOTTLENOSE DOLPHIN HEALTH	27

2. RESULTS AND DISCUSSION	33
<hr/>	
PART I. THE DOLPHIN TRANSCRIPTOME	35
2.1 THE DOLPHIN MICROARRAY	35
2.1.1 WILD DOLPHINS RESPONSE TO STRESS	35
2.1.2 THE DIFFERENTIALLY EXPRESSED GENES	38
2.1.3 INTERLEUKIN-8 REAL TIME PCR (<i>qRT-PCR</i>)	42
2.2 MICROARRAYS AND ARTIFICIAL NEURAL NETWORKS	45
2.2.1 WILD DOLPHINS AND THE ENVIRONMENT	45
2.2.2 ARTIFICIAL NEURAL NETWORKS (ANNs)	46
2.2.3 ANNs DISCRIMINATION OF SEX DIFFERENCES IN WILD DOLPHINS	47
2.2.4 ANNs DISCRIMINATION OF WILD DOLPHIN'S GEOGRAPHICAL LOCATIONS	50
2.2.5 WILD DOLPHIN POPULATIONS TRANSCRIPTOMIC SIGNATURE	51
2.3 THE DOLPHIN GENOME SEQUENCING PROJECT	57
PART II. DOLPHIN CELL BIOLOGY	59
2.4 QUANTITATIVE CHARACTERIZATION OF MAMMALIAN CELL LINES	59
2.4.1 QUANTITATIVE METRICS TO CHARACTERIZE A DOLPHIN CELL LINE	60
2.4.1.1 <i>MORPHOLOGICAL ANALYSIS: CELL AREA, ROUNDNESS AND CLUSTERING</i>	61
2.4.1.2 <i>VOLUME DISTRIBUTION AND GROWTH RATE CALCULATION</i>	67
2.4.2 THE DOLPHIN LUNG CELL LINE	73
2.4.3 ANALYSIS OF LUNG ENDOTHELIAL CELL MARKERS	83
2.4.4 ANALYSIS OF LUNG EPITHELIAL CELL MARKERS: ALVEOLAR CELLS AND SURFACTANT PROTEIN B	87
2.5 DEVELOPMENT OF MARINE MAMMAL PRIMARY CULTURES	93

2.6 DEVELOPMENT OF MARINE MAMMAL INDUCED PLURIPOTENT STEM CELLS	95
3. CONCLUSIONS	101
3.1 FUNCTIONAL GENOMICS OF THE DOLPHIN	105
3.2 CELL BIOLOGY OF THE DOLPHIN	107
3.3 FINAL CONCLUSIONS	110
4. MATERIALS AND METHODS	111
PART I. MICROARRAY ANALYSIS	113
4.1 OVERVIEW OF THE DOLPHIN MICROARRAY	113
4.1.1 GENERATION OF CDNA LIBRARIES AND COLLECTION OF ESTs	113
4.1.2 EST COLLECTION, GRIDGING AND REARRAYING	114
4.1.3 TARGETED GENE CLONING	115
4.1.4 cDNA MICROARRAY PRODUCTION	118
4.2 BLOOD SAMPLE COLLECTIONS	118
4.2.1 BLOOD SAMPLES FOR THE STRESS INDUCED STUDY	118
4.2.2 BLOOD SAMPLES FOR THE ARTIFICIAL NEURAL NETWORK STUDY	119
4.3 PREPARATION OF RNA	120
4.3.1 RNA EXTRACTION	120
4.3.2 SYNTHESIS OF LABELED RNA	120
4.4 MICROARRAY HYBRIDIZATIONS	121
4.5 STATISTICAL ANALYSIS OF MICROARRAY DATA	121
4.5.1 STATISTICAL ANALYSIS OF MICROARRAY DATA OF THE STRESS INDUCED STUDY	121
4.5.2 STATISTICAL ANALYSIS OF MICROARRAY DATA FOR THE ARTIFICIAL NEURAL NETWORK STUDY	124

4.5.2.1 DATA PROCESSING VIA BIOCONDUCTOR	124
4.5.2.2 GENE SELECTION VIA ANNs	125
4.5.2.3 MACHINE LEARNING ANALYSIS	125
4.6 REAL-TIME PCR (<i>qRT-PCR</i>)	127
4.6.1 <i>qRT-PCR</i> PROTOCOL	127
4.6.2 <i>qRT-PCR</i> DATA ANALYSIS	127
4.7 DOLPHIN GENOME SEQUENCING PROJECT	128
4.7.1 GENERATION OF cDNA LIBRARIES	128
PART II. DOLPHIN CELL BIOLOGY	130
4.8 CELL CULTURE, FIXING AND STAINING	130
4.8.1 CELLS AND CULTURE CONDITIONS	130
4.8.2 CELLS FIXING AND STAINING	131
4.9 MORPHOLOGY ANALYSIS	131
4.10 CELL VOLUME DISTRIBUTION MEASUREMENTS	133
4.11 DOLPHIN CELLS VIDEO-IMAGING	134
4.12 ANALYSIS OF ENDOTHELIAL AND EPITHELIAL CELL MARKERS	135
4.12.1 IMMUNOCYTOCHEMISTRY	135
4.12.2 IMMUNOHISTOCHEMISTRY	137
4.12.3 ACETILATED LOW-DENSITY LIPOPROTEIN ASSAY	138
4.12.4 WESTERN BLOT ANALYSIS	138
4.13 DEVELOPMENT OF PRIMARY CULTURES	140
4.13.1 DEVELOPMENT OF PYGMY SPERM WHALE ALVEOLAR TYPE II	140
4.13.2 DEVELOPMENT OF PYGMY SPERM WHALE FIBROBLASTS	142
4.14 MARINE MAMMAL INDUCED PLURIPOTENT STEM CELLS	142

5. APPENDIX **145**

<i>Table A1</i> Dolphins sampled in the stress induced study and their correlated microarray records.	147
<i>Table A2</i> Genes showing significant regulation in pre versus post blood samples.	149
<i>Table A3</i> Dolphins sampled in the ANN study and their correlated microarray records	151
<i>Table A4</i> List of most significantly differentially regulated genes selected from ANNs for the determination of sex in dolphins from 4 geographic locations.	154
<i>Table A5</i> List of genes showing highest sensitivity values selected from ANNs for the determination of the location in male (I) and female (II) dolphins.	161
<i>Table A6</i> List of most significantly differentially regulated genes selected from linear statistical analysis (Bioconductor) for the determination of the location in male (I) and female (II) dolphins.	165

6. REFERENCES **169**

7. ACKNOWLEDGEMENTS **187**

SUMMARY

The development of genetic information, molecular tools and reagents for biomedical research in the dolphin (and marine mammals in general) has been slow. Progress in the field has been weakened by the protected status of these animals, which makes obtaining samples difficult. Classical measures of environmental quality for the marine ecosystem have included assessment of the relative abundance of species, and the levels of pollutants found in the environment and in indigenous organisms. These measures are valuable but they do not provide the most sensitive nor most rapid information on the effects of multiple environmental stressors.

Major advances in the knowledge of dolphin biology and the unique adaptations of these animals in response to the marine environment are being made as a result of 1) the development of cell-lines for use in *in vitro* experiments 2) the production of monoclonal antibodies to recognize dolphin proteins 3) the development of dolphin DNA microarrays to measure global gene expression and 4) the sequencing of the dolphin genome. These new approaches may permit the discovery of new genes and/or functions of the proteins for which they encode. Hence, they may play a central role in understanding the complex and specialized biology of the dolphin with regards to how this species responds to an array of environmental insults.

The work presented here describes the development of tools for the study of the biology, health and physiology of the dolphin, *Tursiops truncatus*, and its response to environmental stress and infection. Advances in the knowledge of the molecular genetics of the dolphin have the potential not only to supplement and greatly expand upon conventional measures of

dolphin health status, but also to enhance the sensitivity and potential value of the dolphin as a sentinel species for the health of the marine environment. As a mammal that lives its entire life in the sea, it acts as an integrator of the stressors present in the marine environment. Dolphins may have the potential to predict contaminant effects on health, and to be an indicator of infectious disease that may impact humans who have contact with the marine ecosystem through residence, work, or recreation near the coast.

This work presents the creation, characterization and application of new molecular tools to identify genetic and physiological baseline data to better understand the complex and unique biology of the dolphin. The approaches used are 1) the global analysis of the transcriptome and gene expression changes in blood samples of wild dolphins using a species-specific microarray developed by Mancina et al. (2007) specifically for studies of the immune response in *T. truncatus*; 2) the assessment of quantitative measurements describing and characterizing a species-specific cell-line at phenotypic and genotypic level, as a tool to study physical and biochemical signatures of dolphin lung cells.

In conclusion, this work presents studies in the cell biology, biochemistry and functional genomics of the dolphin using biological fluids, tissues or cell lines in an effort to further our understanding of dolphins and their responses to changing environments.

1. INTRODUCTION

INTRODUCTION

1. 1 THE BOTTLENOSE DOLPHIN

1.1.1 DESCRIPTION AND TAXONOMY

The bottlenose dolphin, *Tursiops truncatus*, is one of the best known and abundant marine mammals in the world and the most common and widespread member of the family Delphinidae (Figure 1.1A). The name *Tursiops* means “dolphin-like” and derives from the Latin *-tursio* (=dolphin) and the Greek suffix *-ops* (=appearance), while *truncatus* derives from the Latin *-tronco* (=truncated) apparently referred to the flattened teeth used by Montagu, 1821, as an identifying characteristic [1]. Bottlenose dolphins figure in the legends of ancient Romans and Greeks and they have been the focus of many books for scientific and public audiences [2-6]. The common English name is “common bottlenose dolphin” distinguishing this species from the “Indo-Pacific bottlenose dolphin”, *Tursiops aduncus*.

The bottlenose dolphin is widely distributed in coastal, inshore and offshore regions of tropical and temperate waters, ranging from latitudes of 45°N to 45°S. Molecular studies show that the coastal (or inshore) populations and the offshore populations are 2 different ecotypes genetically isolated, showing morphological and hematological differences [7,8].

Bottlenose dolphins are recognized by their medium-sized, robust body, moderately curved dorsal fin, and dark grey coloration, with a sharp demarcation between the melon and the short rostrum (or beak) (Figure 1.1B). The genus *Tursiops* is distinguished by the well-defined beak which is about 8 cm long and resembling the top of an old-fashioned bottle (hence the name) [9]. Adult lengths range from 2.5 to 4 m, and weigh from 200 to 500 kg,

with the males usually being longer and heavier than females. Body size varies geographically with habitat and also seems to vary inversely with water temperature in many parts of the world. The animals are colored light grey to black dorsally, with a light belly [10] (Figure. 1.1B).

They have 18 to 28 conical teeth on each side of each jaw [11]. Their cone-like teeth serve to grasp but not to chew food. The flukes (lobes of the tail) and dorsal fin are formed of dense connective tissue and do not contain bones or muscle. The animal propels itself forward by moving the flukes up and down. The pectoral flippers, homologous to the forelimbs of land mammals are for steering (Figure 1.1B).

Bottlenose dolphins can live for more than 40 years [11]. However, one study of the lifespan of the wild bottlenose dolphin population off Sarasota (Florida, USA) indicated an average lifespan of about 20 years or less [12]. Females become sexually mature between age 5 and 13, males between age 9 and 14. Female dolphins reproduce every 2 to 6 years. The average gestation period is 12 months. Births can occur at any time of year, although peak births occur in warmer months. A single calf is born, about 1 m long at birth weighing between 9 and 30 kg [9,10] (Figure 1.1B). The bottlenose dolphins have been known to inter-breed with a number of other dolphin species such as Risso's Dolphin, Common Dolphin, False Killer Whale and Atlantic Spotted Dolphin [13,14].

The bottlenose dolphin is a distinctly social species that often travels in groups of up to 15 individuals, though occasionally they aggregate in groups of several hundred [9,10]. They often hunt as a team; they feed on squid, shrimp, eels, and a wide variety of fishes. They have been observed chasing fish onto mudflats and sliding out of the water to seize their prey. They generally consume approximately 6-7 kg of seafood daily [9,10]. The dolphin's search

for food is aided by a form of sonar known as echolocation: they locate objects by producing sounds and listening for the echo. Dolphins are able to extract shape information from their echolocative sense, suggesting that they are able to form an "echoic image" of their targets [15]. They produce and hear these high frequency sounds for foraging and navigation. Bottlenose dolphins communicate with one another through squeaks, whistles, and body language. They produce sounds using six air sacs near their blowhole (they lack vocal cords). Each animal has a characteristic frequency-modulated narrow-band signature vocalization (signature whistle) which is uniquely identifying [16].

Despite its wide distribution and popularity, the taxonomy of the bottlenose dolphin has remained confused for a long time [7] (Figure 1.1A). The bottlenose dolphin has been classified into as many as eight species but most recent analyses lead to the conclusion that only two exist, namely, *T. truncatus* and *T. aduncus*. LeDuc et al. [17] proposed that not only *T. aduncus* is a distinct species, but it appears to be more closely related to the *Stenella coeruleoalba* than to the *T. truncatus* [17]. This is supported from a recent analysis by Xiong et al. [18], who concluded that the genera *Stenella* and *Tursiops* are not monophyletic, thus suggesting the importance of adaptive convergence and/or retention of ancestral body form.

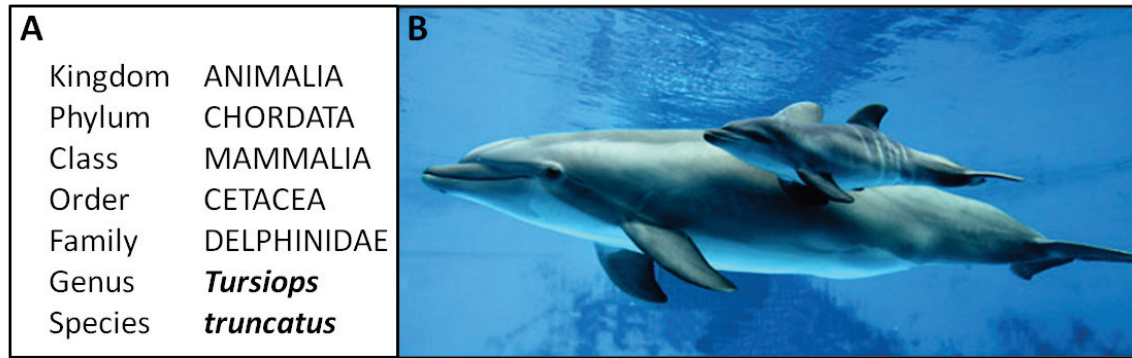


FIGURE 1.1 The bottlenose dolphin, *Tursiops truncatus*.

(A) Taxonomy: *T.truncatus* is a mammal belonging to the order of Cetacea, family Delphinidae. **(B)** Image of an adult female and newborn calf showing some of the characteristics of the species: robust body, moderately curved dorsal fin, and dark grey coloration, a sharp demarcation between the melon and the short well-defined rostrum.

1.1.2 PHYLOGENY AND EVOLUTION

The bottlenose dolphin belongs to the mammalian order of Cetacea (from the greek *-ketos*, whale), sub-order Odontoceti (or toothed whales), family Delphinidae.

Linnaeus, in the early editions of *Systema Naturae* (1735), included cetaceans among the fishes, but by the tenth edition he recognized them as a distinct group unrelated to fishes. Recently, the order of Cetacea has been grouped with the order of Artiodactyla in the clade of Cetartiodactyla, owing to the strong relationship between species of the two orders [19,20]. Flower (1883) was the first to propose a close relationship between cetaceans and ungulates, the hoofed mammals [21]. Prior to 1994, it was believed that artiodactyls and cetaceans both shared a condylarthran ancestry and the whales belonged to a sister-taxon of the extinct mesonychids. This view was confirmed by modern morphological evidence [22]. By contrast, the majority of post-1994 molecular studies resolved a paraphyletic Artiodactyla, with Cetacea nested within the Artiodactyla as sister to hippopotamids and forming a clade known as Cetartiodactyla [23,24]. This designation is supported by the

recent description of two archaic whales with morphological homology between Cetacea and Artiodactyla and the exclusion of the mesonychids [25,26].

Mitogenome (mitochondrial genome) data analysis, both at gene and protein level, has provided an estimated time of divergence between Cetacea and Hippopotamidae at about 53-54 MYA [18]. Cetaceans (together with sirenians) are the earliest recorded marine mammals and the most diverse mammalian group to adapt to a marine life [21]. Within Cetacea, a basal split was identified between Mysticeti and Odontoceti at about 30 MYA, from a common Archaeocete (primitive whale) ancestor. The Archaeocete (early Eocene, 52-42 MYA) deposits have been found in Africa, North America, Pakistan and India. They have been divided into 5 families, the oldest of which (Pakicetidae) includes the most basal cetaceans [27]. Modern whales possess newly derived characters compared to the Archaeocete's with the most noticeable being the association of the bones in the skull in response to the migration of the nasal openings to the top of the skull (telescoping) (Figure 1.2). The modern whale skull has premaxillary and maxillary bones that have migrated posteriorly and presently form most of the skull roof resulting in a long rostrum or beak and dorsal nasal openings, the blowhole [21](Figure 1.2).

Odontoceti split then into 4 basal lineages: sperm whales, beaked whales, Indian river dolphins and delphinoids (river dolphins, narwhals/belugas, porpoises and true dolphins), with the last lineage including the bottlenose dolphin, *T. truncatus* [18].

The whales belonging to the group of the Odontoceti show a wide variety of morphologies including the large, deep-diving sperm whale with few teeth that captures squid by suction feeding and the smallest cetacean, the porpoises with many spade-shaped teeth for seizing fish. The distinguishing feature is the presence of the melon, a region of adipose and

connective tissue on top of the skull correlated to their ability to echolocate. It has been suggested that *Tursiops* originated in the Mediterranean region. Fossil remains of *Tursiops* species have been traced back to the Pliocene (2-5 MYA) and Pleistocene (less than 2 MYA) [28].

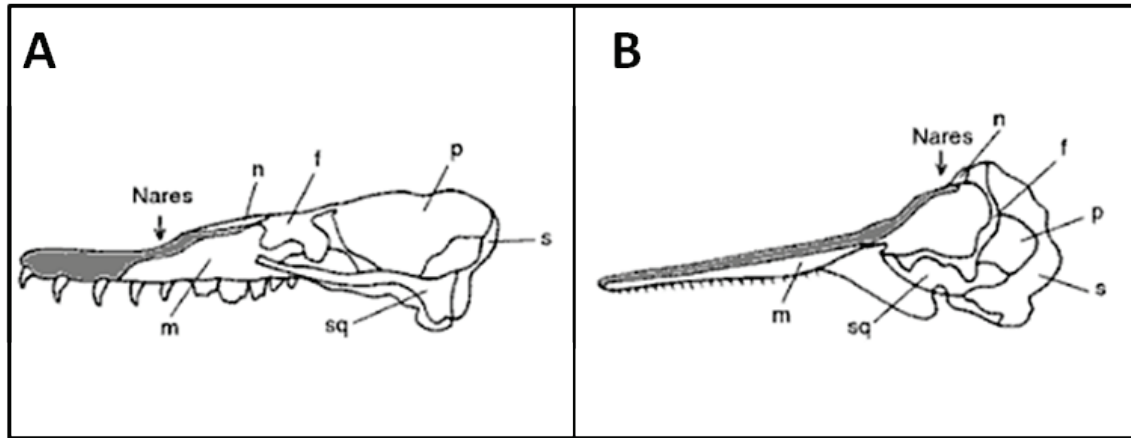


FIGURE 1.2 Telescoping of the skull in archaic and modern dolphins.

Cranial bones are rearranged and the nares are in a posterior position. Skull of (A) archaeocete and (B) modern odontocete. Cranial bones: premaxilla (stippled), frontal (f), maxilla (m), nasals (n), parietal (p), squamosal (sq), supraoccipital (s). Modified from Berta et al., 2006 [21].

1.1.3 ADAPTATION TO THE AQUATIC ENVIRONMENT

Dolphins have adapted to a completely dissimilar environment from that of terrestrial mammals and developed unique adaptations for 1) swimming 2) respiration 3) diving 4) thermoregulation and 5) sleep.

1) To aid in swimming they have developed a streamlined and fusiform body shape; the bottlenose dolphin routinely swims at speeds of about 5-11 kph with *burst* (maximum) speeds of 29-35 kph [29].

2) To aid in respiration they breathe through a single blowhole (nasal opening) on the dorsal surface of their head consisting of a hole and a muscular flap (Figure 1.3A). The muscular flap (muscle sphincter) is closed during muscle relaxation and opens during contraction. The larynx is composed of two elongate cartilages providing a more direct connection between nose and trachea. The trachea is short and broad, consisting of several cartilaginous rings that are interconnected with each other (Figure 1.3B).

Dolphins hold their breath while underwater and begin to exhale when they reach the surface; they are conscious breathers. During each respiration a dolphin exchanges 80% or more of its lung air (humans exchange only 17%) in about 0.3 seconds (exhaling and inhaling) [30,31]. A bottlenose dolphin average respiratory rate is about two to three breaths per minute [30] but, if necessary, it has the ability to remain submerged for several minutes.

3) To aid in diving they have developed physiological adaptations to maximize the conservation of oxygen while underwater and to prevent the “bends” (decompression sickness). Most bottlenose dolphins regularly dive to depths of 3 to 45 m for 8 to 10 min but they are capable of diving much deeper. Under experimental conditions, the deepest trained dive is 547 m [32].

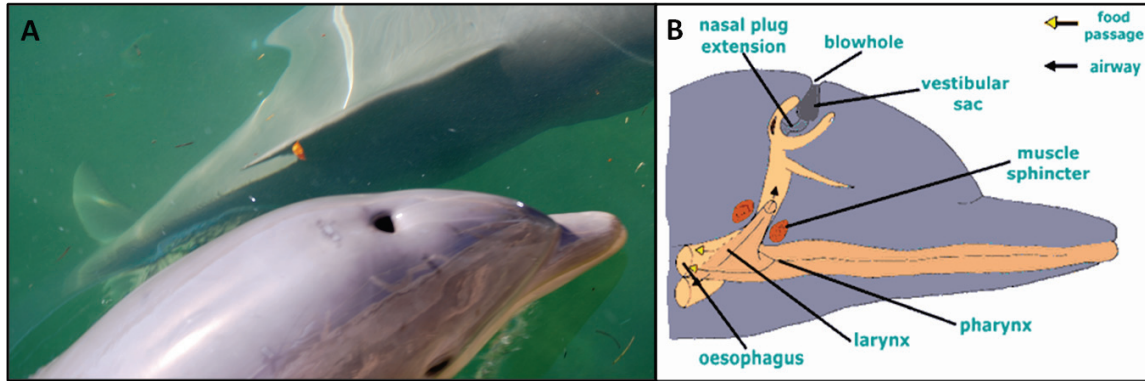


FIGURE 1.3 Dolphin blowhole and upper respiratory tract.

(A) The Dolphin's nasal opening is on the dorsal surface of their head, the blowhole. (B) Representation of the upper respiratory tract; the muscular flap is closed during muscle relaxation and opens during contraction allowing the gas exchange.

While diving, dolphins have a slower heartbeat and blood is shunted away from tissues tolerant of low oxygen levels toward the heart, lungs, and brain, where oxygen is needed. Oxygen is stored in the muscle which has a content of myoglobin (an oxygen-binding protein) that is 3 to 10 times higher than in land mammals. The oxygen is also stored in the blood and in the lung (Figure 1.4) [21].

Dolphin calves as young as 1.7 years old have already developed several elements of cardiac control but the development of the oxygen stores in the skeletal muscles [33], blood [34] and the ability to induce bradycardia [35] in bottlenose dolphins are not fully developed until 3 years postpartum. Their diving and breath-holding capacity increases as they mature and increase their body size. It has been suggested that this may explain in part the long associations (3–6 years) observed between bottlenose dolphin mother and calf in the wild [36].

During the dive the dolphin's lungs collapse completely. Any residual air is squeezed out of the alveoli and into the bronchi and trachea. The collapse and reinflation of the lungs are

facilitated by the position of the diaphragm, which is set at an acute angle to the long axis of the body. This mechanism of lung collapse allows for the tolerance of extreme pressures during deep dives and allows avoidance of decompression sickness (bends) and nitrogen narcosis.

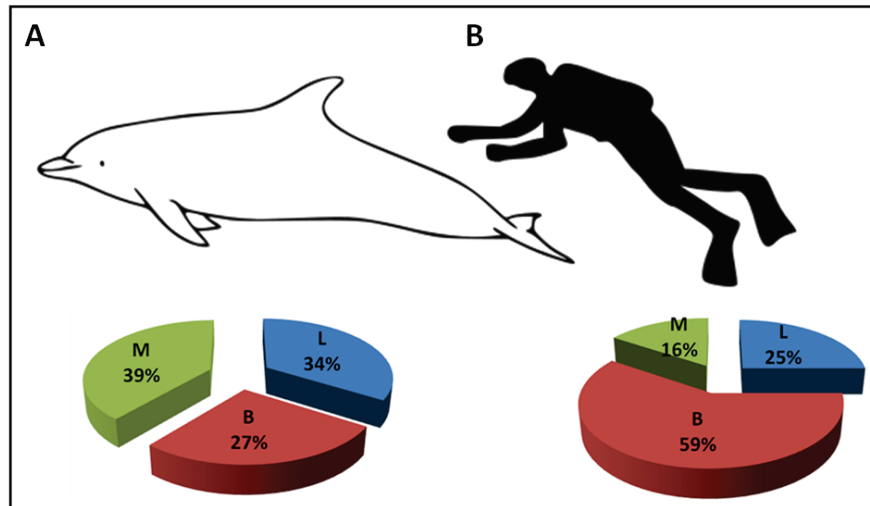


FIGURE 1.4 Comparison of oxygen store in bottlenose dolphins and humans.

Values are for a for a body mass of 200 kg for the dolphin (A) and 70 Kg for a human (B).

M, muscle; L, lung; B, blood.

4) To prevent heat loss, dolphins have developed a thick layer of blubber that lies just underneath the skin and which provides insulation but also acts a food reserve and enhances buoyancy. A bottlenose dolphin's body fat generally accounts for about 18% to 20% of its body weight [31]. A dolphin's core temperature is about 36.9°C. There is a heat gradient throughout the blubber to the skin [30]. The dolphin's fusiform body shape and reduced limb size decrease the surface area exposed to the external environment and helps dolphins to conserve body heat [30]. Their circulatory system adjusts to conserve or dissipate body heat and maintain body temperature; arteries in the flippers, flukes, and dorsal fin are surrounded

by veins so that some heat from the blood traveling through the arteries is transferred to the venous blood rather than the environment (Figure 1.5). This countercurrent heat exchange aids dolphins in conserving body heat. Moreover, when they dive, blood is shunted away from the surface of the body and this decrease in circulation helps to conserve body heat [30].

5) To maintain their conscious breathing functioning during sleep, deep sleep in bottlenose dolphins may occur in only one brain hemisphere at a time. The sleeping cycle lasts for approximately 8 hours during each 24 hour period (33% of the day). During the sleeping cycle dolphins remain near the surface swimming slowly [32,37].

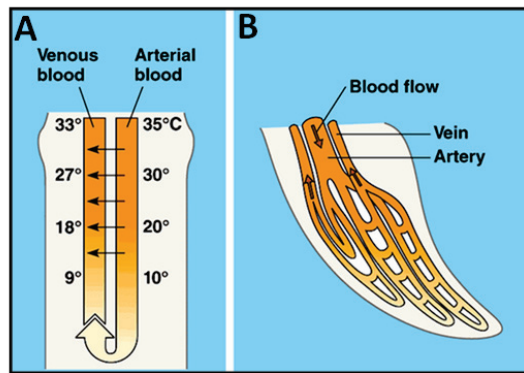


FIGURE 1.5 Heat exchange in dolphin flippers, flukes and dorsal fin. (A) General pattern of a countercurrent system and (B) simplified vascular exchange network in bottlenose dolphin flippers. Modified from Berta et al., 2006 [21].

1.2 BOTTLENOSE DOLPHINS AND THE COASTAL ENVIRONMENT

1.2.1 EFFECTS OF ENVIRONMENTAL CONDITIONS

The increasing number of humans inhabiting the coast and the increasing consumption (and destruction) of resources place enormous pressures on the environment. The effects can be found in every ecosystem but the major impact is observed in the ocean which covers 79% of the Earth's surface. The effects can be direct such as alteration in the abundance of fish or shellfish and the prevalence of infectious/toxic agents, or indirect, through the effects of runoff and climate change. Oceans facilitate the distribution of toxic contaminants such as heavy metals and organochlorine chemicals (e.g. polychlorinated byphenyls, PCBs and chlorinated pesticides, like DDT) which tend to be stable and lipophilic. Runoff from urban, industrial and agricultural activities bioaccumulate up the food chain, with the greatest concentrations in animals at the highest trophic levels, such as marine mammals (Figure 1.6). Previous studies have shown that dolphins can accumulate anthropogenic contaminants such as organohalogen and heavy metal contaminants [38-41]. Dolphins are also subject to the stress posed by biotoxins (e.g., brevetoxins, ciguatoxin/maitotoxin, saxitoxins, domoic acid and okadaic acid) produced by harmful algal blooms (HABs), which are periodically experienced by coastal waters around the world and have been increasing over the last quarter century [42-44](Figure 1.7). For example, between August 1999 and February 2000, 120 bottlenose dolphins stranded in the Gulf of Mexico, Florida and 2 peaks of stranding coincided with *Karenia brevis* blooms [45]. Histopathological analysis showed significant upper respiratory tract lesions but the highest concentrations were found in the stomach

contents, followed by liver and kidney suggesting that the dolphins obtained the toxin via the food chain, rather than by inhalation [45].

The extent of the environmental impact can be a dramatic event such as the death of the dolphin but it can also be less evident, affecting their health, immune system and reproductive function.

Dolphins inhabiting coastal and inshore waters are mainly resident populations, remaining within a limited, definable range for most of their lives, although adult males may range outside of the general community on occasion [46,47]. Genetic data provide additional evidence that discrete bottlenose dolphin populations exist on a local scale and that regional variations in body burdens of some contaminants may be correlated to local environments and the restricted movements of these animals. Studies of contaminants found significant elevation in a number of organic contaminants in several geographic locations in the South East coast of the USA [38,39,48] [40,49]. These results suggest that dolphin populations cannot escape the legacy of contamination of the areas in which they live, as their philopatric nature precludes occupation of new and less-contaminated areas. Studies on the impact of organic contamination on dolphins have shown elevated CYP1A1 levels correlated to PCB levels [50,51], elevated risks to first-born calves [52], and increases in contaminant loads with increasing age in males [48,52].

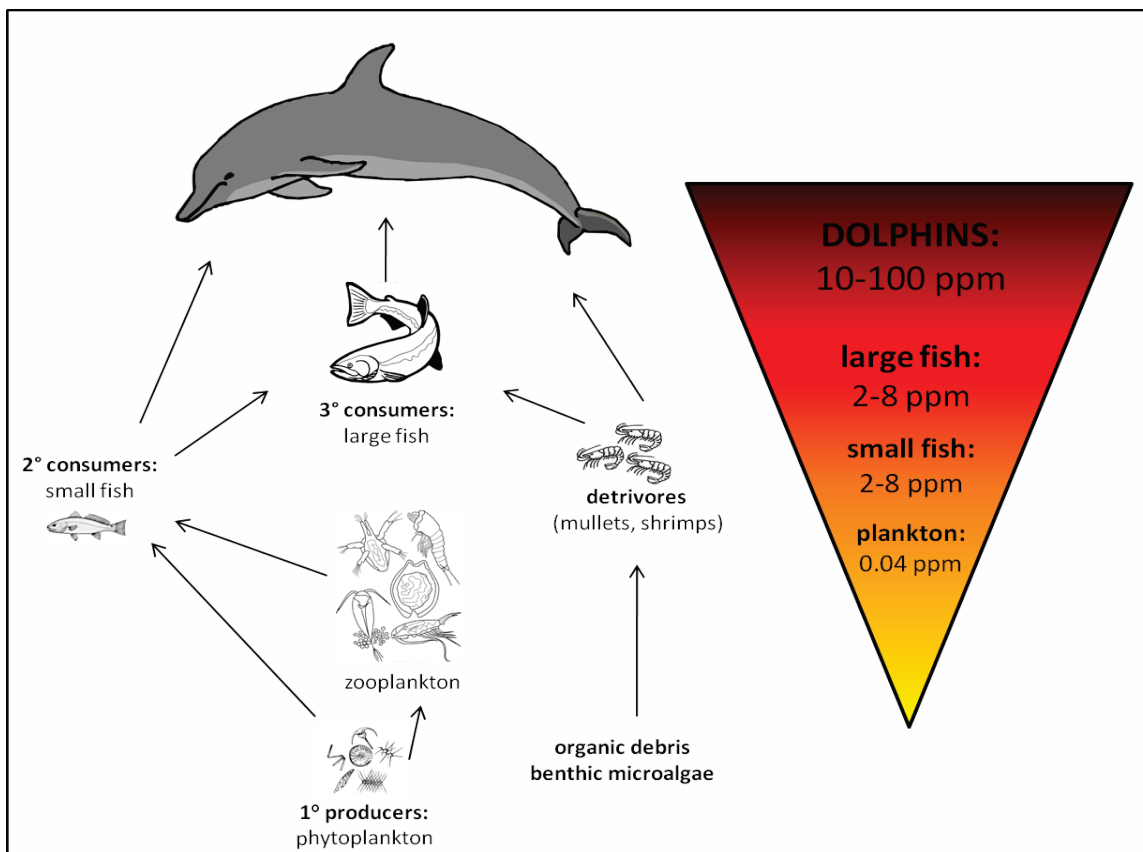


FIGURE 1.6 Biomagnification in the food chain.

Runoff from urban, industrial and agricultural activities have the greatest concentration in animals at the highest trophic level such as the dolphin. An example of biomagnifications of persistent contaminants (e.g. PCBs) is showed on the pyramid on the right.

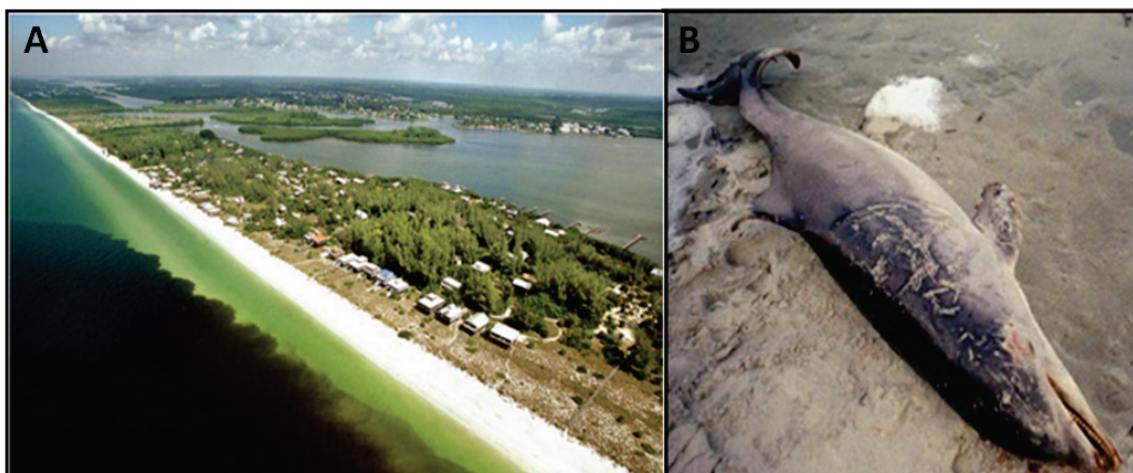


FIGURE 1.7 Red tides on the coast of Florida, USA.

Red tides are caused by harmful algal blooms, such as the dinoflagellate *Karenia brevis* which produces brevetoxin. *K. brevis*'s blooms (A) cause severe pathological symptoms in both humans and marine mammals. Stranding of a bottlenose dolphin thought to be a victim of a red tide is shown in (B).

1.2.2 EMERGING DISEASE AND PATHOLOGY

In the past decades, emerging disease agents have been reported in dolphins including various papillomaviruses [53], dolphin poxvirus [54], and other viral infections [55], lobomycosis [56,57], toxoplasmosis [58-61] and various neoplastic diseases (urogenital cancer, lingual papillomas, squamous cell carcinomas and genital papillomas) that may be direct or indirect consequences of pathological infections [62-64](Figure 1.8). In some cases they are caused by new species-specific pathologic agents, like the dolphin papillomavirus, the etiologic agent of several benign and malignant tumors. In dolphins, it has been shown that at least 4 distinct species-specific forms of papillomavirus exist [53]. In some cases, they are caused by agents pathogenic to man as well; an example is the fungus *Loazia lobo*, a pathogenic agent causing lobomycosis and resulting in dermal and subcutaneous granulomas, which has been described only in humans and dolphins[65](Figure 1.9).

Effective methods for monitoring and assessing the emergence of new diseases caused by the impact of contaminants and marine pathogens are essential for evaluating the status of the marine environment and of the health hazards posed to dolphins and humans.

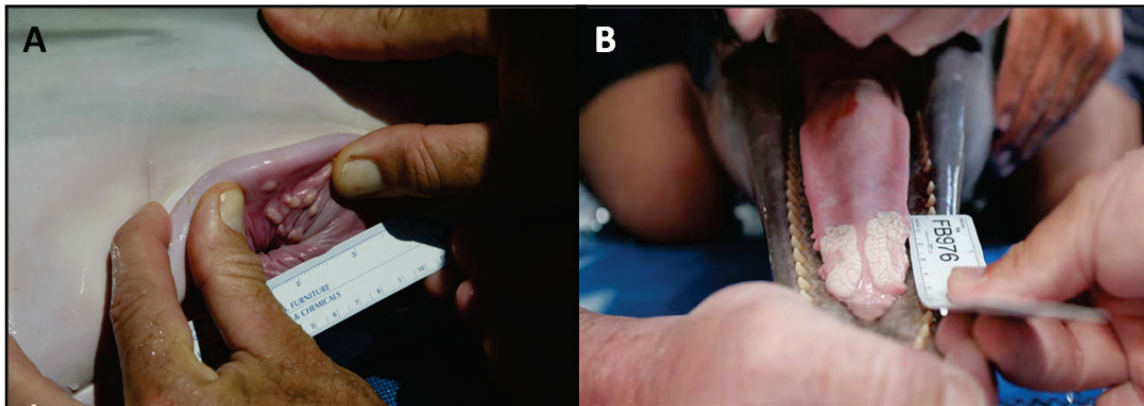


FIGURE 1.8 Papilloma virus infection in free-ranging bottlenose dolphin. (A) Genital lesions typical of papilloma virus infection in female dolphin. (B) Tumor in the tongue of a bottlenose dolphin associated to papilloma virus infection. Bossart *et al.*, 2006 [66].

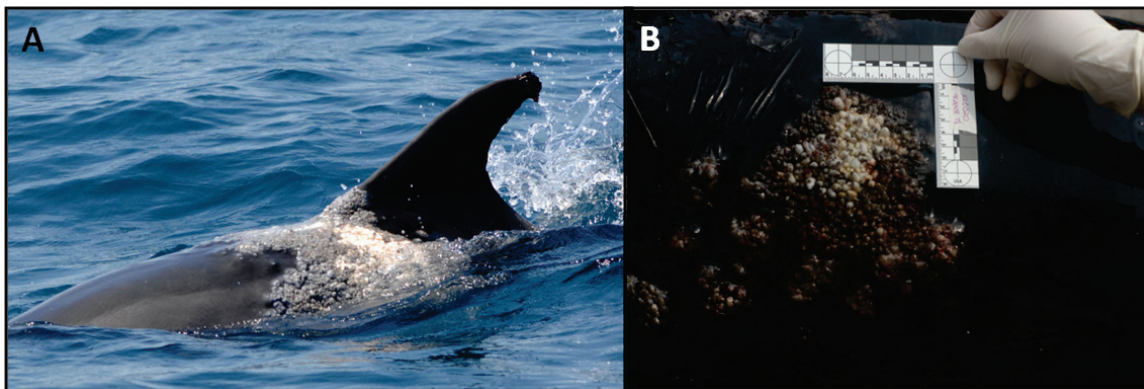


FIGURE 1.9 Lobomycosis skin lesion in free-ranging bottlenose dolphin. (A) Dorsal skin lesion associated with the pathogenic fungus *Lacazia loboi* infection. (B) Close view of the skin lesion adapted from Rotstein *et al.*, 2009 [65].

1.2.3 THE BOTTLENOSE DOLPHIN, SENTINEL FOR THE COASTAL ECOSYSTEM

Marine mammals have been proposed as sentinel organisms for the health of the marine environment because most of the species, including dolphins, present characteristics that can be informative of the status of the marine ecosystem in which they live. Furthermore, assessing the health status of dolphins can provide valuable information for evaluating the relationship between exposure to biological and chemical agents and health effects on humans.

Dolphins have long life spans, feed at a high trophic level and have extensive fat stores that can serve as accumulation beds for anthropogenic toxins. They live their entire lives in the aquatic environment where they are directly and constantly exposed to a variety of pathogens and other stressors of natural and anthropogenic origin. Their blubber that plays a major role in nutrition, buoyancy and thermoregulation is also an ideal repository for some contaminants. Lipophilic contaminants may remain stored in the blubber until the animal dies but others can be metabolized in times of physiological challenge (illness, nutritional compromise, pregnancy, etc...) [67]. The first to propose the use of marine mammals as environmental sentinels was Holden, in 1972. In 1998 the Marine Mammal Commission identified the California sea lion (*Zalophus californianus*), the harbor seal (*Phoca vitulina*), the beluga whale (*Delphinapterus leucas*) and the bottlenose dolphin (*Tursiops truncatus*) as model species for investigation into the effects of environmental contaminants on marine mammals.

1.3 METHODS TO STUDY BOTTLENOSE DOLPHIN HEALTH

1.3.1 WILD DOLPHIN SAMPLES COLLECTION

The study of dolphin biology is challenging given their status as a protected species. One approach is to study dolphins in captivity, which allows veterinarians and biologists to collect valuable information on the physiology of diving, sleeping and social behavior and to monitor their health status [59,68-72]. However, due to limitations in specimen acquisition, limited relevance when compared to the animal in their natural habitat and restrictions on human intervention (e.g. as set forth by the Marine Mammal Protection Act in the US), conclusions drawn from dolphin research on captive animals should be treated with caution.

A good source of information on dolphins in their natural habitat comes from necropsy (an animal autopsy) of stranded animals [73-75] (Figure 1.10). The breadth of samples that can be collected using this approach is more extensive than that of captive or capture-release, and includes organ biopsies, and collection of parasites and stomach contents. *Post-mortem* investigations and forensics have reported interesting findings about bacterial infections, disease and traumatic injury [76-81]. The downside of this procedure is that the subjects often have been deceased for several hours, and significant decomposition is likely to have occurred prior to sample collection and analysis which would compromise its value.

The study of free-ranging animals in their native environments is more informative than the examination of stranded animals or captive animals. Currently, marine scientists monitor coastal and offshore (in less degree) populations of dolphins using 1) photo-identification together with tagging and tracking using Time-Depth-Recorder (TDR), radio transmitters and

GPS locators that allow continuous monitoring of the tagged animal (Figure 1.11) [56,82-85], 2) skin and blubber biopsy sampling (Figure 1.12) [86,87] and 3) capture-release health assessment events (Figure 1.13). Recently the US National Marine Fisheries Service (NMFS) started issuing research contracts for health assessment projects by which it became feasible to capture free-ranged dolphins, followed by release after sampling. Experienced veterinarians perform a physical examination and collect a variety of samples which are analyzed for a variety of components including blood chemistry, serology, immune function, microbiology and contaminant levels [57] (Figure 1.13).



FIGURE 1.10 *Post-mortem* physical exam and necropsy of a stranded bottlenose dolphin.

The dolphin stranded in January 2009 in Charleston, SC. The biologist (Wayne McFee) examined the dolphin in order to understand the cause of death. After a physical exam (A, B), the dolphin was taken to the laboratory where necropsy was performed (C). Photos: courtesy of NOAA (Coastal Strandings Assessment Project at NOAA's Center for Coastal Environmental Health and Biomolecular Research).

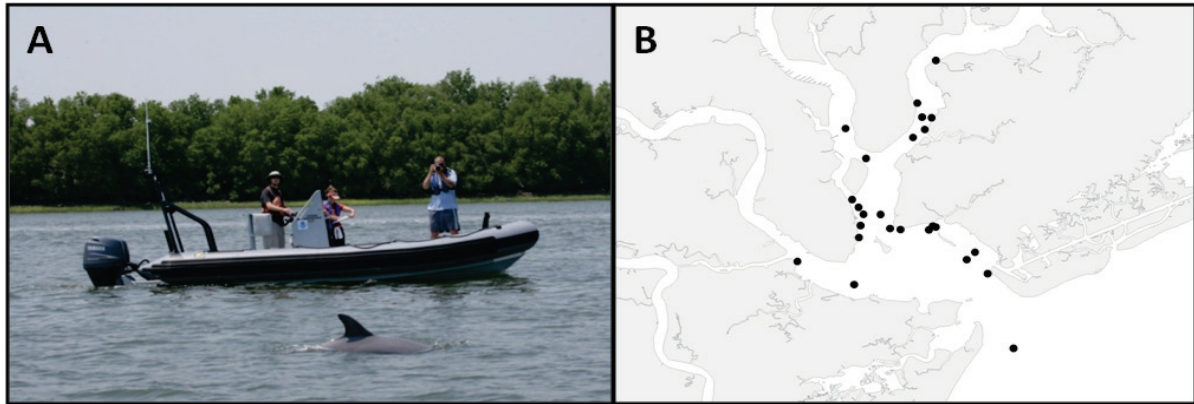


FIGURE 1.11 Photo-identification studies of free-ranging bottlenose dolphins.

Dorsal fins are uniquely characteristic. Photos of dorsal fins are collected from dolphins of resident populations (A) and uploaded on the local database regularly. This method is useful to generate dolphin residence and distribution patterns which can enable a comparison of dolphin health with environmental exposure (B). Photos: courtesy of NOAA (Permit no. 932-1489 issued by NOAA National Marine Fishery Service).



FIGURE 1.12 Skin biopsy collected from free-ranging bottlenose dolphins.

The dart is shot from a vessel (A, B) and it generally collects skin and blubber (~1-1.5 cm) (C). Photos: courtesy of NOAA (Permit no. 932-1489 issued by NOAA National Marine Fishery Service).



FIGURE 1.13 Capture-release health assessment studies.

“Catch boat” used to transport and release the net once the dolphin (or a group of dolphins) has been located (A). Physical examination and sample collection on the “Dolphin Processing” boat (B). “Sample Processing” boat (C). Release of the dolphin after examination, sample collection and radio tagging (D). Photos: courtesy of NOAA. (Permit no. 932-1489 issued by NOAA National Marine Fishery Service).

1.3.2 TRADITIONAL APPROACHES TO STUDY DOLPHIN HEALTH

Many groups are investigating the dolphin immune system using samples acquired from capture-release programs, providing data from environmental effects on the dolphin’s health status may be predicted. Different parameters are being evaluated applying laboratory methods widely used for other species; for example, blood samples for hematology are collected from the dolphin fluke and used for complete blood count and morphologic analysis using automated analyzers. Goldstein et al. performed a screening on 62 wild healthy bottlenose dolphins representing hematology baseline data [88]. Dubey et al. on the other hand compared several techniques (modified agglutination test, MAT; the indirect

fluorescent antibody test (IFAT), the Sabin–Feldman dye test (DT), an indirect hemagglutination test (IHAT), enzyme-linked immunosorbent assay (ELISA), and Western blot) for identification of *Toxoplasma gondii* in dolphin blood serum [89]. Mumford et al. in 1975 and Colgrove GS in 1978 [90,91] analyzed the activation of dolphin peripheral blood lymphocytes using phytoimitogens and since then the mithogens concanavalin A (ConA) and phytohemagglutinin (PHA) have been routinely used to study lymphocytes proliferation in marine mammals [92-94]. Tissues most commonly analyzed are serum and plasma (immunology, contaminants, bacteria, and hormones), blubber (contaminants), urine (protein, glucose) and feces (bacteria), and skin (contaminants).

1.4 MOLECULAR BIOLOGY OF THE BOTTLENOSE DOLPHIN

1.4.1 DOLPHIN IMMUNITY: GENES AND PROTEINS

The response of the dolphin to infection or to environmental stressors is neither well characterized nor understood, especially when compared to what is known in species such as human or mouse. However, this is an important area of investigation given its relevance to dolphin health. Knowledge of the cetacean immune system is being expanded primarily through the cloning of cardinal genes involved in the immune response. The dolphin immune system, as for all mammals, is characterized by both an innate immune response as well as an adaptive immune response. Adaptive immunity (cytokine dependent) is further divided into two arms 1) humoral immunity and 2) cell mediated immunity, which involve activation of B lymphocytes (antibody production) or T lymphocytes (phagocyte activation or induction of apoptosis), respectively. Pathways of immune response activation are well known in humans. The cloning of the major cytokines and immunoglobulins through RT-PCR supports their likely role in the immune response in marine mammals and strengthened the inferred phylogenetic relationship between Cetaceans and Artiodactyls (Figure 1.14) [72,95-105].

In addition to confirming the presence of a transcript, RT-PCR is widely used to accurately assay the levels of expression (e.g. number of message copies) for a specific gene using quantitative real time PCR or qRT-PCR. This method measures amounts of cDNA (derived from RNA) comparing their levels to that of housekeeping genes. Spinsanti et al. [106] cloned and partially sequenced 10 different housekeeping genes from skin biopsy RNA of striped dolphin (*S. ceruleoalba*) and used the sequences to design specific oligo nucleotide

primers to test quantitative changes in expression of those genes using qRT-PCR. Of the 10 housekeeping genes examined, 3-monooxygenase (YWHAZ) and glyceraldehyde-3P-dehydrogenase (GADPH) were found to be the most stably expressed (i.e., showing minimal variation under different experimental conditions) genes and thus were used as controls for the normalization of qRT-PCR data in the analysis of striped dolphin biopsies. Ribosomal protein L4 and S18 expression also appeared to be stable. Mollenhauer et al. (2009) used ribosomal genes for the normalization of expression for genes following exposure of dolphin skin cells to methylmercury [107].

To identify immune system perturbations induced by environmental insults, Sitt et al. [70] performed a screening of 9 cytokine genes (IL-2, IL-4, IL-10, IL-12, IL-13, IL-18, TNF α , TGF β and IFN γ) in cetacea (bottlenose dolphin, beluga whale and pacific white-sided dolphin) using qRT-PCR to quantify the variation in expression in leukocytes induced by mitogen with S9 ribosomal gene as the housekeeping gene.

While qRT-PCR has become a routine technique and remains an important tool for analysis of immune responses in bottlenose dolphin and cetacean species, the availability of more global methods to assess immunological responses via gene expression (e.g., microarrays) is still at his infancy.

A better understanding of the dolphin immune system is also the result of development of novel assays for measuring dolphin-specific antibody and cellular responses and producing monoclonal antibodies to define distinct subpopulations of dolphin lymphocytes or other cell biomarkers [72,95-97,100,103-105,108-112]. Currently little is known about dolphin proteins and by extension their sequences or similarity to those of other species. There are 273 protein sequences available in NCBI for the genus *Tursiops*, most of which are mitochondrial

proteins. In addition, the structure for only a single dolphin protein has been resolved (protein sequence S, Structure Of The Signal Recognition Particle Interacting With The Elongation-Arrested Ribosome [113]).

In general cross-reactivity of antibodies designed and available for proteins of terrestrial species with cetacean proteins has not been determined [72,114]. Dolphin specific antibody development or screening of a large set of mono- and polyclonal antibodies must be performed to find those that best detect the protein of interest, due to unsuccessful or ambiguous cross-reactivity [89,115,116]. Nollens et al. have recently published data about the variation in cross-reactivity of a dolphin specific immunoglobulin G antibody between species of dolphins and whales [117]. They demonstrated that the percent cross-reactivity of the IgG antibody was highest for the dolphins tested and was lowest (17%) for the mysticetes; they were also able to correlate the antigenic cross-reactivity to the genetic distances between the species tested [117]. The availability of dolphin specific antibodies at the time of this publication is limited to monoclonal and polyclonal anti-bottlenose dolphin IgG [118], monoclonal antibodies against bottlenose dolphin neutrophils [119] and lymphocytes [71], and monoclonal anti-cetacean homologs of CD2, CD19, CD21, beta-2 integrin and CD45R [108-110].

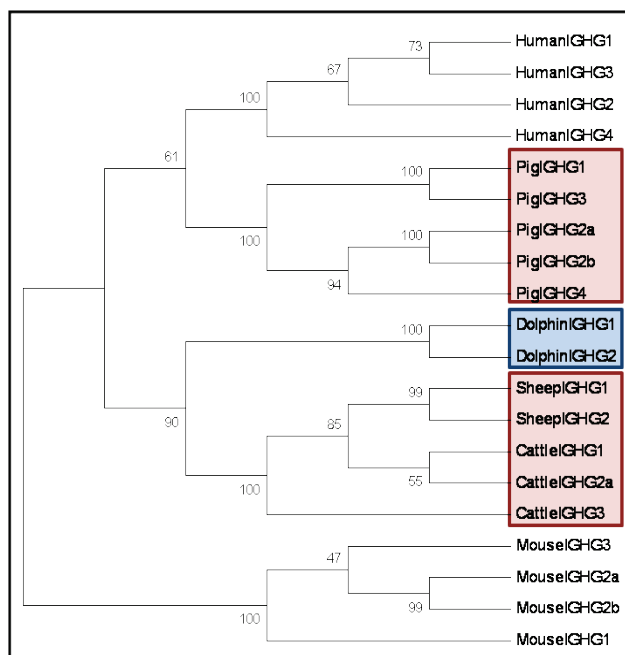


FIGURE 1.14 Phylogenetic tree of selected mammalian Immunoglobulin G Heavy Chain (IGHG) sequences.

The phylogenetic tree was constructed using Mega3 from the amino acid sequences of the IGHG chains of various mammalian species. Bootstrap values (%) in support of each node are indicated. The 2 bottlenose dolphins IGHG sequences are shown in the blue box. Artiodactyla IGHG (pig, sheep and cattle) are shown in the pink box. Adapted from Mancia et al., 2006 [120].

1.4.2 OVERVIEW OF MOLECULAR APPROACHES TO STUDY BOTTLENOSE DOLPHIN HEALTH

Amongst the new molecular technologies that can (and are) being applied to studies of dolphin health are genomics, proteomics, metabolomics and cellomics.

Genomics technology and functional genomics in particular can accelerate novel gene discovery, offering the opportunity to study molecular physiological responses on a broad ecological scale through the deployment of gene microarrays as transcriptomic biosensors [121-123]. The underlying paradigm of the transcript profiling approach is that all stimuli impinging on a cell will affect both gene and protein expression in that cell. Transcript profiling yields a quantitative “snapshot” of an entire expressed genome and is now an

established technique in the biomedical models of human physiology and disease [124-127]. Thousand of genes can be examined simultaneously resulting in large amounts of information about the interactions of many physiological systems. Furthermore, functional genomics approaches can yield results that are characteristic of the sum total of the environmental impacts an organism is experiencing [128], thus making it not only informative of basic mechanisms, but also a valuable diagnostic tool for health and disease.

Functional genomic analyses can be complemented by proteomic approaches. Proteomics is the large-scale study of proteins, their quantity, quality, structure and functions. Transcript profiling analyzes the expressed genomes, the coding region of DNA that is transcribed in mRNA. But mRNA is not always translated into protein, and the amount of protein translated depends on gene-specific translational efficiencies, the physiological state of the cell, mRNA stability and on proteasome activity. The genome is constant but the proteome differs from cell to cell under different physiological conditions. With a proteomics approach it is feasible to analyze cell signaling cascades and identify new proteins, therapeutic targets and biomarkers of a wide variety of diseases [129-134].

Cellomics represents the study of cellular phenotype and function and the relationships between all cellular components and how they work together in context, and it is typically approached through the use of cell lines. The use of cell lines for *in vitro* experiments is a widely used technique to study physiological events under normal or diseased condition [135] and in response to exposure to toxins.

Various studies have examined the effects of environmental factors (such as toxins and contaminants) on dolphins and other marine mammals all over the world [39-42,136-141]. The majority of these studies have focused on effects of specific toxins as determined by cellular/tissue distribution and more descriptive biological outcomes. These are necessary to develop an understanding of how the compromised status of the oceans may affect the resident organisms. However, in order to determine more specific effects as well as the long term implications, further investigations are needed using reproducible systems that allow the monitoring of the quantitative changes both at phenotypic and genotypic levels.

Investigators have been trying to develop dolphin cell lines for a long time [142-144] but despite the effort and the great applicability of cell lines as tools to study the mechanisms of dolphins biological processes, only a few such lines are available. This is due in part to the protected status of the animal and/or the stringent federal permits needed to deal with the samples.

Previous studies have shown interesting applications of marine mammal cell lines to study infection, such as hepatitis A and herpesvirus [144-146] but also to study the effect of chemical contaminants including mercury or perfluorinated compounds [147-150]. The susceptibility of dolphins to chemicals and toxins may be very different from what has been previously described for human (for example, for bottlenose dolphin the minimal body burden of methylmercury that produces mild symptoms is 2mg/kg, which is seven times the human threshold for symptoms [151]). In addition, the response to a specific stressor may vary dramatically as a function of a specific cell type (for example, epithelial vs. endothelial, or kidney vs. liver).

The dolphin kidney cell lines previously used and cited in the literature are from Atlantic spotted dolphins (Sp1K) [148,149] and bottlenose dolphin (TuTruK) [152]. B. Middlebrooks at the University of Southern Mississippi, isolated the dolphin kidney (TuTruK) and also a lung (TuTruL) cell line [152] from a stranded stillborn bottlenose dolphin. The skin cell line DS1 used by Yu et al [153] and Ellis et al. [154] was developed from bottlenose dolphin skin biopsy samples at the Medical University of South Carolina in Charleston, SC. The skin cell line was also successfully immortalized. Successful skin cell cultures were also obtained from *S. coeruleoalba*, *T.truncatus* and *D. delphis* skin biopsy as described by Marsili et al. [155,156].

Cell based phenotypic assays, genomic and metabolomic analyses of cells are included as technologies to predict the potential for toxicity of chemicals that could represent the greatest hazard to human health and the environment in the “ToxCast” research program, developed by the U.S. Environmental Protection Agency (EPA) [157].

In order to understand the biology of an organism it is necessary to identify biomarkers of the healthy and diseased state, which requires having sufficient genomic information and an understanding of the relationship between genes and proteins in the cellular context. The combination of genomics, proteomics and cellomics data is basic to today’s molecular biology research. In the study of organisms which also are protected species, like dolphins, these approaches that are capable of sensitive and real-time pictures of environmental impacts of stressors are going to be even more powerful and essential.

The work presented here is a contribution to the field of dolphin molecular biology and describes the development and applications of molecular tools specifically generated to gain insight into the biology, health and physiology of the bottlenose dolphin, *T. truncatus*.

2. RESULTS AND DISCUSSION

RESULTS AND DISCUSSION

PART I. THE DOLPHIN TRANSCRIPTOME

2.1 THE DOLPHIN MICROARRAY

The microarray used in this work was a species-specific cDNA microarray designed for studies of immune and stress response in dolphin, *T. truncatus*. The dolphin microarray was generated from ESTs of cDNA libraries from dolphin peripheral blood leukocytes (PBL) stimulated with LPS (lipopolysaccharide) and IL-2 (interleukin-2) representing a random sampling of the transcriptomes of stimulated B and T lymphocytes, respectively. The unigene collection (1343 unigenes) printed on the microarray was supplemented with the 52 targeted PCR-cloned stress and immune function genes as well as with unsequenced ESTs selected at random from both the IL-2 and LPS libraries. The microarray was validated and its performance as a probe to interrogate the transcriptome of dolphin cells was investigated as described in Mancina et al., 2007 [120] and, briefly, in the first sections of the Methods.

The work presented in the following section of the results describes the applications of such tool to study wild dolphins. The microarray was used a) as prognostic tool to monitor stress-induced changes in gene expression in wild dolphins and b) as a diagnostic tool, using a machine learning approach to define transcriptional signature of wild dolphin populations.

2.1.1 WILD DOLPHINS RESPONSE TO STRESS

Assessing the health of dolphin wild populations is necessary in order to monitor their status and for scientifically based management of the ecosystem. Health assessments of wild

dolphins typically rely on study of animals that are captured, examined and released. The process of chase, capture, examination and sampling of wild dolphins subjects these animals to some degree of both behavioral and physical stress. Previous reports have shown the activation of the hypothalamic/ pituitary/adrenal (HPA) axis, as measured by increased levels of corticosteroids in dolphins subjected to capture/ release studies [158].

In order to understand the extent and impact of such stress and to establish baseline normal values for sensitive physiological and biochemical functions during capture/release studies, blood samples were drawn from dolphins immediately upon capture (*pre*) and then, following veterinary examination, just before their release (*post*). The RNA extracted from blood samples was hybridized to the dolphin cDNA microarray previously described to determine changes in global gene expression changes between *pre* and *post* samples (e.g. genes up or down regulated following the capture/release event). The study reported here was undertaken specifically to address changes in dolphin molecular physiology that occur during health assessment studies.

There are many potential sources of variation in gene expression in wild dolphins, including sex, age, nutrition, disease (e.g. infections) and genetic factors. The population utilized in this study was balanced with respect to the geographical location, sex and number of animals sampled, but the age distribution was unbalanced and the genetic background and health/diseased status of each animal are additional examples of potential sources of variation in these animals (Figure 2.1; Table 2.1). Thus, an approach was taken in which comparisons were made between the two blood samples taken from each animal at the beginning (*pre*) and after (*post*) the veterinary examination. 20 dolphins were sampled, 10 (5 male and 5 female dolphins) for each one of the 2 geographical locations, (Charleston, SC and Indian River

Lagoon, FL), and 2 samples were collected (*pre* and *post*) from each dolphin; a total of 40 samples were hybridized to the microarray (Table A1). The unique properties of each animal (such as age, health and genotype) were considered constant between the *pre* and *post* samples.

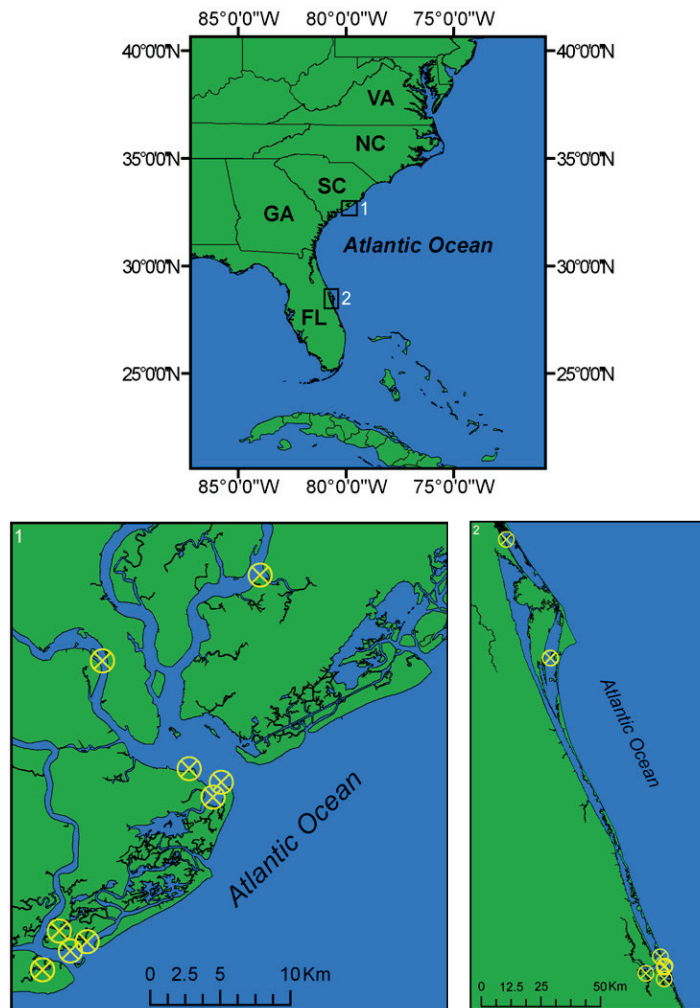


FIGURE 2.1 Map of the sampling locations along the South East coast of the United States. Samples were collected in Charleston, SC (1) and Indian River Lagoon, FL (2). Yellow circles represents the specific site of sampling for each dolphin.

TABLE 2.1 List of the dolphin used in this study.

#	DOLPHIN ID	LOCATION	YEAR	SEX/AGE/GROUP
1	FB8180803	CHS	2003	AM
2	FB8210803	CHS	2003	JF
3	FB8250803	CHS	2003	AF
4	FB8330804	CHS	2004	JF
5	FB8450804	CHS	2004	JF
6	FB8530804	CHS	2004	JF
7	FB8740804	CHS	2004	AM
8	FB8760804	CHS	2004	AM
9	FB8900804	CHS	2004	JM
10	FB8940804	CHS	2004	AM
11	FB9190603	IRL	2003	F
12	FB9360604	IRL	2004	AM
13	FB9390604	IRL	2004	JF
14	FB9410604	IRL	2004	AF
15	FB9470604	IRL	2004	AF
16	FB9490604	IRL	2004	JF
17	FB9520604	IRL	2003	AM
18	FB9540604	IRL	2004	AM
19	FB9660604	IRL	2004	JM
20	FB9720604	IRL	2004	JM

Pre and *post* blood samples were collected from 20 dolphins in Charleston, SC (CHS) and Indian River Lagoon, FL (IRL). F, female; M, male; J, juvenile; A, adult. AM, adult male 10 years and greater; AF, adult females 7 years and greater; JM, juvenile male less than 10 years; JF, juvenile female less than 7 years. Dolphin #11 (FB9190603) unknown age.

2.1.2 THE DIFFERENTIALLY EXPRESSED GENES

The examination of the transcriptomic changes in the gene expression profiles of peripheral blood cells that occurred between the taking of the two samples (*pre* and *post* veterinary examination) revealed a clear and complex response to stress. All of the significantly regulated genes are shown in Table A2. These genes showed significant differential expression not only in individual animals, but also when the group of 20 animals was considered collectively. More genes were up-regulated than were down-regulated, although the down-regulated group contains some important immune-function genes such as the innate

immune response receptors TLR2 and TLR3 and the T cell receptor (TCR) gamma chain. The significantly up-regulated genes include two notable categories identified according to their gene ontology. The first category (Table 2.2) consists of genes involved in energy generation; this is predictable given the known up-regulation of energy metabolism induced by glucocorticoids [159,160]. The second category (Table 2.3) is that of immune function and stress-responsive genes. While some transcriptomic responses indicative of stress were expected, the changes in gene expression observed in this study were greater than anticipated. In particular, the up-regulation of the pro-inflammatory chemokine IL-8, the cytokines IL-1 α and IL-1 β , and the pre-B cell colony enhancing factor (which is up-regulated in response to infection [161]) was surprising. In addition, significantly up-regulated genes included immune receptors such as a precursor of β 2- microglobulin (a component of the major histocompatibility complex 1 molecule), signal transduction molecules such as the Fc receptor γ chain (expressed as a component of Fc receptors for IgE and IgG on many inflammatory cells) and the CD3 γ chain (a component of the T cell receptor complex), as well as stress-responsive molecules such as thioredoxin.

Altered gene expression was seen in a large proportion of the dolphins that were studied. All dolphins showed up-regulation of cytochrome *c* oxidase subunit 1, and 19 up-regulation of ATP synthase F0 subunits 6 and 8. In the case of stress and immune response genes, 19 out of 20 showed up-regulation of pre-B-cell colony-enhancing factor, 17 out of 20 up-regulation of IL-8 and 16 out of 20 up-regulation of the γ component of the T-Cell Receptor Complex. This result indicates that the induction of these changes in gene expression was robust enough to be discerned against a background of variation in the sample population that was known to include geographical location, sex and age and which must also include differences

(of unknown degree) in genetics, physiology and disease status. Studies on global gene expression associated with acute-phase responses (typically provoked by bacterial endotoxin stimulation) have been reported in several species, including mice, dogs and humans [162-164], and gene expression patterns have been studied in both liver and blood. To compare the previously reported results with those obtained in the present study, using a relatively restricted suite of dolphin genes, necessitates extrapolations across species between different tissues and following very different treatments. Despite this, it is clear that certain features are common to the responses documented in these studies. For example, the pre-B-cell colony-enhancing factor that was up-regulated in 19 of the 20 dolphins was found up-regulated in the acute-phase response of both mouse and dog [162,164]. Families of genes identified in this study as regulated by stress in the dolphin and whose expression has also been reported to change significantly in acute-phase responses include IL-1 α , IL-1 β , IL-8, haemoglobin β chain, Fc receptor γ chain, histones, elongation factors, ferritin polypeptides, T cell receptor γ , and the CD3 γ subunit. IL-8 up-regulation was investigated through real-time PCR (*qRT-PCR*).

TABLE 2.2 Summary of significantly regulated genes associated with energy metabolism.

FREQUENCY†	IDENTITY‡
20	Cytochrome c oxidase subunit I
18	Cytochrome c oxidase subunit II
18	Cytochrome c oxidase subunit III
17	Ubiquinol-cytochrome-c reductase
11	Cytochrome b
19	ATP synthase F0 subunit 6
19	ATP synthase F0 subunit 8
13	NADH dehydrogenase subunit 3
10	NADH dehydrogenase subunit 4L
8	NADH dehydrogenase (ubiquinone)1a

*Genes selected from those presented in Table A2; †number of dolphins in which significant regulation was observed; ‡highest value match from a blastx search.

TABLE 2.3 Summary of significantly regulated genes associated with stress and immune response.

FREQUENCY†	IDENTITY‡
19	Pre-B-cell colony-enhancing factor 1
17	Bos taurus interleukin 8 mRNA
16	Beta-2-microglobulin precursor
16	CD3G gamma precursor: T cell receptor
10	Interleukin-1 beta
8	Bos taurus interleukin 1, alpha (IL1A)
8	Fc receptor gamma-chain
18	Thioredoxin
9	ferritin, light polypeptide
19	Pre-B-cell colony-enhancing factor 1

*Genes selected from those presented in Table A2; †number of dolphins in which significant regulation was observed; ‡highest value match from a blastx search.

2.1.3 INTERLEUKIN-8 REAL TIME PCR (*qRT-PCR*)

Of the immune function genes, IL-8 was up-regulated in 17 of the 20 dolphins, and showed the highest levels of induction (as assessed from the *df* values, Tables A1 and Table 2.3). Thus, confirmation of this result was sought using an independent method, quantitative real-time PCR. The levels of message for IL-8 (and as a control GAPDH) were measured in the *pre* and *post* samples of eight dolphins (Table 2.4). The level of IL-8 message, expressed as a ratio to GAPDH levels, was elevated in seven of the eight dolphins (Figure 2.2). Statistical analysis of the data (Table 2.5), correcting for GAPDH levels, showed a highly significant ($P < 0.001$) up-regulation of IL-8 message in *post* as compared to *pre* samples. It should be noted that in Table 2.5, the larger mean values indicate lower relative expression values as Ct is inversely related to the copy number of the target message. This analysis also clearly indicated that IL-8 was significantly up-regulated regardless of the assumptions concerning equivalency of the variances in the samples (Table 2.5).

IL-8 is a gene whose expression is strongly associated with the onset of an acute-phase response, and in the present study, it was shown by both microarray and *qRT-PCR* analysis that IL-8 message was significantly upregulated in wild dolphins during capture/release health assessment. IL-8 is a chemokine, a chemotactic cytokine responsible for migration of cells to a site of inflammation.

It is produced early in the inflammatory response by monocytes, neutrophils, macrophages and endothelial cells and activates acute inflammatory cells [165] in response to stimulation from different agonists including lipopolysaccharide (LPS), bacteria, viruses, and cellular stressors [166-172]. During an infection, neutrophils are rapidly recruited to sites of inflammation where they amplify the inflammatory response and increase tissue

concentration of pro-inflammatory cytokines such as IL-1 α , IL-1 β , IL-6, IL-8, TNF- α , IFN- γ , and GM-CSF [173,174]. Collectively, these events reflect the activation of the acute-phase response which is seen in reaction to infection, injury, trauma, surgery or immune disease [175]. However, IL-8 is only one of several acute-phase response-associated genes identified by the microarray analysis as significantly different between pre and post examination. While the expression patterns for dolphin genes other than IL-8 were assessed only by microarray analysis, the collective data from both microarray and *qRT-PCR* analysis argue strongly that the capture/ release health assessment study of wild dolphins can induce an acute-phase response. It can be noted that the majority of dolphins responded very similarly to the veterinary examination. Thirty-four of the genes listed in Table A2 (53%) were significantly regulated in half or more of the dolphins examined. The failure of some individuals to follow the 'species norm' could be interpreted as an indication of idiosyncratic response and perhaps a result of pre-existing conditions. From the present data, these effects cannot be evaluated. However, as the preponderance of individuals exhibited a concordant response in the expression of these genes, this reinforces the view that sources of variance (whatever their nature) in the sampled population did not obscure the analysis or the conclusions of this study.

TABLE 2.4 Ratio between IL-8/GAPDH mRNA levels in *pre* versus *post* samples.

#	DOLPHIN ID	<i>pre</i>		<i>post</i>		<i>post vs pre</i> expression	
		RATIO	SD	RATIO	SD	up	down
1	FB8180803	0.9192	0.0021	0.9424	0.0004	↑	
3	FB8250803	0.8408	0.0085	1.0001	0.0061	↑	
8	FB8760804	0.8109	0.0022	0.9214	0.0041	↑	
9	FB8900804	0.9319	0.0049	0.9646	0.0025	↑	
12	FB9360604	0.8938	0.0026	0.9224	0.0056	↑	
15	FB9470604	0.8802	0.0027	1.0061	0.0047	↑	
16	FB9490604	0.9429	0.0678	0.8593	0.0095	↑	
19	FB9660604	0.8806	0.0038	1.0201	0.0117		↓

Ratios were calculated using the x values derived from the standard curve equations for GAPDH ($y=-3.05x+36.435$; $R^2=0.9994$) and IL-8 ($y=-3.3874x+41.748$; $R^2=0.9982$), where y is the mean of Ct values for replicate measurements.

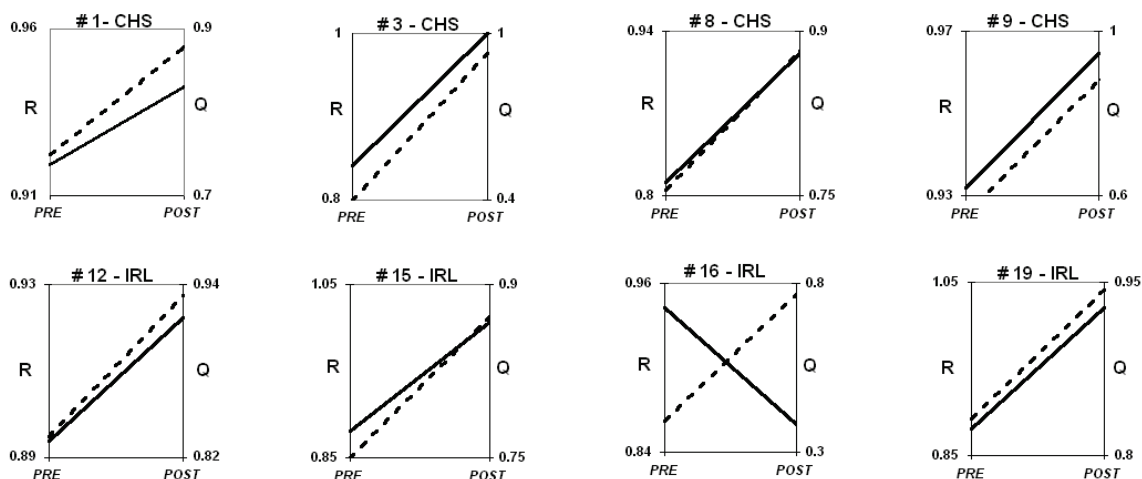


FIGURE 2.2 Comparison of IL-8 message levels as measured by *qRT-PCR* and microarray analysis. Microarray data are shown as quantile values [176] for IL-8 in *pre* and *post* samples (dashed line). *qRT-PCR* data (solid line) are shown as the ratio between IL-8 and GAPDH from relative quantification analysis as shown in Table 2.5.

TABLE 2.5 T-test for significance of IL-8 up-regulation in *post* vs *pre* samples.

	T-test: paired two sample for means		T-test: two sample assuming unequal variance	
	<i>pre</i>	<i>post</i>	<i>pre</i>	<i>post</i>
<i>pre post</i>				
Mean	5.511	4.4	5.511	4.4
Variance	0.549	0.76	0.549	0.76
Observations	16	16	16	16
d.f.		15		29
t Stat		3.402		3.884
P(T≤ t) one-tail		0.002		0.0003
T critical one-tail		1.753		1.699
P(T≤ t) two-tail		0.004		0.0005
T critical two-tail		1.131		2.045

The statistical analyses were carried out on the measured Ct values for IL-8 and GAPDH. The mean values reported in this table for the *post* samples are lower than those for *pre* values because the value of Ct is inversely related to the level of message.

2.2 MICROARRAYS AND ARTIFICIAL NEURAL NETWORKS

2.2.1 WILD DOLPHINS AND THE ENVIRONMENT

PBL samples were collected from 151 bottlenose dolphins in the course of capture/release health evaluation studies at 4 different sites: Charleston Harbor, SC, Indian River Lagoon, FL, Sarasota Bay, FL and St Joseph Bay, FL (Figure 2.3, Table A3). RNA was extracted and hybridized to the dolphin microarray as previously described (see also Materials and Methods and Mancina et al., 2007 [120]). The purpose of this study was to understand the impact of the marine environment on wild dolphin populations examining the differences in gene expression profiles using a combination of microarrays and machine-learning analytical approaches. Differences between the 4 dolphin populations may result from genetic or environmental factors (including for example diet, infection, contaminant load or exposure to

biotoxins) or a combination of these factors. Thus, the hypothesis tested was that individual dolphins could be assigned to their home regions (by machine learning methods) using only their transcriptomic signatures as classifiers. The machine learning approaches used in this study were artificial neural networks (ANNs).

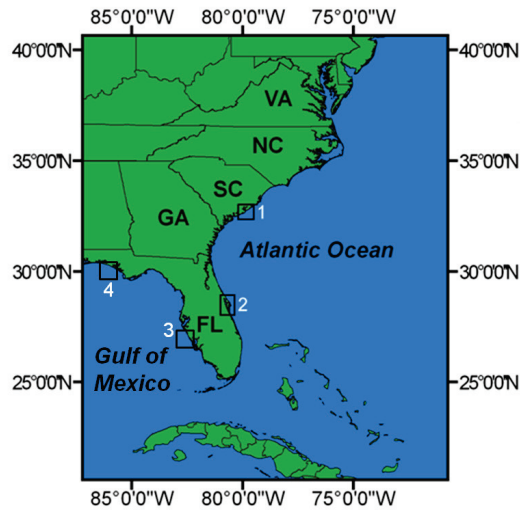


FIGURE 2.3 Map of the sampling locations along the South East coast of the United States. Samples were collected in Charleston, SC (1) and Indian River Lagoon, FL (2) on the Atlantic Ocean and in Sarasota, FL (3) and St. Joseph Bay, FL (4), on the Gulf of Mexico.

2.2.2 ARTIFICIAL NEURAL NETWORKS (ANNs)

While the ability of machine learning methods to fit any given input data set to an output is a general property of artificial intelligence (eg. machine learning tools), the artificial neural networks (ANNs) that have been primarily used in this study have some particularly attractive properties for forecasting and modeling dynamic systems [177,178].

In particular, ANN's thrive in modeling non-linear interactions among input variables as output classifiers and are therefore, well suited to dealing with transcriptomic signatures,

which almost certainly involve non-linear interdependencies among the inputs. ANN's have been used extensively in medical science to classify disease status based upon expression profiles [179-182]. Most studies employing ANN modeling approaches of microarray data have used linear analysis tools (significant up or down regulation), expert knowledge, principal component analysis or some combination of these, to select genes for inputs to the ANNs. This re-introduces linear methods to the analyses since linear tools are being used to select inputs for a non-linear analysis and has the potential to degrade the predictive value of microarrays. However, ANN's also provide a potential solution to this problem in that they can select genes, using non-linear methods, for input into the analysis. Specifically, the models generated by an initial training session using all genes present on a microarray (after filtering non-responsive elements), can be interrogated for responses of the outputs associated with changes in these inputs. These are essentially the derivatives of the ANN function but are computed numerically and called 'sensitivities' as they are an assessment of the sensitivity of the output (dependent variable) to changes in the inputs (independent variables). The accuracy, as classifiers, of analytical methods using genes selected in this manner can be estimated by Receiver Operating Characteristic (ROC) curves (Figure 2.4).

2.2.3 ANNs DISCRIMINATION OF SEX DIFFERENCES IN WILD DOLPHINS

As males and females are likely to express a somewhat different suite of genes and the individual locations were not always balanced with respect to sex ratios, it was possible that comparisons of locations using all individuals could be biased by gender differences in each location. To assess this bias we compared the expression profiles between sexes using ANN's as described in Figure 2.4 on the basis of their sensitivities (ANN selected genes are

listed in Table A4). These results (Table 2.6) clearly indicate gene expression differences between the sexes in Charleston Harbor and St. Joseph Bay, but not between the sexes in Indian River Lagoon and Sarasota Bay. This difference in gene expression between the sexes could bias discrimination of dolphins from Charleston Harbor, St. Joseph Bay and (to a lesser extent) Sarasota Bay and the assessment of between-location population differences should be conducted for each sex independently. We deem this finding an important cautionary note. Whilst sexual differences in gene expression have received considerable attention in the past decade [183], few investigators addressing the impacts of environmental conditions on natural populations have accounted for this potential bias in sexually dimorphic species [184,185]. If the sample sizes within contrasted groups are fairly large (>30) and the sex ratios relatively stable, it is unlikely that this complication will strongly influence the results. However, if sample sizes are small, unequal sampling of the sexes could influence the results.

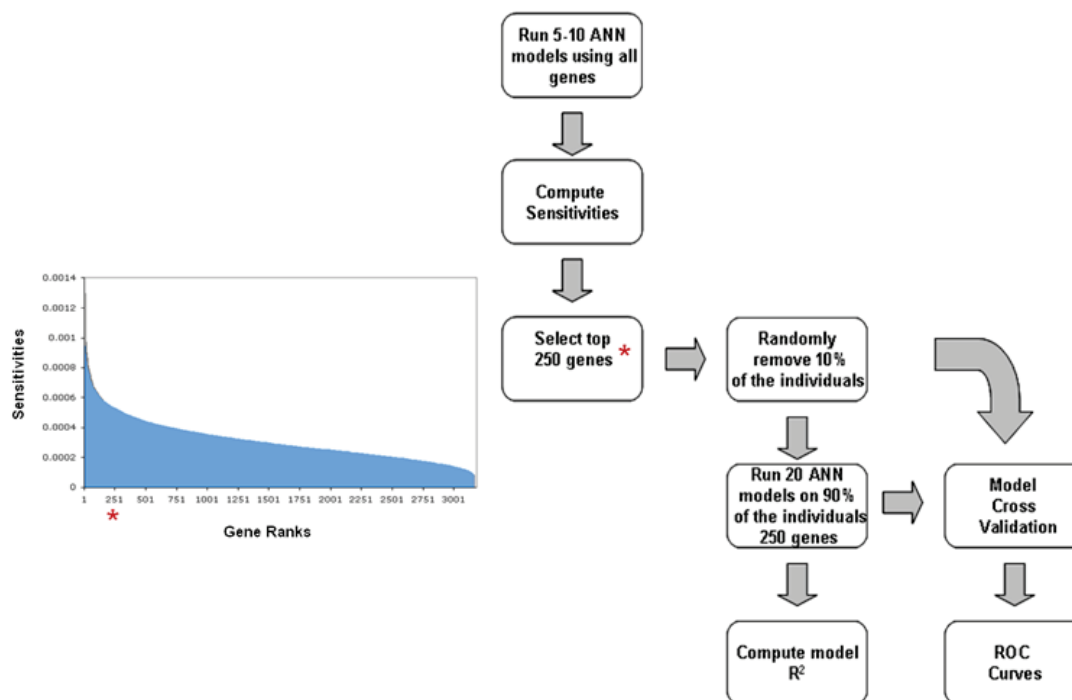


FIGURE 2.4 Schematic flow chart of the ANN analysis of microarray data.

An initial training of ANNs was conducted using the entire set of the microarray filtered data. Five models were run for each population keeping the sexes separate, using a *one-vs-rest* approach (eg. Charleston Harbor males vs males in all other populations) withholding a random selection (1/7) of the microarray records from each population as a cross validation set to prevent over training of the ANN (Haykin 1999). The model with the highest R-square for the training data from each population comparison was used to compute the sensitivities of the individual genes. The sensitivities across all populations were then averaged and ranked to select the top 250 most ‘important’ genes. Sensitivities (plotted on the ordinate) provide an assessment of how changes in the input (gene number) impact the output. ANN, artificial neural network. ROC, receiver operating characteristic curves.

TABLE 2.6 Discrimination between male and female dolphins at four locations.

	CHS	IRL	SAR	SJB
NO.GENES	AUC (SE)	AUC (SE)	AUC (SE)	AUC (SE)
250	0.6598 (0.0416)	0.5843 (0.0708)	0.6275 (0.072)	0.7019 (0.0749)

Areas under the ROC curves (AUC) and their standard errors (SE) for classification of male and female dolphin via ANNs are shown within each sample location. The number of genes used in the test is indicated on the left (250). These genes (Table A4) were identified according to sensitivities from the best of 5 ANN models run on the full suite of genes on the microarray. The values in bold type are significantly different from random expectations at $p < 0.05$. CHS, Charleston, South Carolina; IRL, Indian River Lagoon, Florida; SAR, Sarasota, Florida; SJB, St. Josephs Bay, Florida.

2.2.4 ANNs DISCRIMINATION OF WILD DOLPHIN'S GEOGRAPHICAL LOCATIONS

The results of the ANNs classification of individual transcript profiles to location are presented in Figure 2.5. In all comparisons both males and females were correctly assigned to location of collection above random expectations and of the 10 total comparisons all but 2 were greater than 90% accurate. Both of these involved comparison of male dolphins. This should not be taken as an indication that classification of males should have been less precise than females as this difference is not significant via a sign test. The expected result was that, when differences in the discrimination appeared between the sexes, the classification of females should have been less precise due to their ability to shed certain contaminants [52] via lactation and, thus, their gene expression profiles would have been less discriminatory. This was not the case.

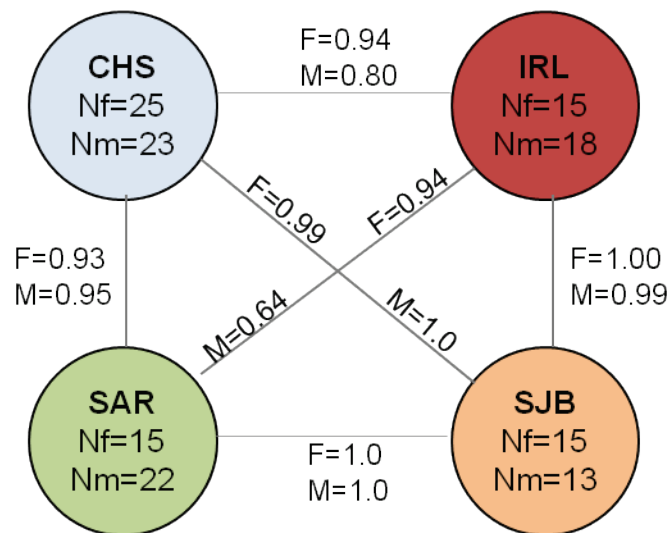


FIGURE 2.5 Classification precision of dolphins to location based upon transcriptional signature.

CHS, Charleston, South Carolina; IRL, Indian River Lagoon, Florida; SAR, Sarasota, Florida; SJB, St. Josephs Bay, Florida. Nf, female sample size. Nm, male sample size. F, percent correct classification for females. M, percent correct classification for males.

2.2.5 WILD DOLPHIN POPULATIONS TRANSCRIPTOMIC SIGNATURE

Although the gene expression profiles, considered as overall signatures, provide useful classificatory tools, there is also a great deal of information that can be inferred from examining which genes show significantly different levels of expression.

The 250 selected genes from the ANNs analyses, with the highest sensitivities were identified (Table A5) for both male and female dolphins, and used to generate heatmaps (Figure 2.6A-B). The results showed identical clustering patterns for males and females, with the closest relationship being between the dolphins from the Southeast US (Charleston and Indian River Lagoon) with the Saint Joseph Bay animals being the next most-closely related and the Sarasota Bay animals forming a separate basal branch.

When a more traditional linear method of microarray data analysis was used (Bioconductor) to look at differentially expressed genes, the selection identified 171 unigenes for male dolphins and 195 for females as being significantly differentially-regulated (less redundancies). These genes, listed in Table A6, were used to generate heatmaps using Euclidean distance and hierarchical clustering as implemented in the R package “gplots”.

As for the ANNs-selected genes, these analyses showed that for both males and females the dolphins from Charleston and Indian River Lagoon clustered together. However, whilst the males showed the Saint Joseph Bay dolphins as being the next most-closely related (Figure 2.7A), for females it was the Sarasota Bay dolphins (Figure 2.7B). A global comparison of the genes differentially expressed both in male and female dolphins in the 2 types of analysis, selected the 130 genes that have been used to generate the Venn diagram in Figure 2.8. This shows the number of differentially expressed genes, for males and females, that were found to be significant in determining the location. Male and female dolphins share 45 genes

uniquely identified by Bioconductor analysis and 44 genes uniquely identified by the ANN analysis. Overall, 41 genes were identified as significantly informative in both ANN and Bioconductor analyses (Figure 2.8). Although a large proportion of the genes identified as differentially regulated were not common to the ANN and Bioconductor analyses (Figure 2.8), nevertheless when typical cluster analyses were carried out the inferred relationships were almost identical (Figure 2.6; Figure 2.7).

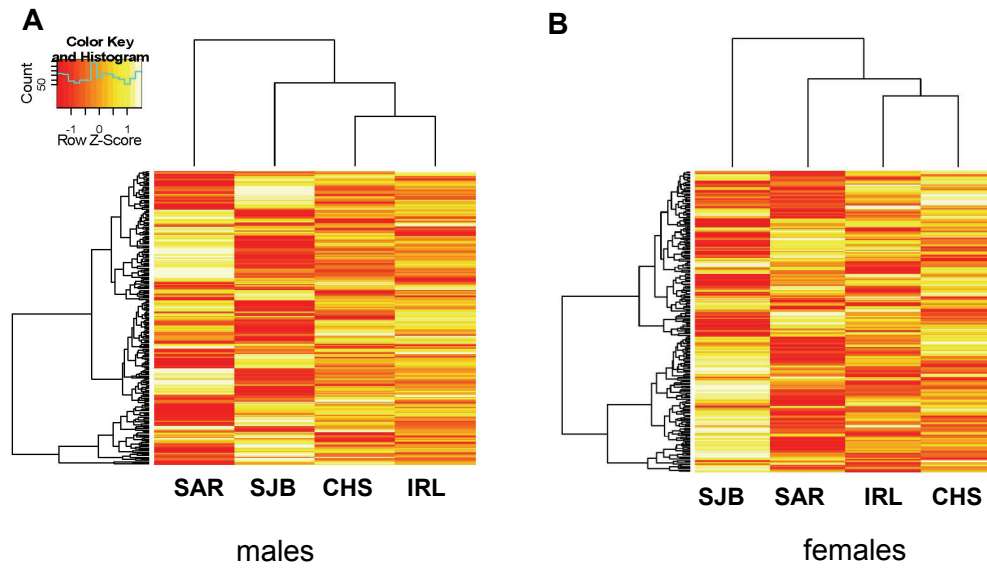


FIGURE 2.6 Intensity values (scaled by row) for the 250 genes selected by the ANN of the male (A) and female (B) populations.

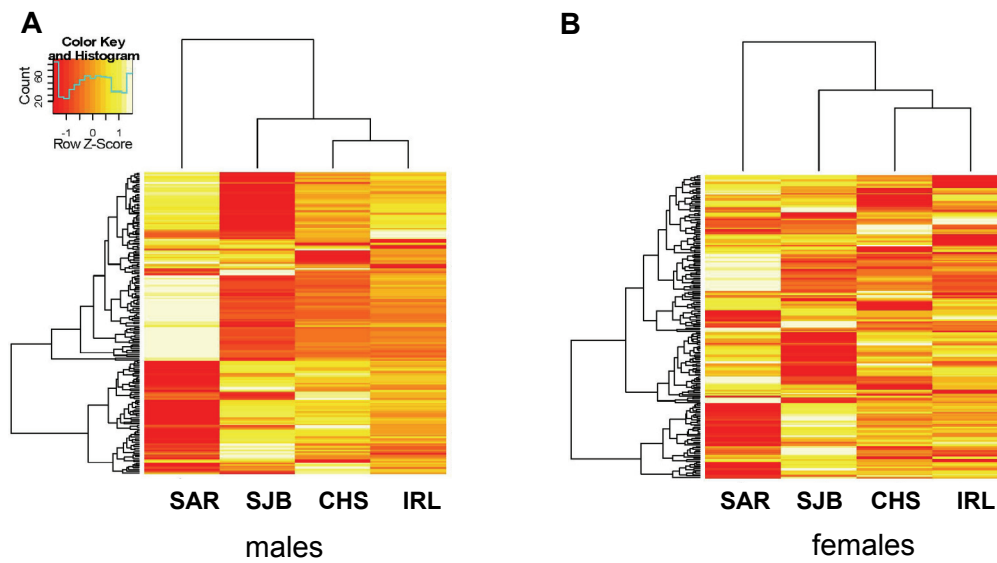


FIGURE 2.7 Intensity values (scaled by row) for the genes selected by the Bioconductor of the male (A) and female (B) populations.

CHS, Charleston, South Carolina; IRL, Indian River Lagoon, Florida; SAR, Sarasota, Florida; SJB, St. Josephs Bay, Florida.

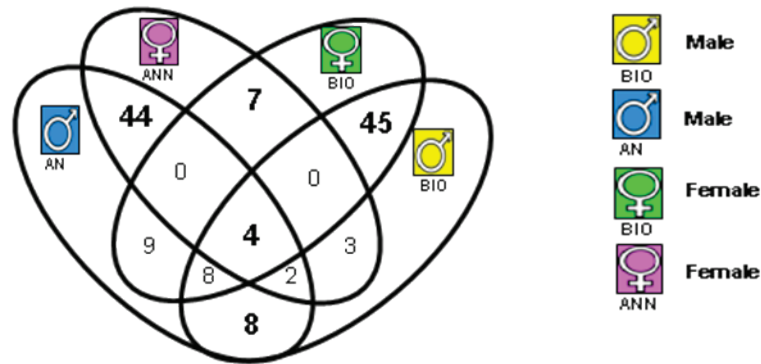


FIGURE 2.8 Venn diagram of the significant genes for the prediction of the location from the ANN and Bioconductor analysis in female and male populations.

ANN genes are indicated with the symbols for the correspondent sex in pink and blue (on the left) while the Bioconductor genes are indicated with the symbols for the correspondent sex in green and yellow (on the right) as explained in the figure legend (left box).

As would be expected with an array that was focused on stress and immune-response, many of the genes found to be differentially expressed between populations reflect this bias of the array. However, this does not detract from the legitimacy of the observed changes in gene expression. It is interesting that while some of the genes that were differentially expressed between males and females are sex-specific (for example, the breast and ovarian cancer susceptibility protein, the ribosomal protein X-linked, dpy-30 homolog), major differences between the sexes were observed in immune function genes (Table A5; Table A6). The Bioconductor and ANN analyses identified in females a variety of innate and adaptive immune receptors (including TLR-1, TLR-4, TLR-7, TLR-8, TCR and CD48). In contrast, in males the informative regulated genes included not only receptors and signal transduction molecules (TLR-1, TLR-3, TLR-6, BCR, CD47, CD79, STAT1) but also interleukins (IL-1 α and IL-13). Male populations also showed differential expression of genes for muscle structural proteins such as myosin and tropomyosin, probably correlated with the relatively greater development of muscle mass in males. Some immune function genes were found

differentially expressed in both males and females (including MHC α , lymphotoxin and a C-type lectin-related protein). A major component of the genes regulated significantly in both sexes (as identified in both ANN and Bioconductor analyses) are the structural proteins, including those of the ribosome and mitochondrion. Not surprisingly, many of the genes identified with both analyses belong to the family of retrotransposons (endonuclease reverse transcriptase), as in mammals almost half the genome (45%) is comprised of transposons or remnants of transposons [186,187].

Another noteworthy set of genes identified in the Bioconductor and ANN analysis in both sexes were metallothionein, ERp44, selenoprotein K, ferritin and heat shock protein (Table 2.7). The expression of these genes is known to protect against oxidative stress-induced cellular injury [188-190]. Table 2.7 shows the expression of these genes relative to the expression in Sarasota dolphins, which exhibited a lower level of expression. Metallothioneins form complexes with heavy metal ions, binding physiological (zinc, copper, selenium) but also xenobiotic heavy metals (cadmium, mercury, silver, arsenic) via the thiol groups of the cysteine residues. Selenium, originally considered toxic, is now known to be an important micronutrient [191]. Deficiency as well as too high concentration of selenium can lead to several disorders and diseases [191]. Endoplasmic reticulum resident protein (ERp44 or thioredoxin domain-containing protein 4) is an ER-resident that contains a thioredoxin domain and is induced during ER stress. Its overexpression alters the equilibrium of the different Ero-1 (endoplasmic reticulum oxidoreductin) redox isoforms, suggesting that ERp44 may be involved in the control of oxidative protein folding [192]. Little is known of selenoprotein K (SelK). It has been recently identified in *Drosophila melanogaster* where knock-down assays showed that SelK is necessary for normal development [193,194]. SelK

is also present in humans where it exhibits a wider variety of functions; Lu et al (2006) showed its function as an antioxidant in cardiomyocytes [195]. It was very interesting that SelK seemed to be present in dolphin blood. The knowledge of the importance of selenoproteins to the immune system is limited, but it is known that they have a role in the modulation of the inflammatory response [196]. The presence of Selenoprotein K in dolphins requires further study.

TABLE 2.7 Relative expression of oxidative stress-response genes in all 4 geographic locations through the Bioconductor and ANNs analyses.

DOLPHIN ESTs		LOCATION				ANALYSIS/SEX
NCBI ACC.NO.	IDENTITY	CHS	IRL	SAR	SJB	
DV468529	Hsp70 subfamily B suppressor 1 (HBS1)	0.58	0.78	-	1.44	B/M
DV799541	Metallothionein 1	0.07	0.00	-	0.14	B/M
DT661135	ERp44 (thioredoxin domain-containing protein 4)	0.83	0.50	-	3.08	B/M
DV467972	Heat shock factor binding protein 1 (HSBP1)	0.59	0.83	-	1.50	A/M
DV467994	Selenoprotein k	1.84	0.84	-	0.93	B/F
DT660293	Ferritin	0.44	0.04	-	0.89	A/F

Expression of oxidative stress-response genes relative to the expression of that gene for the SAR dolphins. Values are expressed as fold change in expression using Sarasota dolphin values (lower expression) as reference set. The fold changes were obtained from VSN transformed microarray data. B, Bioconductor analysis. A, ANN analysis. M, male dolphins. F, female dolphins. CHS, Charleston, South Carolina; IRL, Indian River Lagoon, Florida; SAR, Sarasota, Florida; SJB, St. Josephs Bay, Florida.

2.3 THE DOLPHIN GENOME SEQUENCING PROJECT

The Human Genome Sequencing Center at Baylor College of Medicine has sequenced the genome of the bottlenose dolphin (*Tursiops truncatus*).

The dolphin has been chosen as one of 24 animals whose genome has been sequenced to 2x coverage as part of the comparative genomic annotation effort which seeks to identify functional elements that are conserved across mammals, a project funded by the National Human Genome Research Institute (NHGRI). We worked with the Human Genome Sequencing Center at Baylor College of Medicine for the sequencing of the genome of the

bottlenose dolphin (*Tursiops truncatus*). The genome was obtained from DNA of a healthy female dolphin and it was sequenced together with ESTs from 5 cDNA libraries that we generated from different dolphin tissues (kidney, spleen, liver, muscle, skin). The sequencing has been carried out using both traditional Sanger sequencing method as well as using the more recently introduced 454 sequencing. The yield accounts for ~8,000 ESTs and ~10,250,000 WGS (Whole Genome Shotgun) from Sanger sequencing and 7 SRA (Short Read Archive) runs from 454 sequencing.

We are currently working to extract unigenes from the combination of all the sequences available in the *T. truncatus* database in order to design an Agilent oligo array comprehensive of the dolphin genome.

The “second generation” dolphin microarray will be used to assess the impact of biological, chemical and physical stressors at the transcriptomic level on 1) wild animals (prognostic tool) and on 2) dolphin cells maintained in culture (diagnostic tool). Gene expression profiles from cells will be integrated with morphological and other image-derived data from cells (phenotypic anchoring).

Given the limitation of dolphin cell lines availability, we are currently developing and optimizing protocols to generate, identify and characterize dolphin cell lines from stranded animals. Progress and results are shown in the next section.

PART II. DOLPHIN CELL BIOLOGY

2.4 QUANTITATIVE CHARACTERIZATION OF MAMMALIAN CELL LINES

Cell lines are widely used to study molecular and physiological events in normal or disease conditions, and in response to drugs or toxins [197]. The reliability of cell lines is critical to assure accuracy of assay outcomes and to allow meaningful comparison of data between different laboratories and under different conditions. Cell lines can be misidentified, contaminated [198-205] and intrinsically unstable in their growth properties and/or genome; furthermore, gene expression and metabolic rate can be sensitive to culture conditions. There are many qualitative descriptions of cell lines reported in the literature, but in the absence of quantitative data, these descriptions can be ambiguous and confusing. Quality control metrics for a cell line that quantitatively describe the phenotype of cells in culture are, therefore, necessary to establish the characteristics of a culture before measurements are made. Such metrics may comprise specifications of the cell culture that can be used to assess comparability of different experiments on different days, and provide assurance of comparability of data collected in different laboratories. Unambiguous quantitative metrics can provide benchmark data to determine changes that may occur in a cell line after sequential passaging or long time in culture or storage, and also provide a benchmark for assessing the effects of toxins or other environmental perturbations.

The presence or absence of receptors or other gene products are sometimes used in evaluating cell lines, but such data are not always available or unambiguous. This is particularly true for rare cell lines such as dolphin cells. The absence of reliable commercially available antibody reagents, and the unknown cross-reactivity of antibodies

against proteins of terrestrial mammalian species with proteins of dolphin cells can prevent clear identification of a cell line [206,207].

2.4.1 QUANTITATIVE METRICS TO CHARACTERIZE A DOLPHIN CELL LINE

This work describes the development of quantitative measurements of some physical properties of cells to describe a dolphin cell line. We utilized optical microscopy to measure cell morphology and cell-cell contact, and we used impedance measurements in a flow-based cell counter to determine cell volumes within the populations, from which we determined cell growth rates. As it will be shown, the methods presented here can be applied to most cultured cell populations thus providing practical physical metrics of cells in culture. This information can provide an easy to acquire specification that benchmarks the phenotypic properties of cell cultures.

We evaluated cells from a marine mammal, the dolphin (*T. truncatus*), and compared them to cells from 3 terrestrial mammals, the human (*Homo sapiens*), the cow (*Bos taurus*), and the mouse (*Mus musculus*).

The metrics used provide evidence to support the unique identity of these cell cultures, and to quickly and easily identify changes in the population of cells undergoing extended passages.

We have established metrics based on cell volumes, morphology, and cell-cell interactions that describe the four populations of cells and their distinguishing characteristics.

The dolphin cell line (TuTruL) has been kindly provided from B. Middlebrooks at the University of Southern Mississippi and it has been previously characterized as a lung microvascular endothelial cell line by Garrick et al. [152]. However, the results presented in the next chapters will argue and further discuss the “endothelial” nature of the TuTruL.

2.4.1.1 MORPHOLOGICAL ANALYSIS: CELL AREA, ROUNDNESS AND CLUSTERING

Visual comparison of representative images of endothelial cells from dolphin lung (Figure 2.9 A-C), bovine lung (D-F), and human umbilical cord (G-I) shows a variety of morphologies and cell-cell contact patterns for these cells grown on tissue culture polystyrene (TCPS) (Figure 2.9). Mouse NIH 3T3 fibroblasts (J-L) are shown for comparison as a non-endothelial cell line. The phase contrast (Figure 2.9, column 1) and Texas-red-Maleimide (Figure 2.9, column 2) stained images suggest morphological differences among the lines. The bovine and human endothelial cells appear to be elongated while the dolphin cells exhibit a more rounded shape. The mouse fibroblasts appear smaller than the other cells. Because such visual inspection of a limited number of cells could be biased and provides only relative characterization, we used automated microscopy to collect several hundred images of each kind of cell for each replicate determination, and applied image analysis procedures to extract quantitative morphological parameters from the images. Texas-red-Maleimide [208] was used to stain cellular proteins, and to provide good optical contrast between cell areas and background (Figure 2.9, column 2), and DAPI staining was used to identify the cell nuclei (Figure 2.9, column 3). A mask of each cell object was generated by applying a single intensity threshold value to discriminate between the Texas red staining and background; the number of pixels within these objects was used to determine the area of the cell object, and therefore the area of the cells were spread. DAPI staining provided validation that the object was a cell, or a group of cells, and allowed determination of how many cells comprised a group.

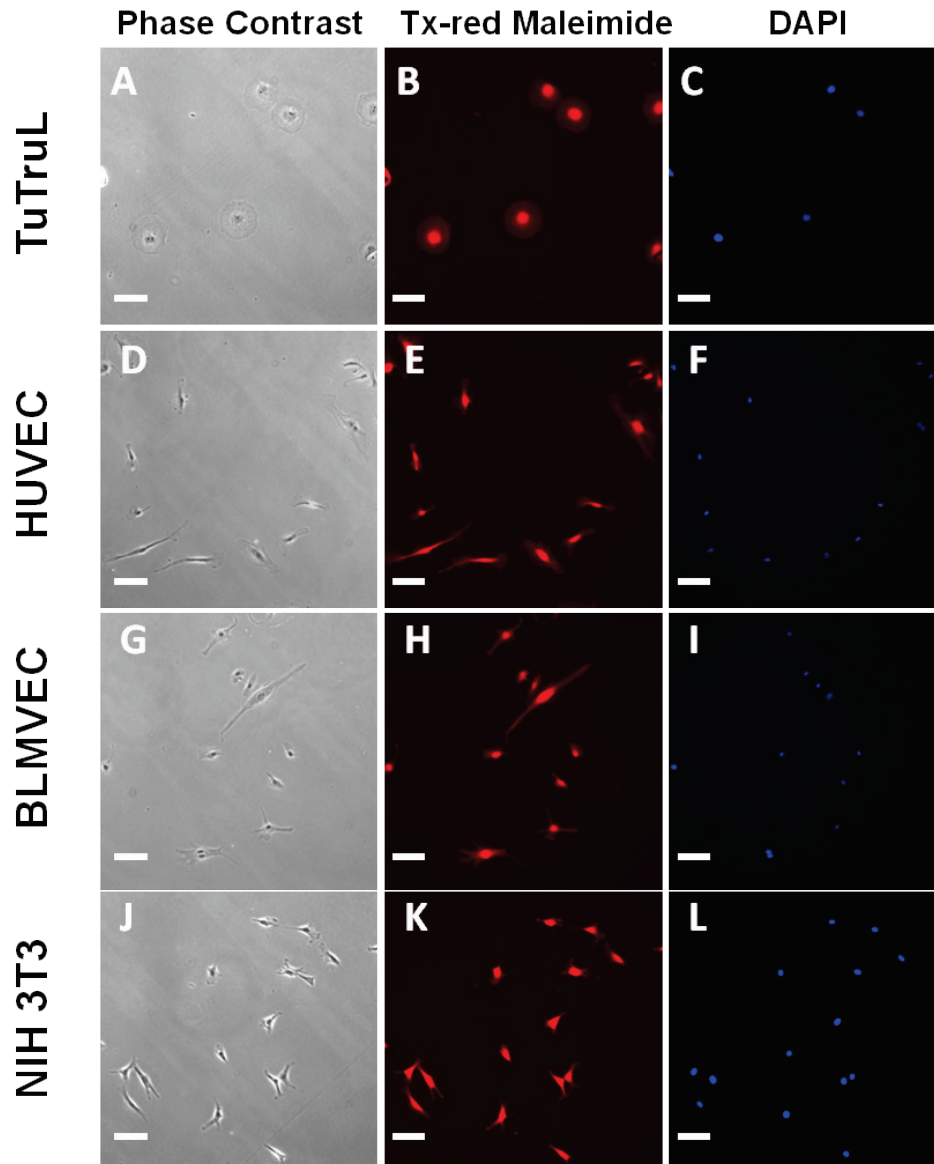


FIGURE 2.9 Phase contrast and fluorescence (Texas-red- maleimide and DAPI staining) microscopy images of 4 cell lines.

Cells were seeded at 1000 cells/cm² and images were collected after fixing the cells 24 hours after seeding. A-C, TuTruL, D-F, BLMVEC, G-I, HUVECs and J-L, NIH 3T3. Scale bar = 100 μ m for A-L.

The results of image analysis indicate that dolphin cells have the largest spread area with an average area of $4470 \pm 487 \mu\text{m}^2$, the human cells have an average spread area of $3208 \pm 259 \mu\text{m}^2$, and the bovine cells average area is $2076 \pm 293 \mu\text{m}^2$. NIH 3T3 fibroblasts had an average area of $1388 \pm 215 \mu\text{m}^2$, which is consistent with previous measurements made in our lab for this cell line ($1182 \mu\text{m}^2 \pm 80 \mu\text{m}^2$, data not shown). These averages are shown in Figure 2.10. The range of cell areas measured within these populations is shown in Table 2.8 and the distribution of the cell areas within the 4 populations is shown in Figure 2.11. From this image data, we also calculated roundness and axial ratio to describe the cell shapes. The dolphin cells are significantly more round than the other cell types and have a lower axial ratio as shown in Figure 2.12A and 2.12B.

Clusters of cells, i.e., cells that are in close contact with one another, are identified as Texas red labeled objects containing more than one DAPI-labeled nucleus. When comparing the number of nuclei per cell object after 24 and 48 hours in culture, the dolphin and the bovine lung cells show a clustering behavior that is not present in the human umbilical vein endothelial cells. At 24 hours the percentage of cells forming clusters was between 20% and 30% for all the cell lines, while at 48 hours almost 90% of the dolphin cells and 55% of the bovine cells formed clusters, and only 31% of the human and mouse cells were clustered together (Figure 2.13). The ability of cells to form clusters may indicate that the cells have low migration rates and do not move away from each other after division. Differences in clustering appear to be a characteristic that distinguishes dolphin cells from the other cell lines, and may be consistent with the “a cobblestone-like morphology” used to describe endothelial cells [209,210].

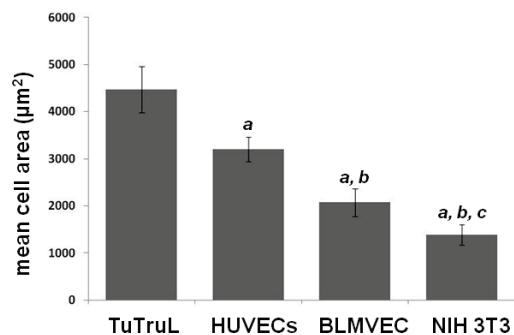


FIGURE 2.10 Average spread area of 4 different cell lines.

Cell area values were determined from Texas-red staining and are a mean of 6 replicates (cell data collected from 100 fields/replicate). TuTruL, dolphin lung endothelial cells; HUVECs, human umbilical vein endothelial cells; BLMVEC, bovine lung microvascular endothelial cells; NIH 3T3, mouse fibroblast. Error bars represent the standard deviation between 6 replicate measurements. Letters (*a*, *b*, *c*) indicate statistical differences between data sets using Student's *t*-test at ($P > 0.05$). *a*, cell line areas statistically different from TuTruL; *b*, cell line areas statistically different from HUVECs; *c*, cell line areas statistically different from BLMVECs.

TABLE 2.8. Cell areas measured for 4 different cell lines.

REPLICATE NO.	TuTruL	HUVECs	BLMVEC	NIH 3T3
1	2534.11	1939.02	1001.324	780.83
2	1992.70	1487.66	1449.158	721.49
3	2694.32	1773.74	1040.58	628.24
4	2295.67	1795.15	1183.965	931.33
5	2796.36	1876.36	1191.59	925.51
6	2624.21	1848.36	1069.457	651.80
Average (pixels)	2489.56±271.00	1786.72±44.17	1156.01±162.93	773.20±120.20
Area (μm²)	4470.26±487.6	3208.23±259.87	2076.74±293.55	1388.36±215.83

Cell area values were determined from Texas-red staining and are a mean of 6 replicates (cell data collected from 100 fields/replicate). Area measurements were obtained by transforming pixel data (pixel*1.7956). TuTruL, dolphin lung endothelial cells; HUVECs, human umbilical vein endothelial cells; BLMVEC, bovine lung microvessel endothelial cells; NIH 3T3, mouse fibroblasts.

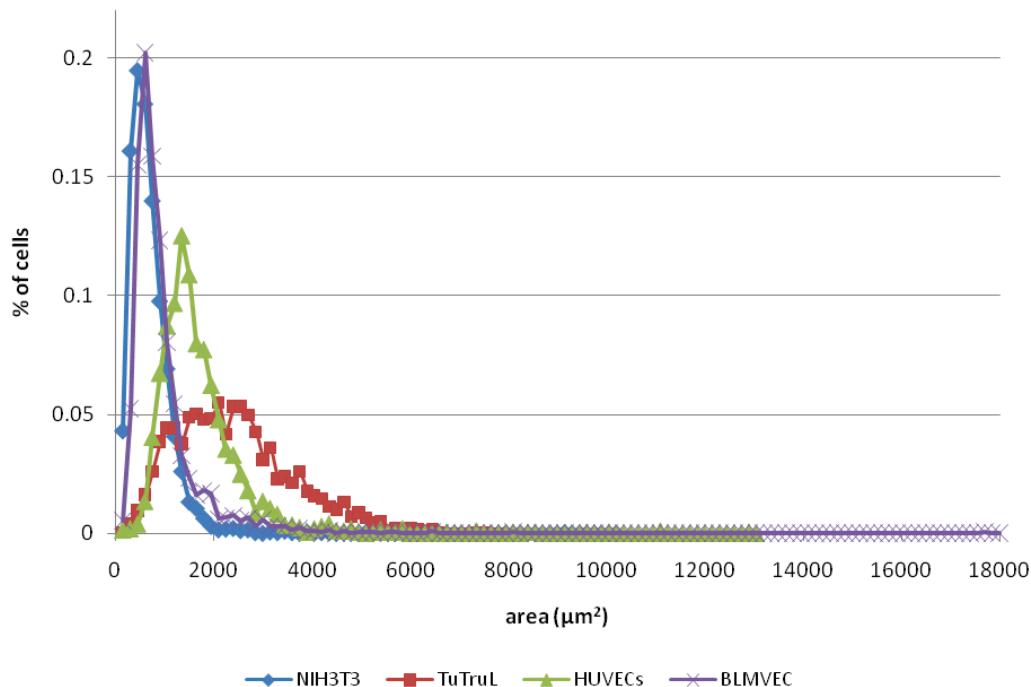


FIGURE 2.11 Distribution of cell areas for 4 different cell lines.

Cell area values were determined from Texas-red staining and are a mean of 6 replicates (cell data collected from 100 fields/replicate). TuTruL, dolphin lung endothelial cells; HUVECs, human umbilical vein endothelial cells; BLMVEC, bovine lung microvascular endothelial cells; NIH 3T3, mouse fibroblasts.

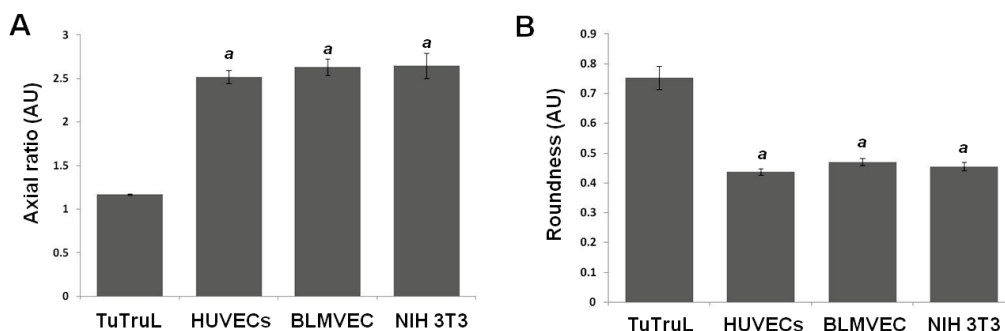


FIGURE 2.12 Average spread areas and roundness of 4 different cell lines.

Mean and standard deviation of axial ratio (**A**) and roundness (**B**). Values are the mean of 6 replicate wells (cell data collected from 100 fields/replicate). Total number of cells was 3,315 for TuTruL, dolphin lung endothelial cells; 2,541 for HUVECs, human umbilical vein endothelial cells; 3,016 for BLMVEC, bovine lung microvessel endothelial cells; 4,083 for NIH 3T3, mouse fibroblasts. Error bars represent the standard deviation between 6 replicate measurements. Letters (*a*, *b*, *c*) indicate statistical differences between data sets using Student's *t*-test at ($P > 0.05$). *a*, cell line areas statistically different from TuTruL.

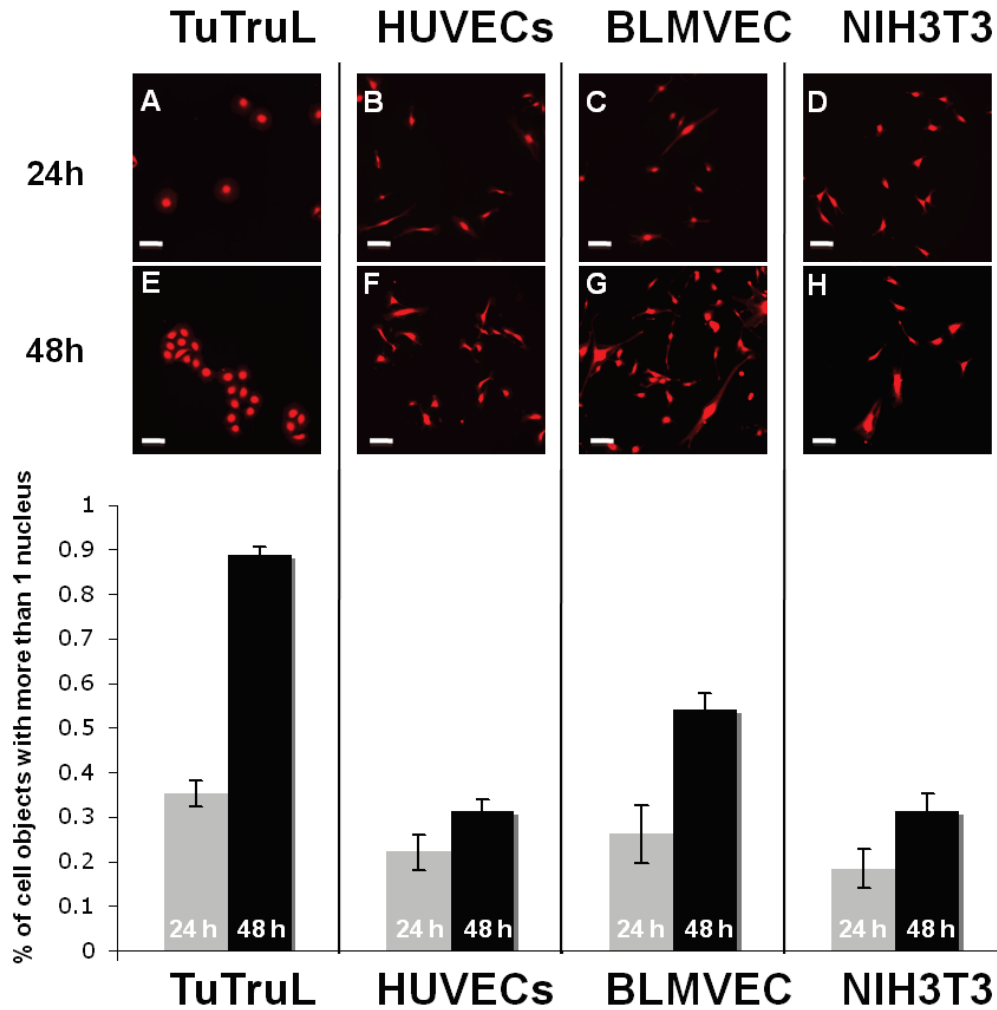


FIGURE 2.13 Cell clustering after 2 days in culture.

Texas-Red-maleimide staining of dolphin lung endothelial cells (TuTruL) at 24h (A) and 48h (E); human umbilical vein endothelial cells (HUVEC) at 24h (B) and 48h (F); bovine lung microvessel endothelial cells (BLMVEC) at 24h (C) and 48h (G); mouse fibroblasts (NIH 3T3), at 24h (D) and 48h (H). Scale bar = 100 μ m for A-H (top panel). DAPI staining was used to count nuclei after 24 hours (grey bars) and 48 hours (black bars). Values are the mean and standard deviation of 6 replicate wells (data collected from 100 fields/replicate). Total number of cells was 3,315 at 24h and 6,914 at 48h for TuTruL, dolphin lung endothelial cells; 2,541 at 24h and 3,578 at 48h for HUVECs, human umbilical vein endothelial cells; 3,016 at 24h and 9,975 at 48h for BLMVEC, bovine lung microvessel endothelial cells; 4,083 at 24h and 12,232 at 48h for NIH 3T3, mouse fibroblast (bottom panel).

2.4.1.2 VOLUME DISTRIBUTION AND GROWTH RATE CALCULATION

We also assessed cell volume distributions to estimate the growth and division properties of the cultures. One relatively easy way of assessing cell lines is to measure cell volumes using an electronic cell particle counter, which determines the volume of each cell by an impedance change that occurs as the cell moves through an orifice. This can be performed during counting of cells for cell passaging. Cells in the population display a range, or distribution, of volumes, as shown in Figure 2.14. The distribution of volumes can be highly reproducible, and appears to be characteristic of a particular cell line in culture. Figure 2.14 shows the distributions of dolphin cell volumes at passage 6 and at passage 10 for 3 different frozen stocks of cells. The stocks were thawed temporally spaced but the cells were grown under the same culture conditions (described in Methods). The data were analyzed by comparing the mean of each measurement set to one another using the “maximum residual test” (the Grubb’s test) to detect outliers in a univariate data set [211]. Volumes are statistically identical to one another both with respect to comparison of passage 6 and passage 10 and when comparing different stocks at the same passage number ($P > 0.05$). The similarity of the volume distributions observed after subsequent passages of the culture suggest that the distribution is stationary, that is, it is the same when measured at different times [212]. A model developed in our laboratory describes the distribution of cell volumes as resulting from the fact that cells in a continuously growing population in culture are at different positions in the cell cycle, and the particular distribution observed is a function of growth rates and division times for cells in that population [212]. Volume growth rates and division times are complex characteristics of cells, in that many intracellular events and culture conditions can affect them. Because of this, such a metric is likely a valuable

indicator of the metabolic state of cells and provides inference as to the genetic stability of the culture.

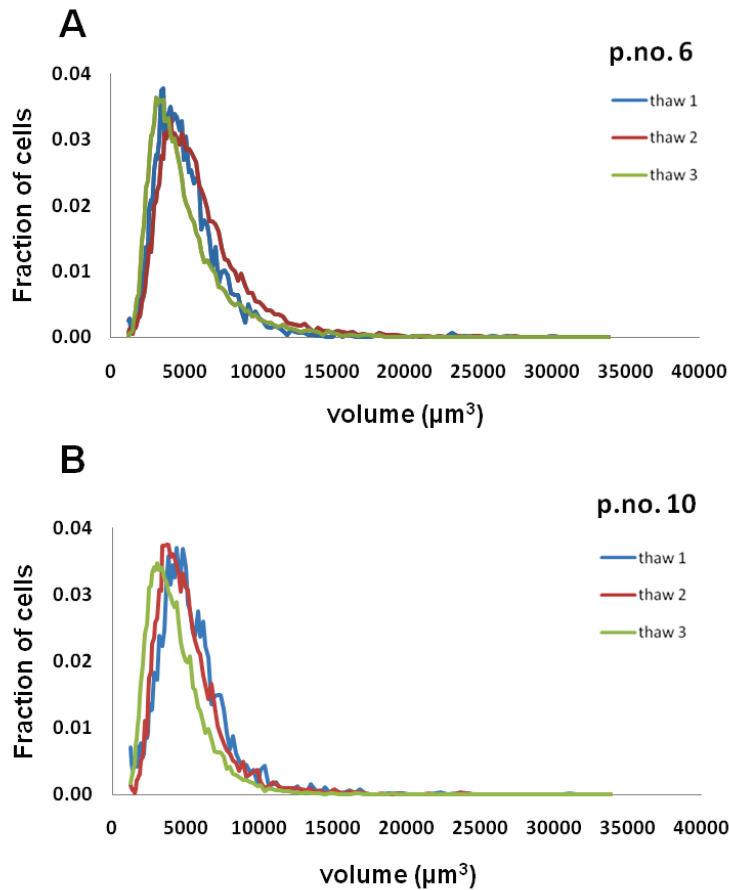


FIGURE 2.14 TuTruL volume distribution data from different starting stocks.

Dolphin volume distribution data collected from Coulter analyzer representing 3 different frozen stocks at relative passage 6 (A, top) and passage 10 (B, bottom) (actual passage nos. 22 and 26). The total number of cells measured was 25,340 at passage 6 and 19,342 at passage 10. Distribution data from frozen stock 1 is represented in blue, distribution data from frozen stock 2 is represented in red and distribution data from frozen stock 3 is represented in green.

These data suggest that the distribution of cell volumes within this population of cells is a characteristic of the cell line. This idea is further borne out by comparison of dolphin cell volumes with those of the other species examined. The data in Figure 2.15 show that each of the four cell lines has distinct volume distributions under the culture conditions used. For

each of the cell lines, the range of cell volumes appears not to change significantly over 6 early consecutive passages ($P>0.05$). The dolphin (TuTruL) cells have an average volume of $5247 \pm 254 \mu\text{m}^3$, the HUVECs and BLMVEC are almost half of the dolphin's cell volume ($2922 \pm 224 \mu\text{m}^3$ and $2606 \pm 349 \mu\text{m}^3$, respectively), and the NIH 3T3 cells have a smaller volume of $2201 \pm 62 \mu\text{m}^3$ (Table 2.9). The total number of cells measured over 6 early consecutive passages was 33,792 for the dolphin cells, 45,459 for the human cells, 69,208 for the bovine cells and 68,180 for the mouse cells. The population doubling time (PDT) was calculated for each cell line during 4 days in culture (see Methods), and the measured volume distributions were fit to the model with 2 adjustable parameters to estimate the average growth rate, and the variance of growth rates, of the cells in the cultures. The PDT calculated for the cell lines were 41 ± 4 hours for the TuTruL, 52 ± 2 for the HUVECs, 19 ± 2 for the BLMVEC and 21.3 ± 0.5 for the NIH 3T3 (Table 2.9). The estimated growth rate for the TuTruL cells ($88 \pm 13 \mu\text{m}^3/\text{hr}$) is statistically equivalent to the BLMVEC and NIH 3T3 cells ($77 \pm 9 \mu\text{m}^3/\text{hr}$ and $71 \pm 2 \mu\text{m}^3/\text{hr}$, respectively) and larger than that for the HUVEC cell lines ($37 \pm 4 \mu\text{m}^3/\text{hr}$). The HUVECs appeared to be significantly slower growing under these culture conditions. These data are shown in Table 2.9.

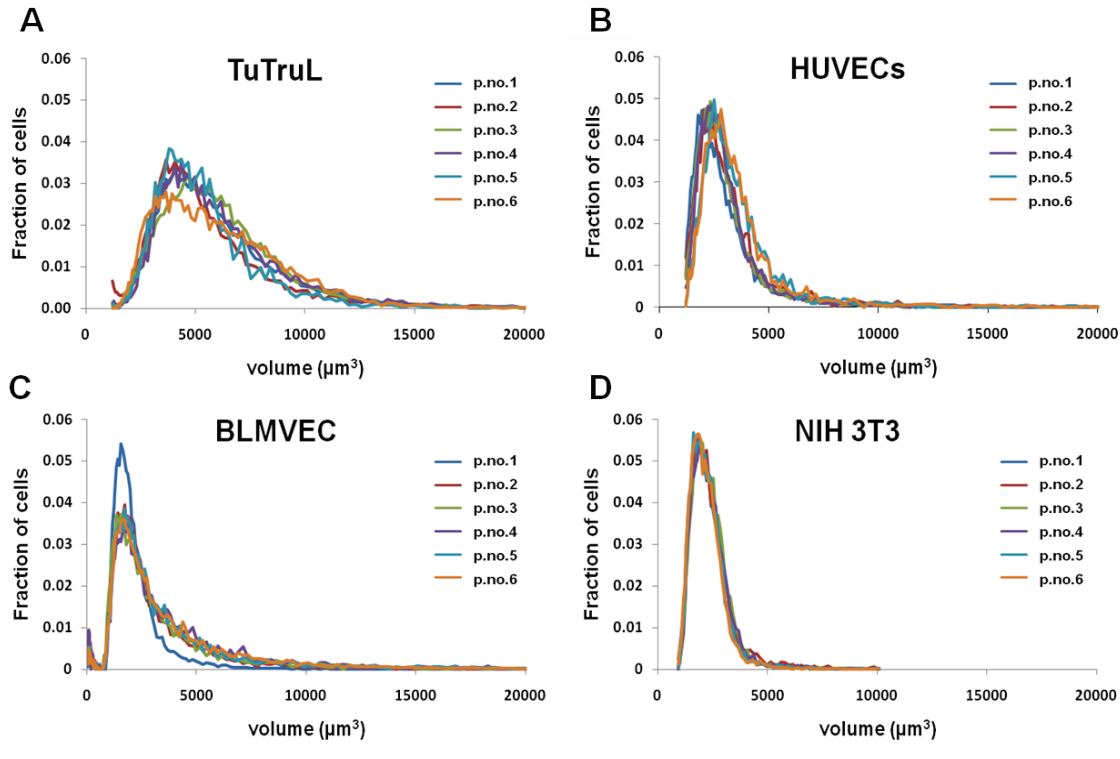


FIGURE 2.15 Cell volume distribution data of 4 different cell populations over the first 6 passages in culture.

A, Dolphin lung endothelial cells, TuTruL, B, human umbilical vein endothelial cells, HUVECs, C, bovine lung microvessel endothelial cells, BLMVEC and D, mouse fibroblast, NIH 3T3. Volume data were collected from a Coulter analyzer and represent 6 consecutive passages of each culture after thawing. Each curve represents the distribution of cell volumes within that population of cells at that passage number. The total number of cells measured was 33,792 for TuTruL, 45,459 for the HUVECs, 69,208 for the BLMVEC and 68,180 for the NIH 3T3. Colors blue, red, green, purple, light blue, orange, correspond to relative passages nos. 1, 2, 3, 4, 5 and 6 (actual passage nos: TuTruL, 17-22; HUVECs, 16-21; BLMVEC, 2-8; NIH 3T3, 11-16).

TABLE 2.9 Volume and population doubling time data for the 4 cell lines used in this study.

CELL LINE	VOLUME (μm^3)	POPULATION DOUBLING TIME (hours)	VOLUME GROWTH RATE ($\mu\text{m}^3/\text{hour}$) ^a
TuTruL	5247 \pm 254	41 \pm 4	88 \pm 13
HUVECs	2922 \pm 224	52 \pm 2	37 \pm 4
BLMVEC	2606 \pm 349	19 \pm 2	77 \pm 9
NIH 3T3	2201 \pm 62	21.3 \pm 0.5	71 \pm 2

Cell volume data were determined using a Coulter counter (Multisizer 3; Beckman Coulter, Fullerton, CA). Volume versus frequency data was obtained by rescaling the diameter versus frequency data within each of the Multisizer 3 files using Excel (Microsoft Corp., Redmond, WA). TuTruL, dolphin lung endothelial cells; HUVECs, human umbilical vein endothelial cells; BLMVEC, bovine lung microvessel endothelial cells; NIH 3T3, mouse fibroblasts. The ‘Volume (μm^3)’, ‘Population doubling time (hours)’, and ‘Volume growth rate ($\mu\text{m}^3/\text{hour}$)’ were computed as described in the Methods using data from six consecutive passages for each cell line. The volumes, population doubling times and volume growth rates are reported as mean \pm standard deviation (n=6).

^a The ‘Volume growth rate’ refers to the average rate at which a cell increases in volume throughout the cell cycle.

Cells in culture can change due to accumulation of genetic errors, senescence, differentiation, or changes in culture conditions. However, while changes in cultured cells are often observed, they are rarely if ever quantified. Volume measurements are a useful indicator of changes in a cell culture. Evaluation of the volume distributions of dolphin cells in culture over extended passages indicate that they often display a distribution of smaller volumes, suggesting that they are dividing more rapidly. Figure 2.16 shows the distribution and the average volumes of early (nos. 1 and 2) and later passages (nos. 23 and 24). The data shown as the first two passages in Figure 2.16 are the same that are shown in Figure 2.15A, where the volume of the dolphin cells does not significantly change for the first 6 passages. However, the volume of dolphin cells was almost halved after 20 passages in culture. On the other hand, the distributions for the other two cell lines analyzed (human and bovine) display

an increase in volume and increase in the PDT with increasing passage number (>8), suggesting a slowing of growth rate with time in culture, which would be consistent with senescence (data not shown). The immortalized NIH 3T3 fibroblast cells do not show significant changes in volume distribution over 20 of passages (data not shown).

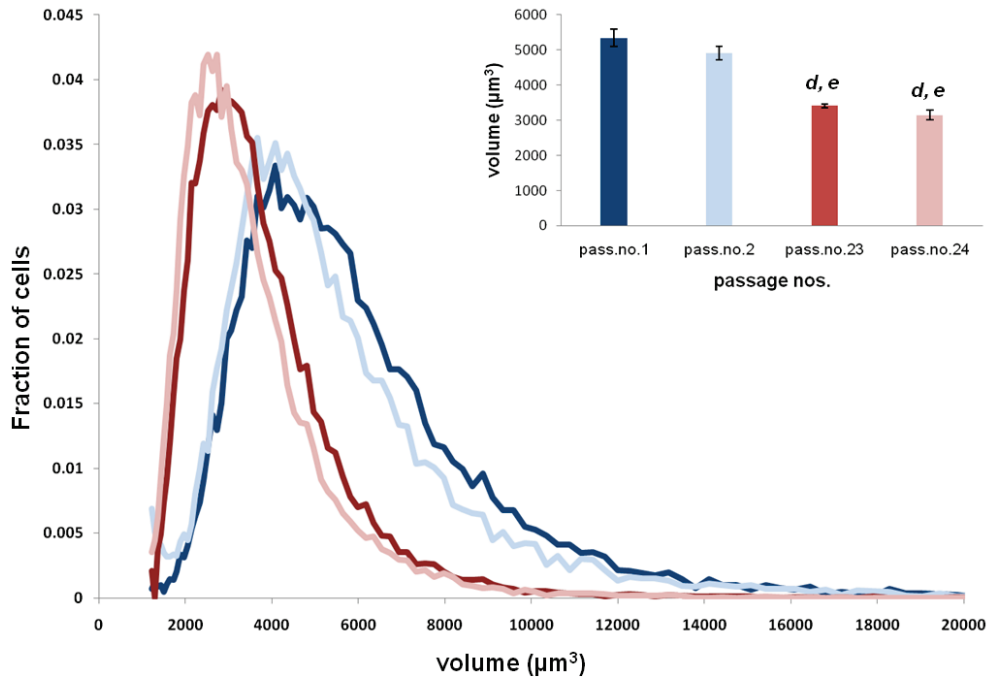


FIGURE 2.16 Cell volume distribution comparison of early and late passages of dolphin lung endothelial cells.

Volume data were collected with a Coulter analyzer and represent early passages (relative passages no. 1 and no.2, blue curves) and late passages (relative passage no. 23 and passage no. 24, light red curves). Data were collected in triplicates at each passage. Each curve represents the distribution of cell volumes within that population of cells at that passage number. The histogram (inset, top right) represents the mean of volume measurements for the 4 passages described. Error bars represent the standard deviation between 3 replicate measurements. Letters (*d*, *e*) indicate statistical differences between data sets using Student's t-test at ($P > 0.05$). *d*, passage no. volume data statistically different from passage no. 1; *e*, passage no. volume data statistically different from passage no.2.

2.4.2 THE DOLPHIN LUNG CELL LINE

In the attempt to further characterize the dolphin primary cell line, we used the quantitative metrics developed to describe the stability of the TuTruL in culture over time. As already discussed in the previous chapter, we observed a decrease in volume over time in culture suggesting more rapid division rates. This was consistent for 3 of the 5 frozen stocks of TuTruL thawed and analyzed; interestingly, for 2 of the stocks analyzed, this change was accompanied by a corresponding change in cell volume and, often, change in morphology.

The cells changed morphology switching from the shape previously described (e.g. round shape) to a “spindly” shape. Figure 2.17 shows the switch from a round morphology at an early passage (passage no. 4, A-C) to a spindly morphology at a later passage (passage no. 29, G-I). At passage 20 (Figure 2.17, D-F) the population was still mixed but the spindly cells had a faster doubling time and quickly became the dominant population. This is reflected in changes of the volume distribution (Figure 2.18A). Figure 2.18 and Figure 2.19 show the volume distributions and the average volumes (insets) of 2 stocks of TuTruL during the first 36 passages in culture when we did observe (Figure 2.18) and when we didn’t observe (Figure 2.19) a differentiation event. The volume decreased in both cases but when we observed a differentiation event, the change in shape morphology corresponded to a dramatic volume decrease at the point where it is possible to identify two population of cells, the original one (passage 1-14) and the spindly one (passage 15-36) (Figure 2.18). The average volume almost halved with the differentiation. During the first 14 passages the volume of TuTruL is $5389 \pm 785 \mu\text{m}^3$ (Figure 2.19). Late passages (passage 30-36) showed an average volume of $3131 \pm 175 \mu\text{m}^3$ consistent with a decrease in volume previously observed and described (Figure 2.16). With the differentiation event, the average volume of

the TuTruL is $5040 \pm 518 \mu\text{m}^3$ for the first 14 passages in culture (Figure 2.18), not significantly different from the average volume of the non-differentiating TuTruL (T test, $P > 0.001$), but at late passages (passage 30-36) the average volume of the spindly cells is $2189 \pm 271 \mu\text{m}^3$.

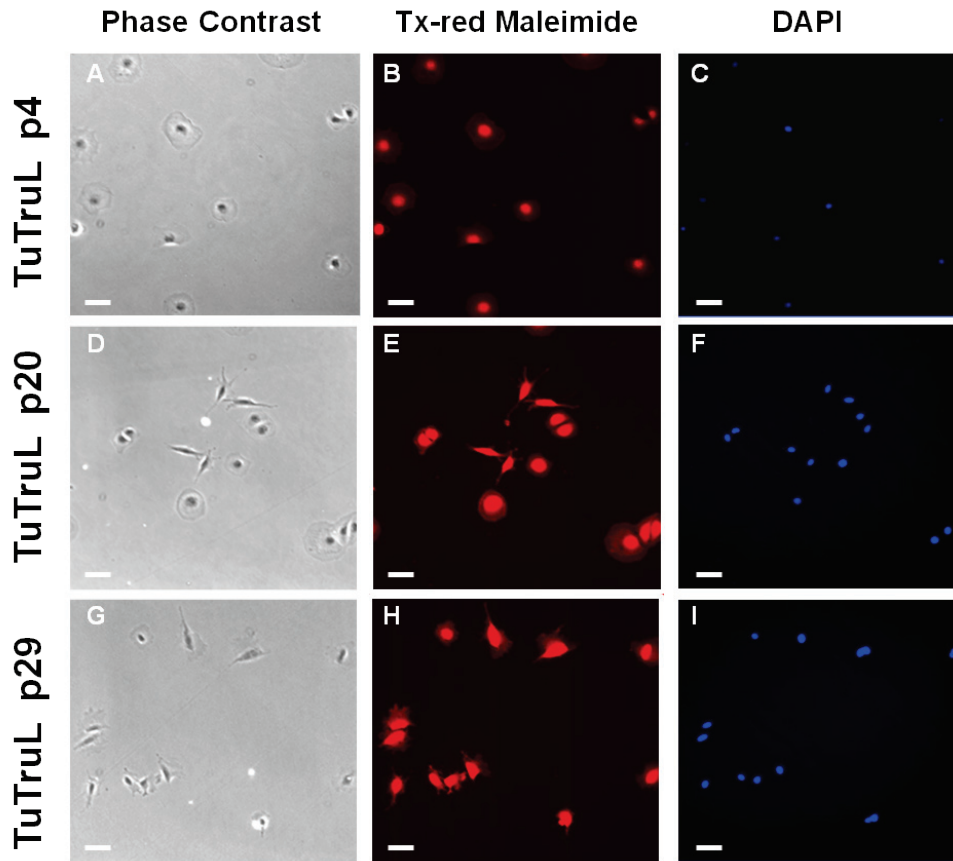


FIGURE 2.17 Phase contrast and fluorescence (Texas-red Maleimide and DAPI staining) microscopy images of TuTruL during early and late passages showing a differentiation event. Cells were seeded at 1000 cells/cm^2 and fixed 24 hours after seeding for image collection. A-C, TuTruL p4, D-F, TuTruL p20, G-I, TuTruL p29. Scale bar = $100 \mu\text{m}$ for A-I.

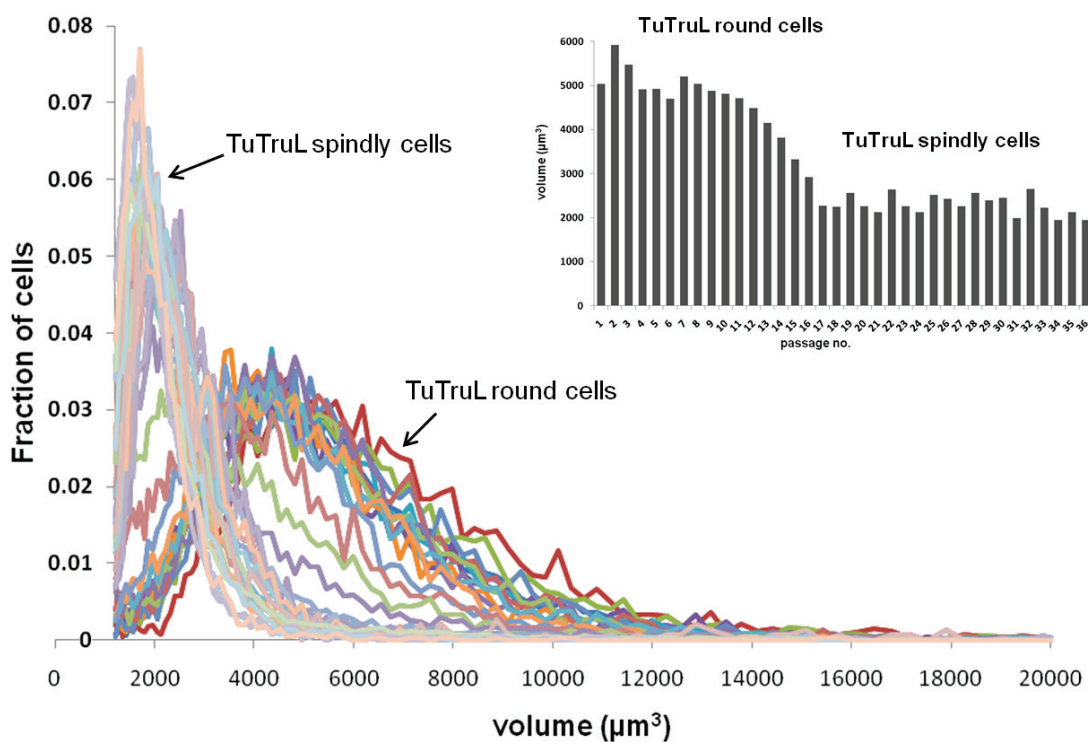


FIGURE 2.18 Cell volume distribution of TuTruL differentiating over time in culture

Volume data were collected with a Coulter analyzer and represent 36 passages in culture. Data were collected in triplicates at each passage. Each curve represents the distribution of cell volumes within that population of cells at each passage number. The histogram (inset, right) represents the mean of volume measurements for the 36 passages described.

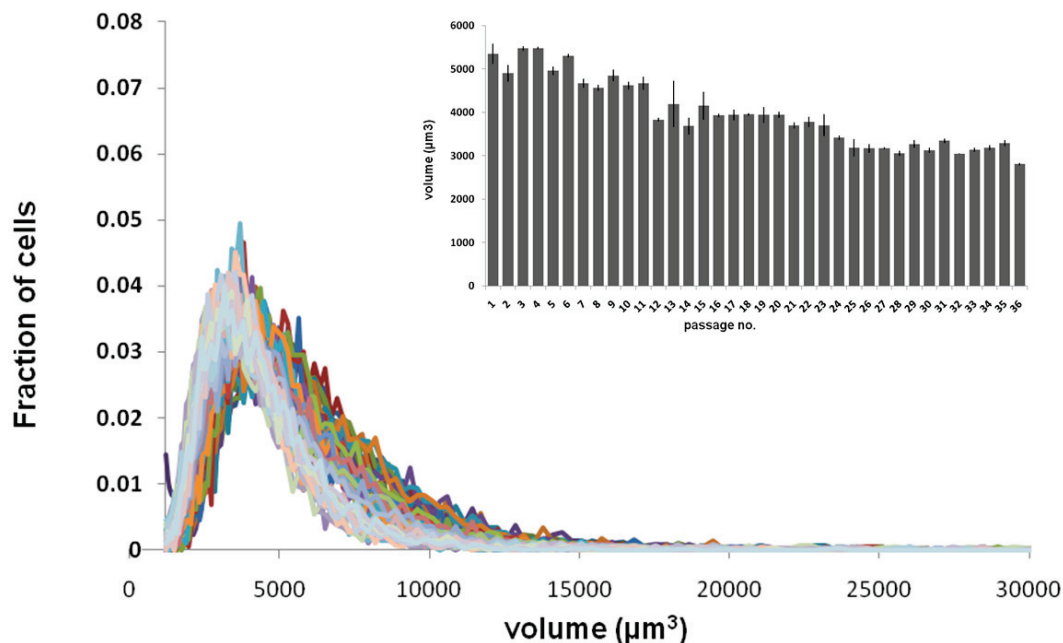


FIGURE 2.19 Cell volume distribution of TuTruL over time in culture.

Volume data were collected with a Coulter counter analyzer and represent 36 passages in culture. Data were collected in triplicates at each passage. Each curve represents the distribution of cell volumes within that population of cells at each passage number. The histogram (inset, right) represents the mean of volume measurements for the 36 passages described. Error bars represent the standard deviation between 3 replicate measurements.

The change in shape was also assessed by morphology analysis, calculating the parameters a) area, b) roundness and c) clustering at 24 and 48 hours using Tx-red Maleimide and DAPI staining to calculate the surface area and the number of cells. The decrease in volume observed (Figure 2.18) is consistent with a decrease in cell area calculated at passage no.4, no. 20 and no. 24 (Figure 2.20A). Like the average volume, mean cell area halved between passage no.4 ($4470.26 \pm 487.6 \mu\text{m}^2$) and passage no.29 ($2037.42 \pm 206.00 \mu\text{m}^2$) (Table 2.10). While getting smaller the cells also lose their round shape (Figure 2.20B).

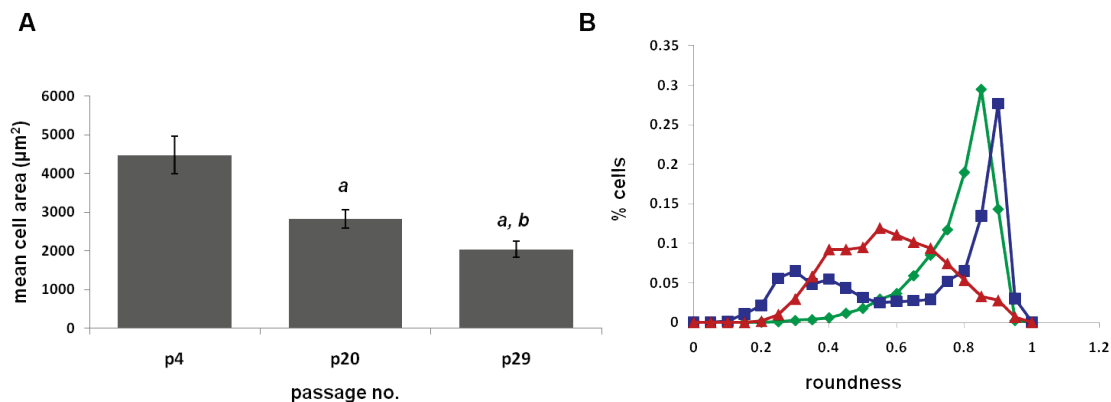


FIGURE 2.20 Average spread area and roundness of differentiating TuTruL at different passage numbers.

Cell area values (**A**) and axial ratio to calculate roundness values (**B**) were determined from Texas-red staining and are a mean and standard deviation of 6 replicates (cell data collected from 100 fields/replicate). (**A**) Letters (*a*, *b*) indicate statistical differences between data sets using Student's t-test at ($P > 0.0001$). *a*, cell areas relative to a passage number statistically different from passage no.4; *b*, cell areas relative to a passage number statistically different from passage no.20. (**B**) green, passage no. 4; blue, passage no. 20; red, passage no. 29.

Table 2.10 Cell areas measured during time in culture for differentiating TuTruL.

REPLICATE NO.	Passage no. 4	Passage no. 20	Passage no. 21
1	2534.11	1673.14	1135.09
2	1992.70	1343.41	1277.75
3	2694.32	1485.52	1173.44
4	2295.67	1637.66	951.73
5	2796.36	1748.07	1026.57
6	2624.21	1572.61	1243.47
Average (pixels)	2489.56 ± 271.00	1576.73 ± 132.37	1134.68 ± 114.72
Area (µm²)	4470.26 ± 487.6	2831.18 ± 237.69	2037.42 ± 206.00

Cell area values were determined from Texas-red staining and are a mean of 6 replicates (cell data collected from 100 fields/replicate). Area measurements were obtained by transforming pixel data (pixel*1.7956).

Clusters of cells (e.g. cells in close contact with one another) were again identified as Texas Red labeled objects containing more than one DAPI-labeled nucleus. When comparing the number of nuclei per cell object after 24 and 48 hours in culture, TuTruL round cells (passage no. 4, Figure 2.20 A-D) present a clustering behavior that is not present in the differentiated TuTruL spindly cells (Figure 2.20 C-F). While at 24 hours the percentage of cells forming clusters was between 35% and 47% for the 3 passages analyzed (Figure 2.20 A, B, C), at 48 hours it was between 87 % and 89% for the TuTruL round cells (passage no. 4) (Figure 2.20D) and for the mixed population (passage no. 20) (Figure 2.20E), while only 60% of the differentiated TuTruL spindly cells clustered together (passage no. 29) (Figure 2.20F).

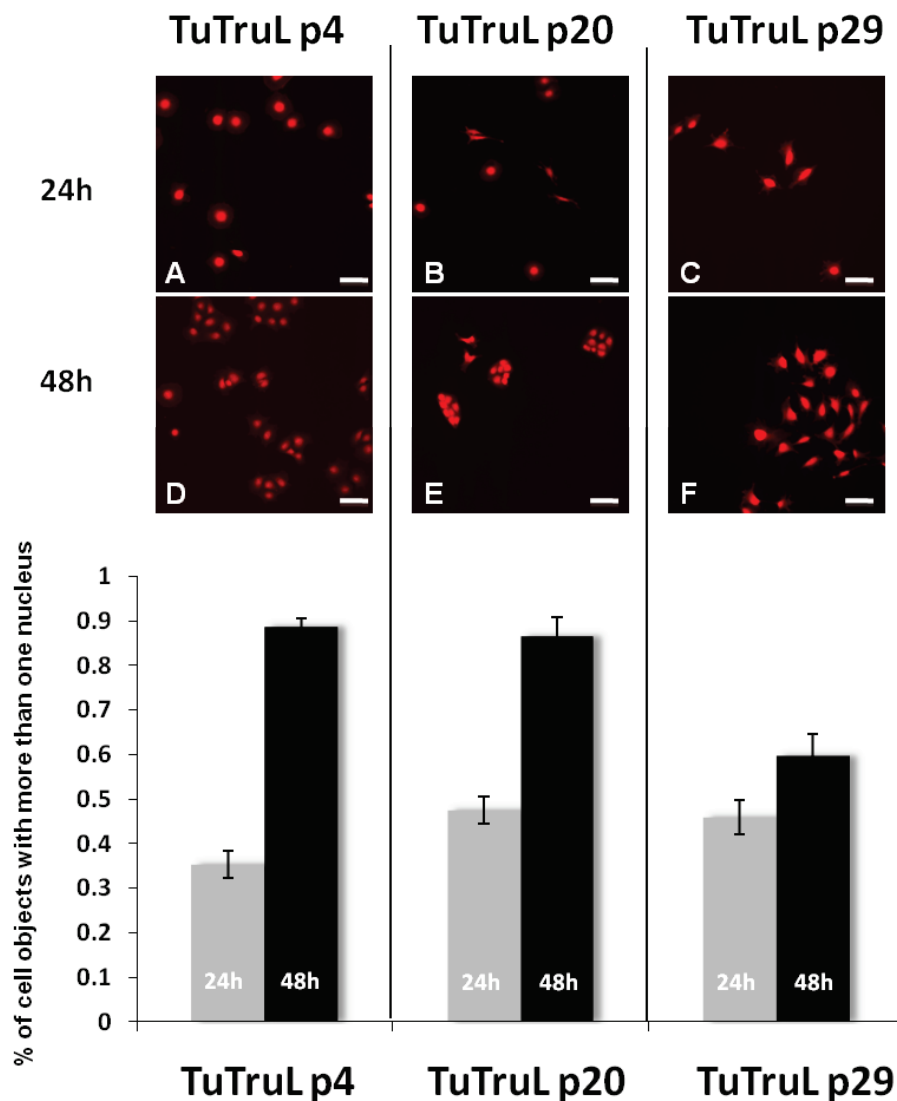


FIGURE 2.21 Cell clustering of differentiating dolphin lung cells after 2 days in culture.

Texas-Red-maleimide staining of TuTruL at passage no. 4 at 24h (A) and 48h (D); TuTruL at passage no. 20 at 24h (B) and 48h (F); TuTruL at passage no. 29 at 24h (C) and 48h (G); Scale bar = 100 μ m for A-F (top panel). DAPI staining was used to count nuclei after 24 hours (grey bars) and 48 hours (black bars). Values are the mean and standard deviation of 6 replicate wells (data collected from 100 fields/replicate). Total number of cells was 3,315 at 24h and 6,914 at 48h for TuTruL at passage no. 4; 3,555 at 24h and 7,272 at 48h for TuTruL at passage no. 20; 2,364 at 24h and 4,506 at 48h for TuTruL at passage no. 29 (bottom panel).

In the attempt to identify how the differentiation event starts, the TuTruL cells (before differentiation) were cultured in an incubator (temperature and humidity controlled) mounted on an inverted microscope with automated stage and CCD camera and imaged for 3 days every 15 minutes. Although we were not able to film a successful differentiation event, we were able to identify events that may have originated a spindly cell from round cells. Figure 2.22 shows 15 snapshots (of 335 total) where a round cell (Figure 2.22, blue arrow, image 1) divides twice. Of the 4 cells, one of them (Figure 2.22, red arrow, image 7-15) is a spindly cell. In this case, the spindly cell dies after the attempt to divide (Figure 2.22, red arrow, image 12-15). This likely describes how a spindly cell can be generated.

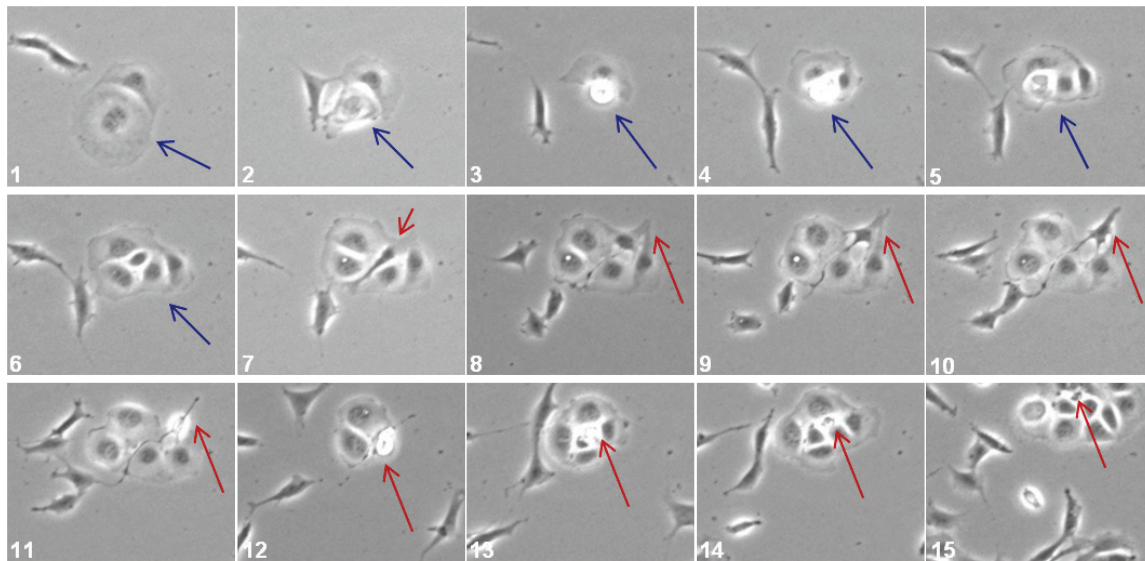


FIGURE 2.22 Differentiation of a spindly cell from a round TuTruL cell.

Phase contrast images were selected from 335 snapshots summarizing 3 days of imaging: 1=74, 2=84, 3=89, 4=102, 5=107, 6=115, 7=130, 8=138, 9=144, 10=149, 11=156, 12=161, 13=185, 14=223, 15=335, respectively. Blue arrows, round cell before (1,2) and during (3-6) division. Red arrows, spindly cell before division (8-10), during division (11,12) and dead (13-15).

The differentiation event of endothelial cells observed is consistent with results previously described [213-216] where the morphology changes are identified as endothelial-to-

mesenchymal transition based on the similarity to the better known epithelial-to-mesenchymal transition (EMT) process. EMT is a program of development of biological cells characterized by loss of cell adhesion, repression of E-cadherin expression, and increased cell mobility, characteristic features of cells undergoing proliferation that can be induced by several oncogenic pathways [217,218]. The endothelial-to-mesenchymal transition (EnMT) has been recently discovered and is less understood than the EMT. Researchers refer to it as a “transition” rather than “differentiation” (or “trans-differentiation”) event as the term transformation classically describes oncogenic conversion, while trans-differentiation refers to a phenotypic switch of cells from one differentiated phenotype into another differentiated phenotype. EnMT is an important event in aortic and pulmonary artery development [219]. During an EnMT, endothelial cells lose endothelial characteristics and gain expression of mesenchymal, myofibroblast-like characteristics and expressed α -smooth muscle actin (α -SMA) [219,220].

We tested the expression of α -SMA on both the TuTruL round (passage no. 8 of a non differentiating stock) and spindly (passage no.26 of a differentiating stock) cells and we found that after the “transition” the expression of α -SMA increased (Figure 2.23). We also observed that the expression of α -SMA in TuTruL was 2 times more than in the HUVECs and 4 times more than the BLMVEC, which are human and bovine endothelial primary cell lines (Figure 2.23).

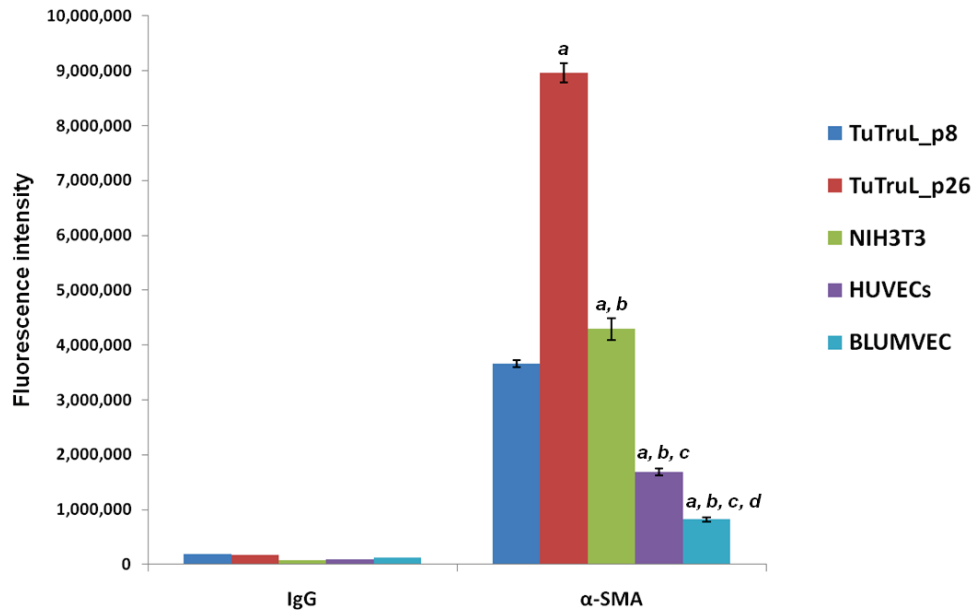


FIGURE 2.23 Expression of α -smooth muscle actin (α -SMA) in different cell types.

Cell area and number of cells values were determined from Texas-red and DAPI staining, α -SMA expression was determined from immunostaining with mouse anti α -SMA primary antibody and goat anti-mouse Alexa-488 secondary antibody. Average fluorescence intensities of Alexa 488 were calculated for α -SMA/cell and are a mean and standard deviation of 3 replicates (cell data collected from 50 fields/replicate). The control, IgG was 1 sample and the data were collected from 50 fields). TuTruL p8, dolphin lung round cells; TuTruL p26, dolphin lung spindly cells HUVECs, human umbilical vein endothelial cells; BLMVEC, bovine lung microvascular endothelial cells; NIH 3T3, mouse fibroblast. Letters (*a*, *b*, *c*, *d*) indicate statistical differences between data sets using Student's t-test at ($P > 0.01$). *a*, cell line α -SMA expression statistically different from TuTruL p8; *b*, cell line α -SMA expression statistically different from TuTruL p26; *c*, cell line α -SMA expression statistically different from NIH 3T3; *d*, cell line α -SMA expression statistically different from HUVECs.

The difference in α -SMA expression, together with the other results presented (e.g. the difference in size, morphology, clustering behavior) on the comparison of the dolphin cells and the endothelial cell types (HUVECs and BLMVEC) analyzed, led us to further investigate the suggested “endothelial” nature of the TuTruL.

2.4.3 ANALYSIS OF LUNG ENDOTHELIAL CELL MARKERS

The endothelium is composed of a thin layer of endothelial cells (EC), which line the interior surface of blood and lymphatic vessels - from the aorta to the smallest capillary. Endothelial cells vary in morphology and functions according to the type and size of the associated vessel. In order to verify the endothelial nature of the dolphin TuTruL cells we repeated the biochemical assay first used to characterize TuTruL [152], e.g. the uptake of acetylated-low density lipoprotein (Ac-LDL). Moreover we tested the expression of 2 adhesion molecules, routinely used as endothelial markers: 1) CD-31, cluster of differentiation 31 also called PECAM-1, platelet endothelial cell adhesion molecule and 2) CD-144, cluster of differentiation 144 also called VE-cadherin, vascular endothelial cadherin.

In the first characterization the TuTruL were identified as dolphin lung endothelial for the positive incorporation of fluorescently labeled Ac-LDL [152]. Ac-LDL is known to be taken up by macrophages and endothelial cells via the "scavenger cell pathway" of LDL metabolism. Ac-LDL is labeled with the DiI, a fluorescent probe (DiI-Ac-LDL) and it has been routinely used to identify endothelial cells [221]. Garrick et al. has shown the uptake of Ac-LDL through imaging of cells after 24hr incubation with 20mg/ml of DiI-Ac-LDL [152]. We repeated this experiment using different concentrations of DiI-Ac-LDL and different time points. We compared the incorporation of DiI-Ac-LDL of TuTruL to other cell lines, used as positive (endothelial, such as HUVECs and BLMVEC) and negative (non-endothelial, such as NIH 3T3 mouse fibroblasts) controls, quantifying the fluorescence intensity of the DiI-Ac-LDL uptake through live flow cytometry. The result of the DiI-Ac-LDL assay was negative for the TuTruL cells (Figure 2.24). Both HUVECs and BLMVEC showed accumulation of Ac-LDL. Given the close phylogenetic relationship between the

dolphin and the cow, the BLMVEC were also used as control for the cross-reactivity of the Ac-LDL, which was of human origin. The dolphin cells, both round and spindly, did not show accumulation of DiI-Ac-LDL like the NIH 3T3, mouse fibroblasts, negative control (Figure 2.24A). We repeated the experiment several times with negative results. The experiment shown in Figure 2.24 was carried out under the same conditions as those used in Garrick et al.; Figure 2.24B shows sample phase and fluorescence sample images of the incorporation of DiI-Ac-LDL in endothelial cells, the HUVECs, compared to that of TuTruL.

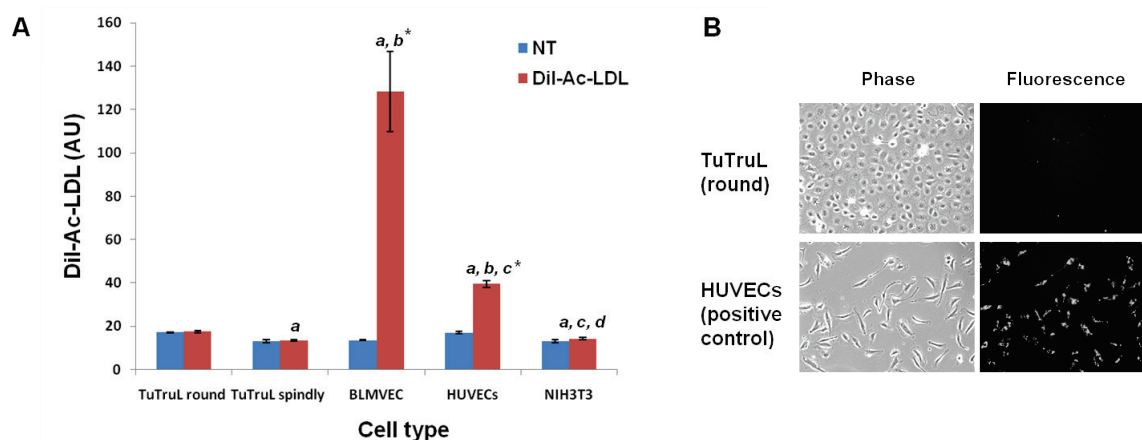


FIGURE 2.24 Fluorescence staining of DiI-Ac-LDL in different cell types.

(A) Cells were labeled with 5 μ g/ml DiI-Ac-LDL and live flow cytometry was carried out after 24hrs incubation. Fluorescence intensity values are a mean of 2 replicate samples/cell type for both untreated (NT, blue) and treated (DiI-Ac-LDL, red) cells. (B) Phase contrast and fluorescence imaging of dolphin cells (TuTruL, round cells) and HUVECs (human umbilical vein endothelial cells) after 4hrs incubation with 5 μ g/ml DiI-Ac-LDL. Letters (*a*, *b*, *c*, *d*) indicate statistical differences between data sets using Student's t-test at ($P > 0.05$). *a*, DiI-Ac-LDL fluorescence statistically different from TuTruL round cells; *b*, DiI-Ac-LDL fluorescence statistically different from TuTruL spindly cells; *c*, DiI-Ac-LDL fluorescence statistically different from BLMVEC; *d*, DiI-Ac-LDL fluorescence statistically different from HUVECs.

(*) indicates statistical difference between the untreated (control) and treated with DiI-Ac-LDL cell lines.

The expression of endothelial cell markers has been investigated through immunostaining and western blot analysis. The antibodies chosen were polyclonal antibodies known for their

cross-reactivity between several species (described in Methods). When available the protein sequence of the antibody was checked and compared to the dolphin sequence for that gene. Results for the immunostaining of both PECAM-1 and VE-cadherin are shown in Figure 2.25. The dolphin cells express PECAM-1 and VE-cadherin at a level not significantly different from the NIH 3T3; the expression for the 2 markers is weak when compared to the HUVECs, endothelial cells and positive control (Figure 2.25A, B). The PECAM-1 expression has also been tested by Western blot and the results confirmed what had been previously observed with the immunostaining (Figure 2.25C). Immunostaining and Western blot analysis were carried out also using different antibodies for the same markers (for both PECAM-1 and VE-cadherin, see Methods) and with another endothelial marker, Von Willebrand factor (vWF). Results were consistent with what was previously shown.

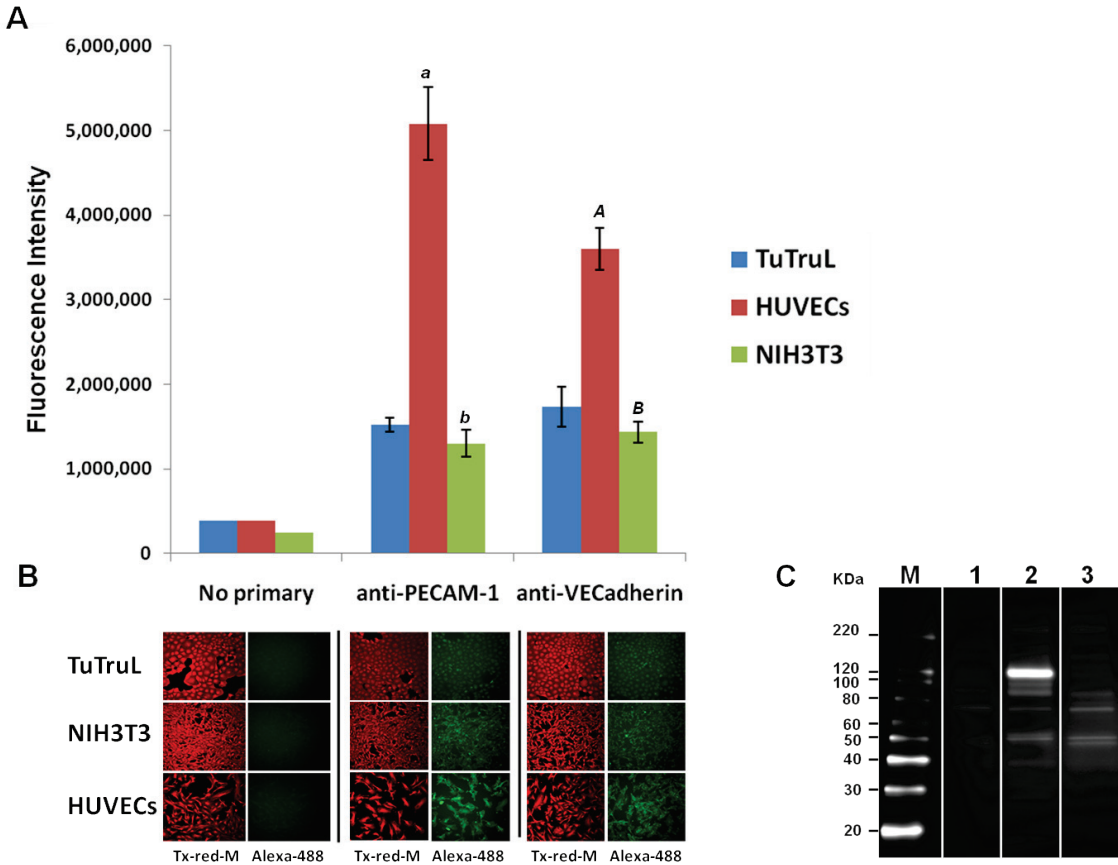


FIGURE 2.25 Expression of PECAM-1 and VE-cadherin in TuTruL, HUVECs and NIH3T3.

(A) Expression of PECAM-1 and VE-cadherin was determined by immunostaining with polyclonal anti-rabbit antibody (1:100) using a fluorescence microscope (see Methods). The quantification of staining intensity of the was determined by intensity of fluorescence/single cell and it represents the mean of 3 replicate samples. Letters (*a*, *b*; PECAM-1; *A*, *B*, VE-cadherin) indicate statistical differences between data sets using Student's t-test at ($P > 0.001$). *a*, *A*, cell line protein expression statistically different from TuTruL; *b*, cell line protein expression statistically different from HUVECs. (B) Texas-red-Maleimide and DAPI (not shown) staining were used to determine cell area values and number of cells (nuclei). Alexa-488 anti-rabbit (1:200) was used as secondary antibody. (C) Western blot analysis for PECAM-1 (~130 kDa) using the anti-rabbit polyclonal antibody used in A (1:100). 1, Marker of molecular weight; 2, NIH3T3; 3, HUVECs; 4, TuTruL.

2.4.4 ANALYSIS OF LUNG EPITHELIAL CELL MARKERS: ALVEOLAR CELLS AND SURFACTANT PROTEIN B

Given the negative results on endothelial cell characteristics, we investigated the nature of the dolphin cells further and tested the hypothesis that the TuTruL cell line was an epithelial cell line.

The mammalian respiratory system represents a complex architecture composed of the lung as well as the conducting airways and respiratory muscles of the thorax. This system can be divided into two functionally and structurally distinct regions, namely the upper and lower airways. Functionally, the upper airway serves to warm, humidify, and filter inhaled air in order to protect the lower tract from infection and damage while the remaining three regions function in gaseous exchange [222]. Associated with each of these regions is a very specific epithelium that changes dramatically in structure from the main bronchi through to the alveolar epithelium of the lower respiratory tract. The alveolar epithelium, which represents the most distal area of the respiratory system, is predominantly comprised of two specialized epithelial cell types, also called pneumocytes: alveolar Type I and alveolar Type II cells. Type I are thin, squamous terminally differentiated Type II cells that form about 93% of the alveolar surface area (33% of alveolar epithelial cells by number) essential for efficient gas exchange. Alveolar Type II cells comprise the remaining 7% by surface area and 67% by epithelial cell number [223]. The considerably smaller cuboidal alveolar Type II cells are confined to the corners of the alveolus and are of special interest in terms of clinical relevance in that their primary physiological function is in the production, secretion, and recycling of pulmonary surfactant [224].

While the majority of surfactant consists of lipids with phosphatidylcholine, about 10% of surfactant consists of proteins, which includes four unique surfactant proteins (SP): SP-A, SP-B, SP-C, and SP-D. SP-A and SP-D are well characterized and represent the crucial hydrophilic proteins involved in the initial interaction, recognition, processing, and subsequent immune response to a wide variety of inhaled pathogens [225-227]. Alternatively, SP-B and SP-C are small, extremely hydrophobic proteins that enhance the transport of lipids into the monolayer and are therefore essential for the regulation of the surface tension in the alveoli during the respiratory cycle [228,229]. SP-C is expressed exclusively by Type II alveolar epithelial cells while SP-A and SP-B are expressed in alveolar Type I cells, subsets of nonciliated cells in tracheal-bronchial glands and cells lining the conducting airways. Thus, surfactant proteins, specifically SP-A, SP-B, and SP-C are useful markers of surfactant synthesis, fetal lung maturation, and the alveolar Type II cell phenotype.

In our laboratory we have previously identified the genomic (and coding) sequences of dolphin surfactant proteins SP-A, SP-B and SP-C (Newton et al., in prep). The sequences of SP-A and SP-C show high sequence homology with those of other mammal (in particular of those mammals belonging to the order of the Artiodactyla) but SP-B has a unique structure. Figure 2.26 shows the genomic organization of dolphin SP-B and the alignment of the mature, secreted form of dolphin SP-B with that of other land mammals. 10 exons encode the SP-B precursor, but only exon 6 and exon 7 encode the mature form. As shown in the alignment, the dolphin secreted SP-B sequence has profound differences compared to land mammals. This difference may result in differential surface activity characteristics

which allow rapid re-expansion of the alveoli after collapse during the dolphin's prolonged dives (Newton et al., in prep).

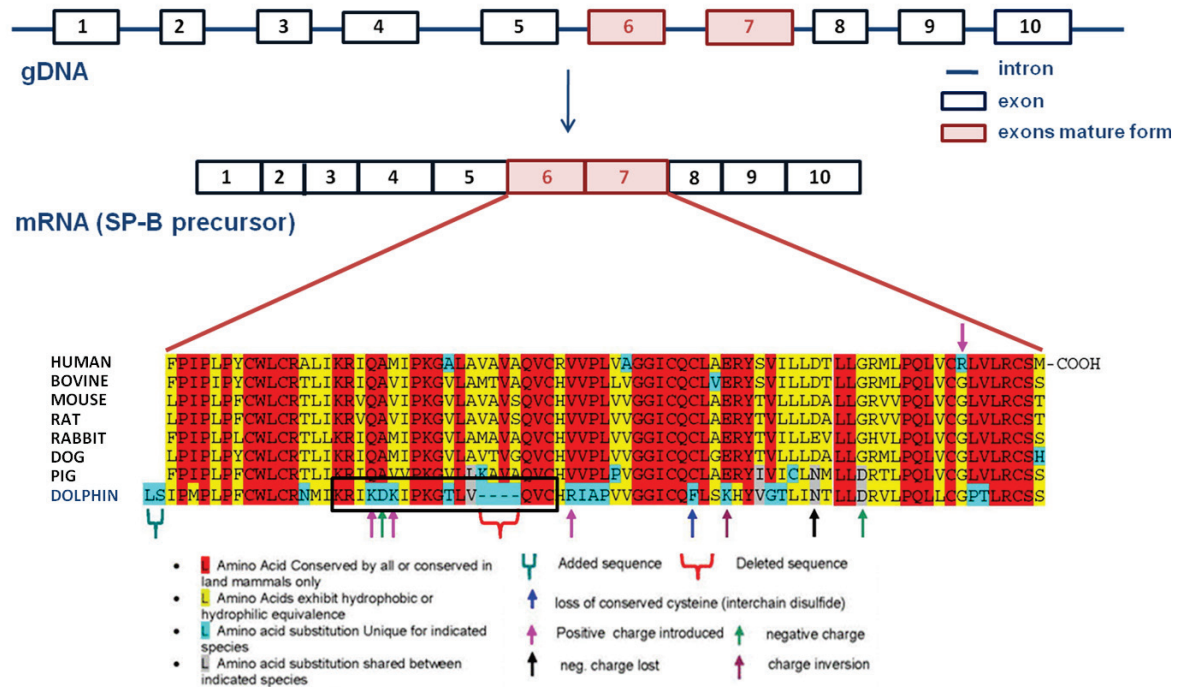


FIGURE 2.26 Dolphin surfactant protein B.

SP-B precursor is coded by 10 exons. The alignment shows a comparison of the mature (secreted) form (exon 6 and exon 7) to that of land mammalian species.

A stretch of 16 amino acids selected in the dolphin SP-B mature form, containing 4 mutations and 4 deletions (KRIKDKIPKGTLVQVC, black box, Figure 2.26) was used for the synthesis of a dolphin-specific antigenic peptide to generate and purify a goat anti-dolphin SP-B antibodies (Ab). The dolphin specific anti-SP-B Ab has been used to detect SP-B in dolphin lung tissue (Figure 2.27A) showing a very high level of SP-B production. The Western blot in Figure 2.27B shows the species-specificity of the dolphin anti-SP Ab which does not recognize human or purified bovine SP-B.

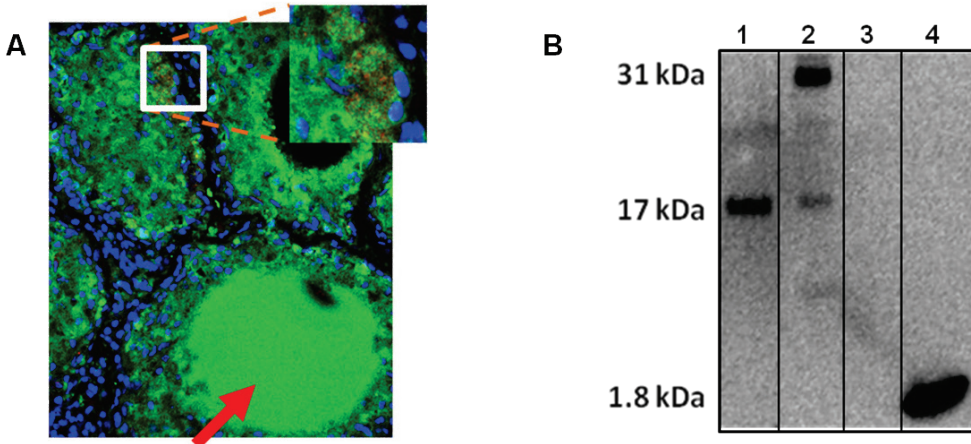


FIGURE 2.27 SP-B expression in dolphin lung tissue.

(A) Immunohistochemical detection of SP-B in dolphin lung tissue, alveoli (inset) and small airways (red arrow, bottom). SP-B, green; nuclei, blue. (B) Western blot analysis of dolphin lung samples SP-B using goat anti-dolphin SP-B Ab on non-denaturing acrylamide gel. 1, Dolphin airway fluid; 2, Dolphin lung cell lysates; 3, Purified bovine SP-B; 4, SP-B antigenic peptide.

We used the dolphin anti-SP-B Ab to test the expression of SP-B on TuTruL. The SP-B expression has been tested on TuTruL cultured in standard medium and in lung epithelial cell specific medium. The standard medium was the HITES culture medium, an RPMI-160 based medium containing glutamine, insulin, transferrin, sodium selenite, hydrocortisone, β -estradiol and fetal bovine serum. The lung epithelial cell medium was the same used for small airways epithelial cells (SAEC) medium, containing bovine pituitary extract, epidermal growth factor, insulin, hydrocortisone, epinephrine, triiodo-L-thyronine, transferrin, retinoic acid and bovine serum albumin (see Methods).

The choice of the SAEC medium to test the epithelial nature of the dolphin lung cells originated from data on epithelial alveolar primary cells that we successfully isolated from a different marine mammal, the pygmy sperm whale (*Kogia breviceps*), and maintained in culture for up to 3 weeks. We developed a new protocol which allows the isolation and immediate freezing of tissues in appropriate cryopreserving medium, during the marine

mammal necropsy. Later, tissue samples can be thawed and digested. The specific cell type can be selected by growing the cells in specific culture condition. Initially, we cultured the pygmy sperm whale cells in both HITES and SAEC media, harvested the cells for RNA extraction and looked at specific marker expression. RT-PCR showed the presence of SP-B in samples cultured with epithelial medium (SAEC) while SP-B was not detectable in pygmy sperm whale cells cultured in HITES medium (Figure 2.28).

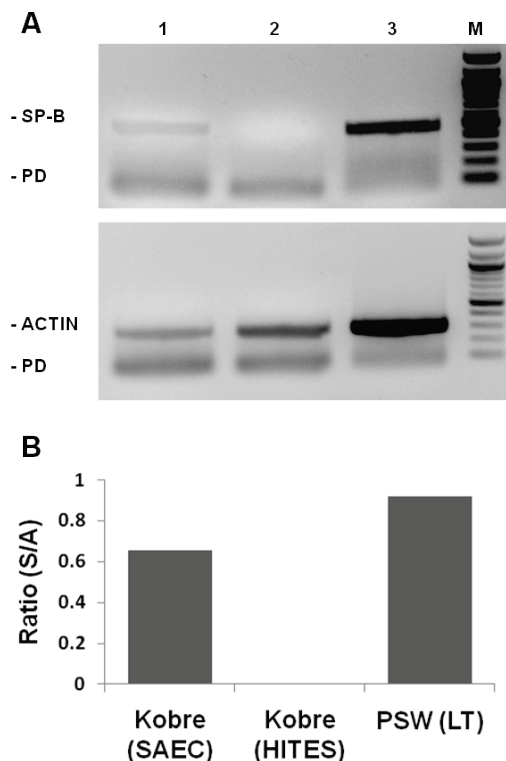


FIGURE 2.28 Whole lung cells cultured in epithelial cell medium favors expansion of alveolar epithelial cells.

Ethidium bromide stained agarose gel of PCR products amplified from pygmy sperm whale primary lung epithelial cells (KobreL) and pygmy sperm whale lung tissue cDNA (PSW LT). Lane 1; PCR products from KobreL cultured in epithelial cell culture medium (SAEC). Lane 2; PCR products from KobreL cultured in endothelial cell medium (HITES). Lane 3; PCR products from pygmy sperm whale lung tissue cDNA. Primers for SP-B (1, 2, 3) and actin (4, 5, 6). M, size marker, 100bp DNA ladder. Histogram represents the SP-B relative expression (data normalized to actin). PD, primer dimer products.

The results of the immunostaining on the TuTruL are shown in Figure 2.29. There is no significant difference between the expression of SP-B in TuTruL cultured in a different medium but when cultured in SAEC medium the number of cells with strong expression is higher (Figure 2.29B).

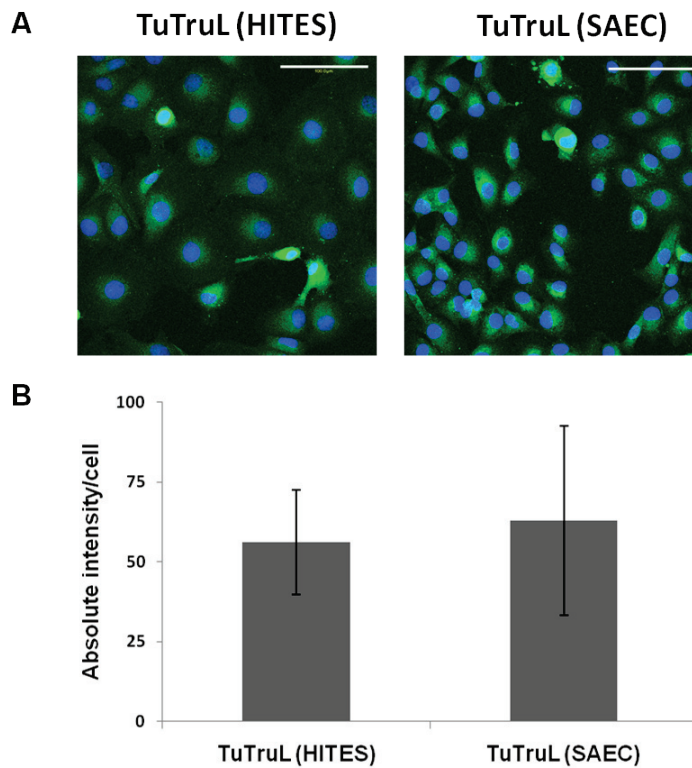


FIGURE 2.29 SP-B expression in TuTruL under different culture conditions.

(A) Confocal micrographs of SP-B stained TuTruL cultured in HITES medium and SAEC medium. Cells were fixed with 4% PFA and stained with goat anti-dolphin SP-B Ab (1:100). Topro3 nuclear stain is showed in light blue. (B) Quantification of SP-B immunostaining/cell after background subtraction. Measurements based on 272 and 234 total cells, for the TuTruL HITES and the TuTruL SAEC respectively.

Moreover, it was interesting to notice that morphology is affected by the culture medium, as TuTruL cells in SAEC medium show a less round shape, consistent with what is expected from alveolar epithelial cells (Figure 2.30).

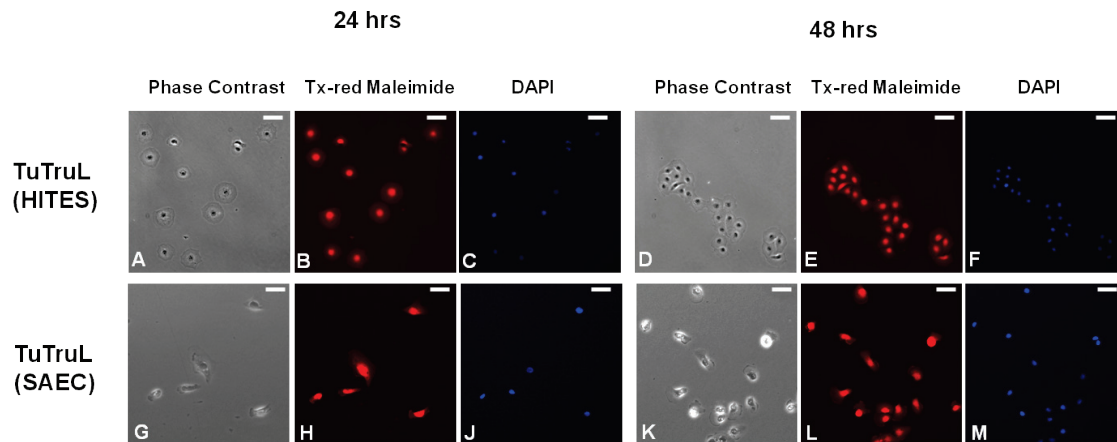


FIGURE 2.30 Phase contrast and fluorescence (Texas-red Maleimide and DAPI staining) microscopy images of TuTruL under different culture conditions.

Cells were seeded at 1000 cells/cm² and fixed 24 and 48 hours after seeding for image collection. A-F, TuTruL (HITES), G-M, TuTruL (SAEC); A-C, G-J, 24 hours; D-F, K-M, 48 hours. Scale bar = 100 μm for A-M.

2.5 DEVELOPMENT OF MARINE MAMMAL PRIMARY CULTURES

So far, only a few cell lines are available to study the mechanisms of marine mammalian biological processes, partly due to the protected status of the animal and/or the stringent federal permits needed to deal with the biological samples. In addition, cell lines often lose some of the characteristics of the primary cells from which they were derived. Necropsies are a good source of samples but most of the time, stranded marine animals are in poor conditions for viable cell/tissue collections.

As discussed in the previous section we have generated alveolar type II primary cells from a stranded pygmy sperm whale (*Kogia breviceps*). The whale was still alive when stranded but the necropsy and the excision of pulmonary tissue were performed 4-6 hours after death (Figure 2.31). After excision of the left lung, a small portion of the pulmonary tissue (~2 cm³) was expanded in cryopreservant, sectioned into 6 pieces and frozen at -80°C (see

Methods). After 1 month, one of the fragments was thawed and digested and the cells (defined as alveolar type II cells by SP-B expression) were selected (Figure 2.32A). After 6 months another fragment of the cryopreserved lung tissue was thawed and cultured in medium optimal for fibroblast expansion (Figure 2.32B).



FIGURE 2.31 Pygmy sperm whale stranded on the beach of South Carolina, USA. (A) Pygmy sperm whale stranded on July 9th, 2009 in Myrtle Beach, SC. (B) Left lung excised during necropsy. Scale bar = 1cm.

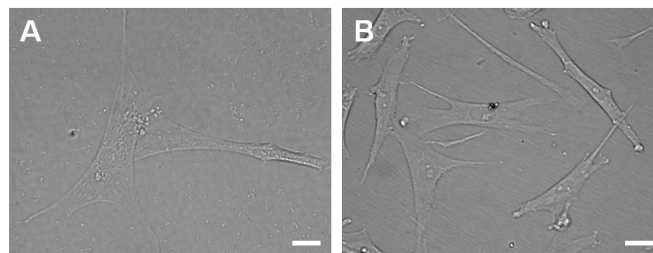


FIGURE 2.32 Phase contrast microscopy images of pygmy sperm whale primary cells. (A) Pygmy sperm whale alveolar type II cells (KobreL) after 3 weeks in culture and (B) pygmy sperm whale fibroblasts (KobreF) after 1 week in culture. Scale bar = 20 μ m.

The approach that we developed is novel and valuable, as we were able to successfully cryopreserve and culture different types of cells from a small fragment of tissue excised from

a dead animal, even months after the animal stranded. The same approach will be taken with dolphin tissues, as soon as the samples become available. The aim is to generate a tissue bank (or biorepository) that will allow researcher to carry out studies when needed, culturing and expanding primary cell types (not cell lines) derived from organs and tissues that may be hypothetical targets of the cause of death, and allow the study of responses to environmental parameters, without limitations in time or availability of samples.

2.6 DEVELOPMENT OF MARINE MAMMAL INDUCED PLURIPOTENT STEM CELLS

Another useful approach to circumvent the limited availability of marine mammalian samples and primary cell types is the development of marine mammalian induced pluripotent stem (iPS) cells, a potentially unlimited source of most primary cell types. Three years ago, 2 groups showed that differentiated human and mouse fibroblasts could be reprogrammed to a pluripotent embryo-like state after introduction and expression of 4 genes (KLF4, OCT3/4 SOX2, and c-MYC; KOSM) [230-232]. After several weeks in culture, the differentiated fibroblast started forming colonies with characteristics similar to human (and mouse) embryonic stem (ES) cells, and with similar differentiation potential [230,231,233]. More recently, iPS cells have been generated from monkey [234], rat [235], and pig [236,237]. The reprogramming of differentiated cells into pluripotent cells is currently widely used as a potential source of most cell types and has many applications from cell-based therapies, toxicology, regenerative medicine, traumatic injuries and genetic diseases [238-243].

We are currently working on deriving iPS cells from dolphin lung epithelial cells (TuTruL) and from pygmy sperm whale lung fibroblasts (KobreF). Dolphin lung TuTruL cells were

infected with KOSM-expressing lentivirus to induce de-differentiation. Lentiviruses are a genus of viruses that can deliver a significant amount of genetic information into the DNA of the host cell and represent a very efficient gene delivery vector. TuTruL cells were infected with pLentG-KOSM lentivirus (see Methods). The successfully infected cells showed the expression of the GFP reporter gene on gelatin coated TCPS within 24-48 hr, (Figure 2.33 and 2.34, respectively). The successfully transfected cells often showed a specific phenotype, losing their flattened shape and adopting a rounded morphology (shown by arrows in Figure 2.33). In one experiment cells were sorted producing 2.5% GFP positive cells (1341 cells) of the TuTruL infected cells (Figure 2.35). Unfortunately, sorted GFP positive cells plated on mouse embryonic fibroblasts (MEFs) often did not readily de-differentiate and maintained their original morphology (Fig. 2.33). One possible explanation for this is that the TuTruL cells are not primary cells, but rather have become a transformed/immortalized cell line. This possibility is supported by their inexhaustible growth capacity (failure to undergo replicative senescence). For this reason, we decided to utilize an established primary cell line, i.e. the KobreF cells.

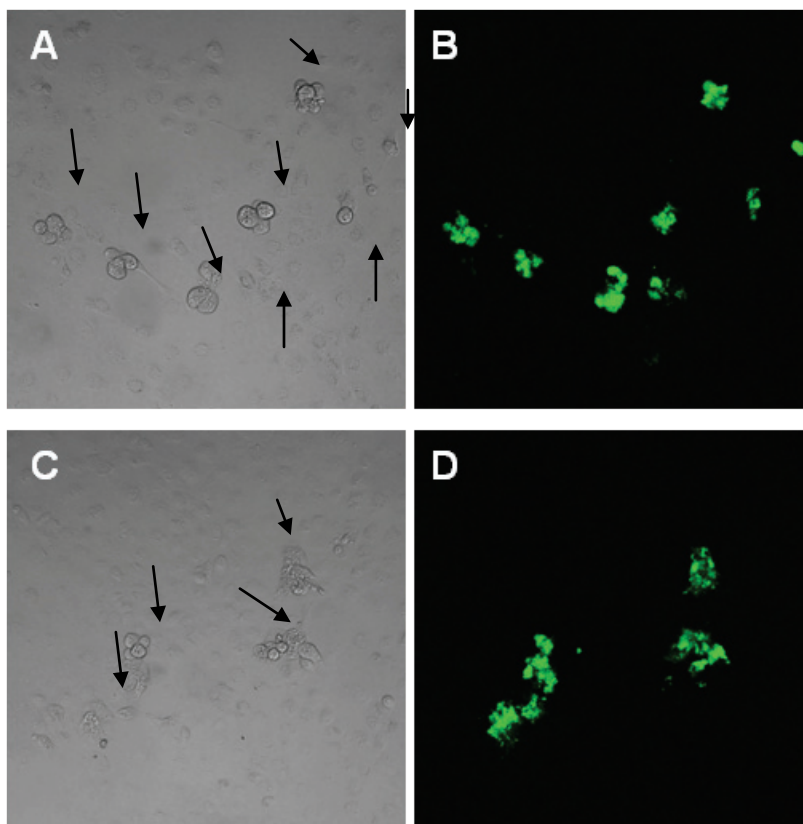


FIGURE 2.33 Expression of GFP in TuTruL cells infected with lentivirus cultured on TCPS 6-well plates. Confocal micrographs of TuTruL 24 hrs after lentivirus infection. A,B and C-D represents 2 different fields imaged. Black arrows in A e C show rounded up TuTruL, corresponding to GFP positive cells. A-C, Bright field images. B-D, GFP fluorescence images.

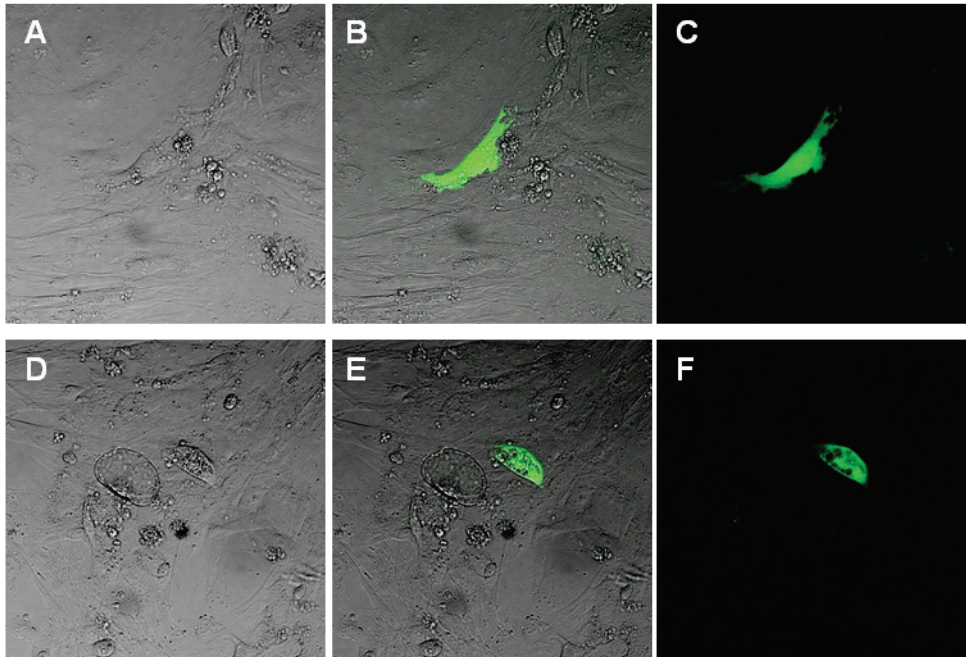


FIGURE 2.34 Expression of GFP in TuTruL cells infected with lentivirus cultured on MEFs. Confocal micrographs of TuTruL 48 hrs after lentivirus infection. A,B,C and D,E,F represents 2 different fields imaged. A-D, Bright field images. B-E, Bright field and GFP fluorescence images. C-F, GFP fluorescence images.

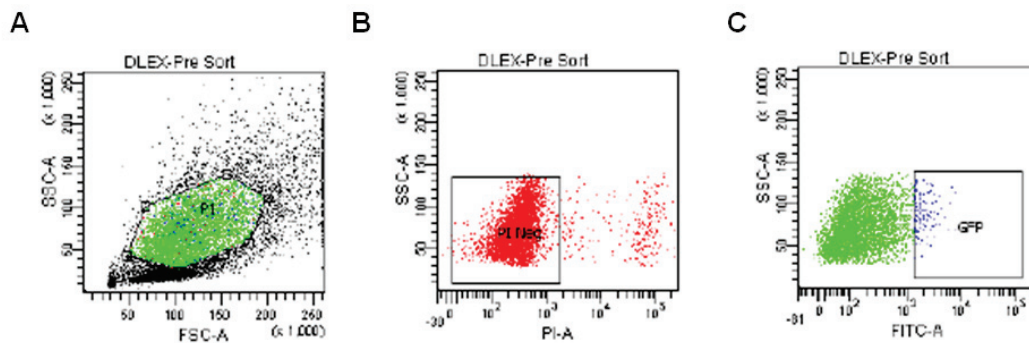


FIGURE 2.35 TuTruL GFP positive sorting results.

Flow cytometer plot of (A) total number of cells from forward (FSC) and side (SSC) scatter measurement, (B) live cells from propidium iodide negative uptake and (C) GFP positive cells from FITC fluorescent signal.

Low passage KobreF, pygmy sperm whale fibroblasts, were infected with pLentG-KOSM (as above), showing high-level GFP expression (Figure 2.36). From cell sorting we observed that 53% of the KobreF cells were GFP positive, producing a total of 1980 cells in one 24 well infection (Figure 2.37). The percentage of GFP positive KobreF cells was almost tenfold higher than that of the control human dermal skin fibroblasts, (data not shown) or of the TuTruL dolphin cell line. The GFP positive cells from the pygmy sperm whale were easily distinguishable from the GFP negative (Figure 2.37C), while in the TuTruL the distinction between the 2 different populations (GFP positive and negative) was not as clear (Figure 2.35C). Subsequent experiments indicated that this enhanced infection/expression may be a reflection of the low passage number of these primary cells.

The GFP positive TuTruL and KobreF cells have been plated on MEFs and Matrigel coated 6-well dishes and we are currently waiting to pick colonies (1-2 weeks) and test the reprogramming efficiency as well as the expression of a broad spectrum of de-differentiating transcription factors.

Once we will have confirmed that the pygmy sperm whale fibroblasts have been genetically reprogrammed to an embryonic stem cell-like state, we will differentiate the iPS cells into specific cell types and characterize their gene expression profiles under normal or experimental conditions (e.g. addition of contaminants or toxins). For example, tissue/cell type specific gene expression patterns obtained from dead/stranded animals will be compared to normal/treated samples. This new approach has the potential to revolutionize our understanding of the basic biology of marine mammals and of the impact of stressors on marine and land animal health.

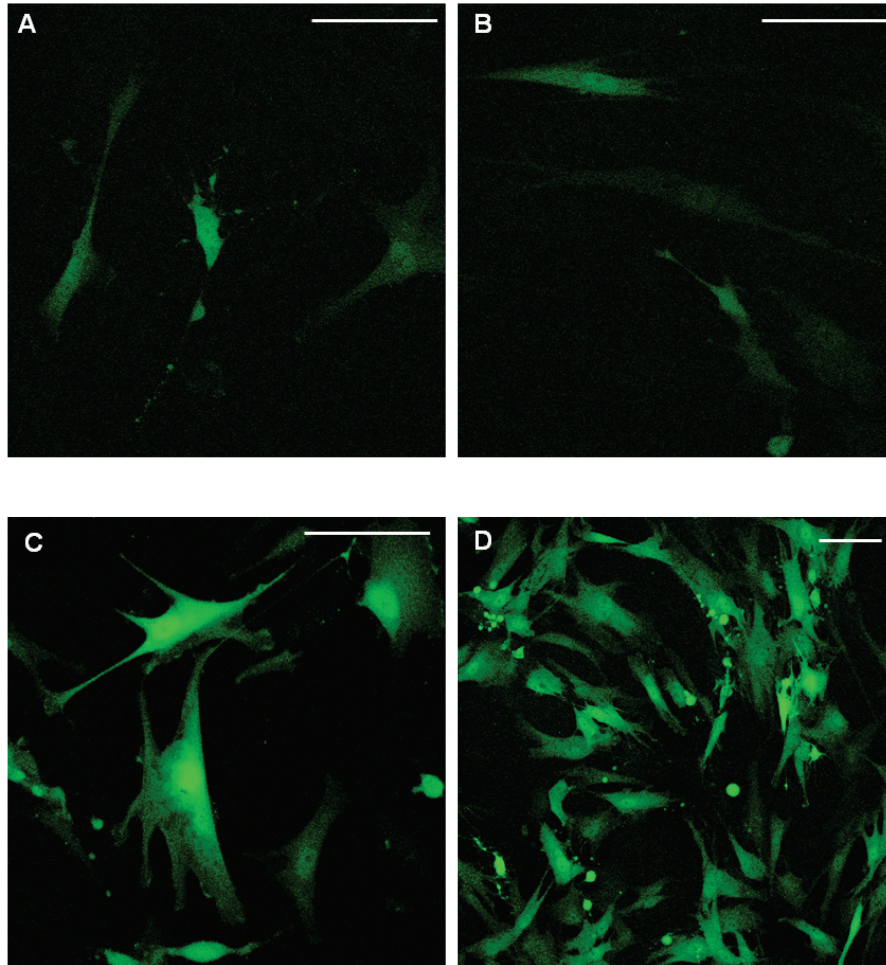


FIGURE 2.36 GFP expression of KobreF after lentivirus infection.

Confocal fluorescent micrographs of KobreF 30 hrs (A, B) and 46 hrs (C, D) after lentivirus infection. Scale bar = 100 μ m.

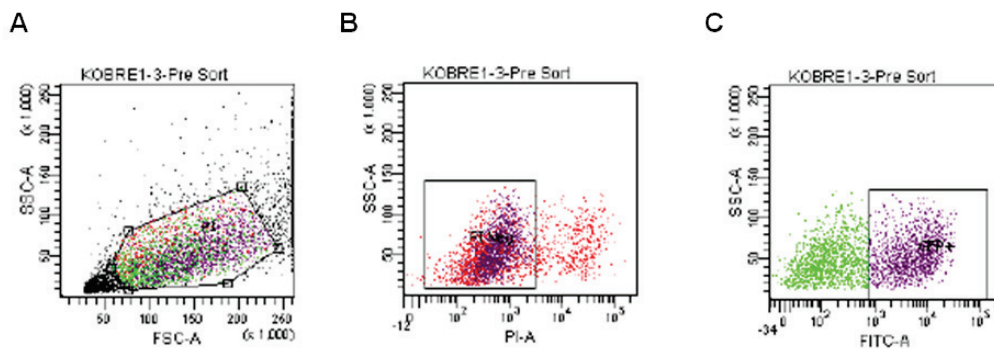


FIGURE 2.37 KobreF GFP positive sorting results.

Flow cytometer plot of (A) total number of cells from forward (FSC) and side (SSC) scatter measurement, (B) live cells from propidium iodide negative uptake and (C) GFP positive cells from FITC fluorescent signal.

3. CONCLUSIONS

CONCLUSIONS

The current status in marine mammal molecular biology methods, specifically in relation to dolphins, remains in its infancy. In order to understand the health of an organism it is necessary to identify biomarkers of the normal and diseased states, which requires not only sufficient genomic, genetic, biochemical and physiological information but also an understanding of the relationship between genes and proteins in the cellular context. The combination of genomics, proteomics and cellomics data is basic to today's molecular biology research. In the study of organisms which also are protected species, like dolphins, these approaches that are capable of sensitive and realtime pictures of environmental impacts (and interactions) of stressors are going to be even more useful. For instance, they can be applied to understand the impact of environmental factors and/or to fully comprehend what threats are posed to dolphin health and to the health of the marine ecosystem. The cetacea (including dolphins) are believed to have evolved from land mammals millions of years ago. The exploration of their genome, both in its coding and non-coding regions, will provide a key to understand the phylogeny and the evolutionary process. Dolphins (and most likely other marine mammals) can be assumed, as a starting point, to share most if not all of the conserved structures and functions (in terms of gene and protein networks) that have a cardinal role in the biological processes of humans, rodents and other terrestrial mammals. It is interesting (but perhaps coincidental) that dolphins have an organization of their nuclear DNA (into 44 chromosomes) which is similar to that of humans.

Dolphins have also adapted to a completely dissimilar environment than that of terrestrial mammals. To aid in swimming they have developed a fusiform body shape; to prevent heat loss, they have developed a thick layer of blubber which provides insulation and also a food reserve and buoyancy. To dive deep, they have developed the capability to collapse their lungs, to reduce their heart rate and the blood flow to the non-essential organs together with increased ability to store oxygen (in both blood and muscle). To find prey, they have developed echolocation by which they emit rapid sound pulses and listen to their echo using the melon on their forehead to focus and direct waves. However, very little is known about the physiology of their unique adaptations to this environment. Furthermore, their position as a top-predator in the food chain, as a result of which they bioaccumulate pollutants and toxins, suggests that they could be an optimum indicator of the health of the coastal marine ecosystem.

In addition to their value as sentinel species of the marine ecosystem, the phylogenetic relationship of cetaceans (including dolphins) to the more extensively studied and more genomically-enabled Artiodactyles such as pigs and cows, offers some unique opportunities at a variety of levels. We can learn from comparative genomics within the Artiodactyl clade about adaptation to a strictly aquatic life style and the demands imposed by this environment on its residents. The cetaceans are not the only phylogenetic group that has made this transition; the list includes also the Carnivora, such as seals, walrus, bears and otters.

The value of molecular techniques for addressing problems in marine biology has only recently begun to be appreciated, and as a result, some of the new technologies are slowly being incorporated into the study of model marine organisms.

The work presented here represents advances in the development and applications of tools for the study of the biology, health and physiology of the dolphin, *Tursiops truncatus*, and their relevance for future studies of the impact of environmental infection and stress.

In particular the focus was 1) on the applications of transcriptomic analysis in wild dolphins and the power of the combination of microarrays studies with machine learning approaches, and 2) on the development and characterization of quantitative metrics to characterize (and develop) cell lines.

3.1 FUNCTIONAL GENOMICS OF THE DOLPHIN

The conservation biology of marine mammals faces many practical problems, prominent amongst which is the difficulty in establishing criteria diagnostic of a healthy normal animal. In order to evaluate the health of wild bottlenose dolphins it is typical to study animals that have been captured and that are then released back into the wild after sampling. We have studied the impact of such capture/release studies on the physiology of the dolphin using measures of gene expression in peripheral blood cells, and shown that changes characteristic of stress and the initiation of an acute-phase response occur.

The induction of the stress responses reported here by the sampling methods themselves has two implications. First, it may complicate the establishment of baseline data for health studies of wild dolphins. Second, the possibility exists that health assessment studies themselves may have an impact on dolphin health or well-being. The second of these implications must be viewed with some reservations as the longer-term impacts of veterinary examination on individual dolphins are unknown. Nevertheless, the present data show clearly a molecular physiological response of dolphins to the stress of veterinary examination. Given

the physiological role of the genes whose expression is altered, it may be appropriate to balance the value of the data generated during capture/release studies against the potential impact on the health of a protected species. These issues deserve further examination with larger and more diverse populations of dolphins.

The use of transcriptomic data for studies of organisms in their natural environment faces many challenges, perhaps the most important of which is the development of appropriate techniques for data analysis. A second problem is that often the full transcriptome has not been characterized for species of ecological and environmental interest, and thus (as in this study) relatively small microarrays must be used. We recognize that recent developments in sequencing technologies are rapidly changing this landscape. Beyond this, a third important problem in the study of protected species, such as dolphins, is the difficulty in obtaining comprehensive, relevant data (such as life-history, genetic and health status information) on the animals that are being studied. Despite these potential problems, we show that a machine-learning approach (ANN) is applicable to the problem of classifying individual animals based on transcriptomic signatures. The dimensionality reduction, which is necessary for any interrogation of transcriptomic data and usually accomplished by linear techniques, can be substantially improved by machine learning approaches which take advantage of the dynamic interdependencies of the components of the transcriptome. This study also shows that, despite a lack of knowledge of the sources or extent of variability in populations of wild dolphins, and the use of a relatively small microarray (that accesses only a small proportion of the total transcriptome), nevertheless accurate classifications reflecting geographic location (determined by the interaction of genetic, disease and environmental factors) could be achieved.

3.2 CELL BIOLOGY OF THE DOLPHIN

Because opportunities for studies on wild and protected organisms such as dolphins are limited, it is critical to have cell lines from these organisms to study as surrogates for the intact animal. Isolated cells are common models for the study of protein functions, cellular mechanisms, organ-specific functions and responses to environmental parameters. Primary cells isolated from tissues typically can be kept in culture for a limited period of time. Conditions must be determined for culturing the cells, such as optimal culture medium and other factors in order to maintain physiological characteristics and viability. The monitoring of cell growth and the characteristics that define their changes is now being accomplished thanks to the development of technologies that enable scientists to look at a living cell in the population but also inside the single cell, gathering information of its behavior in different culture conditions. Specifically, advances in microscopy, image analysis and statistical software over the last few years provide for more accurate assessment of baseline quantitative information needed to understand processes both at a cellular and molecular level.

There is ambiguity in the literature regarding the ‘typical’ characteristics of a given cell line and the sole reliance on visual inspection makes it difficult to describe and compare cell lines across laboratories. Even within a single laboratory, changes can occur in a cell culture, resulting in failure to reproduce data and ambiguity regarding what cell characteristics and responses are ‘correct’. We therefore applied a quantitative approach to several characteristics of dolphin cells in culture, since quantitative evaluations make it easier to accurately and reproducibly compare cells at different times, at different passage numbers,

and in different labs. There are many factors that are important in determining characteristics such as morphology, growth rate, and cell-cell interactions of cells in culture. Such factors include the adhesion matrix, the presence and concentration of growth factors in the medium, the tissue origin and the species and age of the animal from which the cell line was derived. We show here methods that are relatively easy to perform and provide reproducible, high quality, and unambiguous quantitative data on cells in culture comparing cells from three land mammals, cow, human and mouse to cells from a marine mammal, the dolphin. The differences reported for these cell lines may be a function of their species (bovine, dolphin, human, mouse), their tissue of origin (lung, umbilical vein, embryo) and the growth medium (which have been selected for this study in accordance with published data), which include different amounts and sources of serum and added growth factors. The quantitative data presented show that under the culture conditions examined, these cell lines have characteristics that allow them to be unambiguously distinguished from one another, and that changes in these cultures over time can be detected. The data presented here for dolphin cells are particularly important, since very few cell lines of marine mammal origin are available, and the published data and reliable markers for these lines are sparse. We have observed that these cells (dolphin lung primary cells, TuTruL) can occasionally display significant changes over time in culture. We were successful in characterizing these changes by quantifying cell volumes and using volume measurements as a unique identifier for different cell lines.

In the attempt to confirm and authenticate the nature of the cell line used in the quantitative metrics characterization, we used the available biochemical markers, detected by interaction with protein-specific antibodies. The presence or absence of antibody tagging will depend on

protein expression and antibody used. While there are many commercial sources of antibodies (both monoclonal and polyclonal), there are very few commercially available antibodies that are specific to dolphin proteins, so the utility of such antibodies depends on the effective cross-reactivities. The extent to which an antibody prepared against a protein of one species is cross-reactive with a similar protein in other species is dictated by similarity (polyclonal) or identity (monoclonal) of the amino acid (antigenic) sequences of the proteins between species. We tested the cross-reactivity of many antibodies (both mono- and polyclonal), in both western blot and immunocytochemistry analyses, to confirm the endothelial nature of the cell examined. Negative response of the dolphin cells to both biochemical and enzymatic assays, led us to test the hypothesis that the dolphin cells examined were not of endothelial nature. We found a strong expression of SP-B, a lung alveolar cell marker, which led us to the conclusion that the cell line is indeed a lung epithelial cell line.

An important contribution to interpreting the data will be gene expression analysis, and relevant array specific to the dolphin genome is in preparation and will be part of future analysis to better understand the relationships between phenotype and gene expression.

We were also successful in generating primary cultures from cryopreserved lung tissue of a different marine mammal, the pygmy sperm whale, *Kogia breviceps*. One of these cultures, the lung fibroblasts, has also been used to generate induced pluripotent stem cells. Although the results are preliminary and the experiments are still ongoing, the applicability of these methods to the dolphin (and marine mammal field in general) will be extensive.

3.3 FINAL CONCLUSIONS

Compared to human research, marine mammal science is in its infancy. On June 26, 2000, geneticists announced to the world that they had successfully deciphered the human genome. The first complete draft was released in 2003; the human genome contains an estimated 20,000–25,000 protein-coding genes. The ability to measure simultaneously the transcriptional levels of thousands of genes was developed less than 10 years ago, and has been widely embraced as a tool for studying the intrinsic properties of cells and their responses to insult or therapy. Since then the field has grown rapidly, succeeding in several areas. One example is in human cancer. Not only may it be possible in the near future to define distinct classes of tumor within a histological type but transcript profiles can identify markers of disease progression, the potential of a tumor to metastasize, and targets for therapy of specific tumors. Another example in which gene discovery techniques have been widely applied and had substantial success is in toxicogenomics, thanks to the combination of models of *in vitro* toxicity with the analysis of the “transcriptional signature” associated to the treatment of a particular compound.

Eight years after the first whole-genome assembly of the human genome, the light- or sample-sequencing of the dolphin genome is completed, which will initiate a new era of discoveries in the marine mammal field. The exploitation of molecular biological techniques along with focused dolphin cell-based experiments will allow difficult research questions about the interaction between dolphin, human and the ocean, to be addressed and will offer new capabilities to discover a unique and challenging environment and to solve problems associated with the quality and quantity of living marine resources.

4. MATERIALS AND METHODS

MATERIALS AND METHODS

PART I. MICROARRAY ANALYSIS

4.1 OVERVIEW OF THE DOLPHIN MICROARRAY

The microarray used in this work was a species-specific cDNA microarray designed for studies of immune and stress response in dolphin, *T. truncatus* by Mancia et al. [120]. The dolphin microarray is briefly described in sections 4.1.1-4.1.4.

4.1.1 GENERATION OF cDNA LIBRARIES AND COLLECTION OF ESTs

Blood samples were collected from dolphins maintained by the US Navy Marine Mammal Program, San Diego, CA, in accordance with a protocol approved by the Institutional Animal Care and Use Committee (IACUC) under the guidelines of the Association for the Accreditation of Laboratory Animal Care. Peripheral blood leukocytes (PBL) were isolated from dolphin whole blood by centrifugation over Histopaque (Gibco-BRL, Rockville, MD). The cells were stimulated *in vitro* with either lipopolysaccharide (LPS; *E. coli* 111:B4, Sigma, St. Louis, MO) at a concentration of 40 µg/ml for 48 hours or recombinant human interleukin 2 (IL-2; Proleukin, Chiron Corporation, Emeryville, CA) at 250 U/ml for 2 weeks. Cells were washed and fresh medium containing 250 U/ml of IL-2 was added every 3 days. The medium used was RPMI-1640 (500ml RPMI with bicarbonate and L-glutamine, 5ml 100X non-essential amino acids, 5ml 100X sodium pyruvate, 5ml Penicillin/Streptomycin, 5ml 1M HEPES, 50ml FBS, 500µL 2-ME), pH 7.35, sterilized by filtration. Total RNA was extracted and used for the construction of two cDNA libraries using the SMART PCR based system

(Clontech, Palo Alto, CA). The LPS stimulated library had an initial titer of 1×10^5 and was generated from a single individual while the IL-2 library had a titer of 1×10^6 and was constructed from an RNA pool from PBL of 4 animals. Phage libraries were converted to plasmids by infecting 2 ml of fresh BM25.8 culture (grown at 31°C to an OD_{600} of 0.6) without shaking for 30 minutes, followed by addition of 2.5 ml of LB media and growth at 31°C with vigorous shaking for 60 minutes. Finally the volume of the plasmid libraries was doubled with a 50% glycerol-LB freeze media, divided into 1 ml aliquots and frozen at -80°C . One aliquot was thawed on ice and the final titer determined by plating undiluted and diluted library on LB plates containing $50 \mu\text{g/ml}$ of carbenicillin, with $100 \mu\text{g/ml}$ X-gal (BioExpress, Kaysville, UT) and 0.1mM IPTG (EnzyPolLTD, London, Ontario, Canada) induction for blue/white screening to detect the recombinant (white) colonies.

4.1.2 EST COLLECTION, GRIDDDING AND REARRAYING

Approximately 3000 recombinant colony forming units per plate were grown on Q-trays (Genetix, New Milton, UK) containing 200 ml LB-carbenicillin agar with blue/white screening and picked and arrayed (using a Genetix Q-Bot) into 96 well plates containing LB medium with carbenicillin and 7% (w/v) glycerol as cryo preservative. A total of approximately 24,000 clones were picked from the IL-2 library and 3,600 from the LPS library. An initial sequencing of 192 ESTs from each library was conducted to determine the level of redundancy. The entire LPS library and the first 72 96-well plates from the IL-2 library were then spotted onto nylon filters and screened with the most common transcripts. Positive clones were eliminated in a re-arraying process reducing the total number of 96 well plates in the LPS collection from 36 to 11. Re-arraying of the IL-2 library was deemed

unnecessary due to the low redundancy observed (16%). A total of 2784 clones were sequenced and contig analysis yielded 1343 unigenes (archived and annotated at www.marinegenomics.org) and deposited in the NCBI dbEST database (Acc.nos. DT660125-DT661427, DV467741-DT468640). Potential functions were annotated using Gene Ontology (GO) [244] classifiers by blasting the sequences against the gene products in the Gene Ontology database [245].

4.1.3 TARGETED GENE CLONING

A panel of important stress response and immune function genes were specifically cloned for inclusion on the microarray. These included receptors, signal transduction molecules, pro-inflammatory molecules, cytokines, stress proteins, and toxin response molecules (Table 4.1). Degenerate primers (described in [120]) were designed to permit the RT-PCR cloning from dolphin PBL cDNA using alignments of homologous sequences present in the NCBI GenBank non-redundant (NR) database. These alignments included, wherever possible, sequences from members of the Cetartiodactyla (*Sus scrofa*, *Bos Taurus*, *Ovis aries*) or human and mouse sequences (*Homo sapiens*, *Mus musculus*). Obtained dolphin sequences were homology searched using BLAST against the NCBI GenBank non-redundant database.

Table 4.1 Targeted stress and immune function genes of the dolphin cloned by RT-PCR.

FUNCTION	GENE	ACC.NO.
RECEPTORS	TLR-1	DV799564
	TLR-2	DV799561
	TLR-3	DV799560
	TLR-4	DV799558
	TLR-5	DV799591
	TLR-6	DV799545
	TLR-7	DV799543
	TLR-8	DV799544
	MHC-I	DV799539
	MHCIIa	DV799553
	MHCIIb	DV799547
	CD79A	DY470720
	CCR	DV799556
	IL-8R	DV799562
	TCR-a	DV799549
	TCR-b	DV799587
	TCR-b	DV799580
	TCR-g	DV799586
	TCR-d	DV799579
	TCR-d	DV799585
TH1-CYTOKINES	IL-2	DV799577
	IFN-g	DV799583
PRO-INFLAMMATORY CYTOKINES	IL-2	DV799577
	IFN-g	DV799583
	IL-1a	DV799590
	IL-1b	DV799584
	IL-6	DV799581
	IL-12	DV799576
	IL-16	DV799567
	IL-17	DV799566
	GM-CSF	DV799573
	RANTES	DV799578
	RANTES	DV799574
	SIGNAL TRANSDUCTION	IkK-a
IkKb		DV799570
NFkB		DV799552
STAT-1		DV799551
STAT-4		DV799565

	STAT-6	DV799550
	PKC	DV799563
TH2-CYTOKINES	IL-4	DV799593
	IL-10	DV799575
	IL-13	DV799568
OTHER CYTOKINES	IL-8	DV799592
	TGF- β	DV799555
STRESS PROTEINS	Hsp70	DV799559
	MT1	DV799541
TOXICOLOGICAL RESPONSE	AhR	DV799569
	CYP1A1	DV799571
	ARNT	DV799557
	Hsp90	DV799554
MISCELLANEOUS	C3	DV799589
	1-Oct	DV799540
	CDC2	DV799546
	TIGGER	DV799538
	TPX2	DV799588
	CytB	DV799537

4.1.4 cDNA MICROARRAY PRODUCTION

The cDNA microarray contains a set of 3700 dolphin sequences comprising 1343 unigenes obtained from the EST sequencing, 2305 randomly-selected (but unsequenced) ESTs and 52 specifically-cloned target genes. For the microarray, amplicons from this collection were produced by PCR using 2 µl of bacterial culture as template and quantified using the SPECTRAMax PLUS (Molecular Devices, Sunnyvale, CA), vacuum dried and resuspended in H₂O and 30% DMSO to a final concentration of 50-200 µg/ml. Microarray printing was performed using a Genetix QArray^{Max} microarray printer (Genetix Ltd., New Milton, UK) fitted with a 24 pin head, from 12 x 384-well source plates (Genetix) on GAPS II amino-silane coated slides (Corning Inc., Corning, NY). A 20x20 feature per sub-array pattern layout was used with side-by-side duplicates feature and 2 identical full arrays per slide (top and bottom). A total of 48 sub-arrays (12 rows by 4 columns) was printed on each slide, giving a combined total of 19,200 features, including landing lights (Integrated DNA Technologies, Coralville, IA) and controls. Feature diameter was 160 µm diameter and features were printed at a pitch of 212 µm. Slides were fixed by baking for 2 hours at 80°C. Spot check was performed by hybridization with a SpotQC kit using a Cy3TM dye-labeled oligonucleotide probe (Integrated DNA Technologies).

4.2 BLOOD SAMPLE COLLECTIONS

4.2.1 BLOOD SAMPLES FOR THE STRESS INDUCED STUDY

Blood samples were taken from 20 animals included in the Bottlenose Dolphin Health and Risk Assessment (HERA). This project was directed by Dr G. Bossart and Dr P. Fair, whom we thank for their cooperation in providing samples from two sites (Charleston Harbor and

the Indian River Lagoon) in the southeastern USA [246]. Two blood samples were taken from each animal. One (*pre* sample) was taken as soon after capture as practical (4–34 min after the animals hit the net) and the second (*post* sample) was taken after conducting a physical examination and immediately before the release of the dolphin (1–3 h after the presample). Five male and five female animals from each site were examined (Figure 2.1, Table 2.1, Table A1), and RNA was prepared from the *pre* and *post* samples for transcriptomic analysis.

4.2.2 BLOOD SAMPLES FOR THE ARTIFICIAL NEURAL NETWORK STUDY

Blood samples were collected during capture-release study in 4 different locations in the United States. The locations were along the US east coast, in Charleston, SC, Indian River lagoon, FL and in the Gulf of Mexico in Sarasota Bay, FL and Saint Joseph Bay, FL. The samples were collected during health assessment capture-release operations (Wells et al. 2004) under National Marine Fisheries Service (NMFS) Permits # 998-1678-01, 522-1785, 932-1489-09 to Gregory Bossart, Randall Wells and Teri Rowles respectively. A total of 151 individuals were sampled between June of 2003 and June of 2006 of which 59 individuals were from Charleston, 35 from Indian River Lagoon, FL, 32 from Sarasota Bay, FL and 25 from St. Joseph Bay FL. The animal's ID and other available information are listed in Table A3. All of the dolphins sampled from Sarasota Bay, FL were identified as residents of the region based on long-term studies (Scott et al. 1990; Wells 1991).

Many of the individuals were sampled more than once as either part of an investigation of the effect of veterinary examination on transcript profiles or through capture and sample

collection in multiple years. All duplicate samples have been removed from the current data analysis in order to avoid complications of replicate sampling.

4.3 PREPARATION OF RNA

4.3.1 RNA EXTRACTION

Approximately 2.5 ml of blood was collected in PAXgene™ Blood tubes (Qiagen, Valencia, CA), mixed immediately to lyse the blood cells and stabilize the RNA, and stored according to the manufacturer's instructions, i.e. at room temperature for up to 24 hours prior to RNA purification, and at 4°C when longer storage times were needed.

Total RNA was extracted using PAXgene™ Blood RNA kits (Qiagen, Valencia, CA). The quantity and integrity of the extracted RNA was determined by spectrophotometry and electrophoresis in a 1% agarose gel.

4.3.2 SYNTHESIS OF LABELED RNA

Total RNA (1-2 µg) was used to produce Cy3-labeled aminoallyl RNA (Cy3-aaRNA) probe using the Amino Allyl MessageAmp™ Kit (Ambion Inc, Austin, TX), according to manufacturer's instructions and 10 µg of the subsequently produced Cy3-aaRNA was diluted (1:3) in hybridization buffer (50% formamide, 2.4% SDS, 4x SSPE, 2.5x Denhardt's solution, and 1 µl of Mouse Hybloc DNA (Applied Genetics Laboratories, Inc, Melbourne, FL) blocking solution). The probe was then boiled for 1 minute and incubated in the dark for 1 hour at 50°C.

4.4 MICROARRAY HYBRIDIZATION

Microarray slides were pre-washed with 0.2% SDS for 2 minutes, boiled in deionized water for 2 minutes, rinsed in 100% ethanol for 2 minutes and then dried. Slides were pre-hybridized in a hybridization oven with a pre-hybridization buffer (33.3% formamide, 1.6% SDS, 2.6x SSPE, 1.6x Denhardt's solution and 0.1 μ M salmon sperm DNA) in the dark for 1 hour at 50°C. Slides were hybridized with Cy-3-aaRNA in the dark for 16 hours at 50°C. After the hybridization, slides were rinsed in 2x SSC, 0.1% SDS and soaked in 0.2x SSC, 0.1% SDS for 15 minutes in the dark at room temperature, followed by a rinse in 0.2x SSC, soaking in 0.2x SSC for 15 minutes, 0.1x SSC for 15 minutes and, finally, deionized water for 5 minutes in the dark in order to remove carryover SDS. The microarrays were then dried and scanned with ScanArray™ Express and SpotArray software at 80 V PMT and analyzed with QuantArray software (Perkin Elmer, Boston, MA).

The microarray hybridization data and the MIAME protocols have been deposited at the GEO site (www.ncbi.nlm.nih.gov/geo/) with the Acc. nos. GSM186669-GSM186708 and GSM267587-GSM267737, for the stress induced study and the artificial neural network study, respectively. They have also been deposited at www.marinegenomics.org.

4.5 STATISTICAL ANALYSIS OF MICROARRAY DATA

4.5.1 STATISTICAL ANALYSIS OF MICROARRAY DATA OF THE STRESS INDUCED STUDY

Raw data obtained from the QuantArray software package was used as the source for quantification of hybridization of RNA probes to microarray features. Background subtracted intensity values were rank ordered and divided by the number of valid measurements to

obtain the within array quantile. All data analysis operations were performed with original code developed especially for the marine genomics project at www.marinegenomics.org [247]. The significance of apparent differential expression was assessed by calibration of the expression signal to the conditional cumulative probability of expression between replicates of the same sample. The procedure is the same as described previously for normalization of proteomics data [176], except that here a model-free approach was followed to capture the bivariate density distribution using a Parzen window kernel with a Gaussian distribution function [248]. This procedure, which is fully data-driven, was found to be faster, more robust and more accurate in describing the complexity of the data without the drawbacks of assuming a density distribution function. The reason why implicit methods are advantageous (compared with [176]) when dealing with microarray data is that the number of features (microarray probes) is much larger and consequently replicate series provide a finer description of reproducibility. The basic calculations used in this procedure require three input data sets: a) one or reference array, X, b) one or more test arrays, Y, and c) a series of calibration arrays, typically one or more replicate series, and produces two output arguments: 1) the average of the differential expression (df) obtained by projecting the reference and test values on the calibrating conditional cumulative distribution plot and 2) the p value of its consistency/ reproducibility, which is accessed by the Wilcox's sign-rank test of its deviation from the median response (quantile 1/2). For ease of interpretation and to avoid confusing the strength of differential expression (1) with its reliability (2), the former is represented as $df = P(Y|X)*2 - 1$

which projects the values of df between -1 and 1 with positive values indicating over-expression (up-regulation) and negative values indicating under-expression (down-regulation).

The transcriptomic signatures for the *pre* and *post* samples were compared to determine those genes that were significantly up- or down-regulated during the time between taking the *pre* and *post* samples. In assessing the significance of changes in the expression levels of genes, the analysis was undertaken at two levels. The first level considered the regulation of genes in each animal as an individual, and the second then addressed the question of whether a particular gene was significantly regulated in the study population taken as a whole. Genes with negative (-) df values were down-regulated.

All genes listed in this Table A2 showed significant changes in expression between the *pre* and *post* samples in each one of the 20 animals with $df > \pm 0.45$ and $p_i \leq 0.25$ (p_i : significant individual probability value; Wilcoxon probability). The P values showed in Table A2 were total probability P_t values based on likelihood calculations.

Total probability P_t values were calculated according to the following equation:

$$P_t = \binom{n}{k} p_i^k (1 - p_i)^{n-k}$$

n = total number of animals; $k= 0 \rightarrow n$.

P_t values were designated based on the frequency at which a specific gene was up or downregulated across the 20 animals (total number of tests following Chapman, R.W. *et al*, [249]).

4.5.2 STATISTICAL ANALYSIS OF MICROARRAY DATA FOR THE ARTIFICIAL NEURAL NETWORK STUDY.

4.5.2.1 DATA PROCESSING VIA BIOCONDUCTOR

The QuantArray files were uploaded in R/Bioconductor [250] using the “limma” package [251,252]. The data background was corrected using the “normexp” methodology, which fits a convoluted model to the background and foreground intensities using maximum likelihood [253]. The corrected data was normalized using the “loess” method to adjust for print-order effects that could have been generated by differences in the cDNA batches printed onto the microarrays [254]. Following the normalization, the genes for which at least one of the replicates failed to exceed the intensity of non-dolphin genes (e.g. Duck IgY Heavy Chain and *Karenia brevis* photolyase) in more than 10% of the slides were eliminated from the analysis. The remaining spots were normalized using the “VSN” method [255] and the duplicates were averaged using a correlation factor calculated by the “limma” package [252]. In order to select the genes best suited to discern differences between the sexes, an empirical Bayesian approach implemented in the package “limma” was taken to shrink the standard errors towards a common value [256]. Next, moderated t-statistics for each of the probes in each of the populations was calculated [256] and the p-values obtained were adjusted using the false discovery rate method [257]. Gene selection was also conducted via ANN’s between the sexes within each location following similar procedures to those described below.

4.5.2.2. GENE SELECTION VIA ANN

While general machine learning approaches encapsulated in Artificial Neural Networks have been applied to the analysis of microarray data, [179,180], the basic formulation of our approach is shown in Figure 2.4 and is similar to that employed by Wei et al. [180]. An initial training of ANNs was conducted using the entire set of VSN transformed expression data that passed Bioconductor filtering (i.e. above background). Five models were run for each population keeping the sexes separate, using a *one-vs-rest* approach (eg. Charleston Harbor males vs males in all other populations) withholding a random selection (1/7) of the microarray records from each population as a cross validation (CV) set to prevent over training of the ANN [258]. The model with the highest R-square for the training data from each population comparison was used to compute the sensitivities of the individual genes. Sensitivities in this context are the partial derivatives of the weight and sigmoidal transfer function for each gene. The sensitivities across all populations were then averaged and ranked to select the top 250 most ‘important’ genes (Figure 4).

Dolphin ESTs selected by Bioconductor and ANN analyses were blasted against the (nr) non-redundant protein sequences database at NCBI (<http://www.ncbi.nlm.nih.gov/>). Blastx cutoff value was 1.0E-3. The blastx search was updated on October 12, 2009.

4.5.2.3. MACHINE LEARNING ANALYSIS

Following the selection of genes using the sensitivity analysis in the ANNs a second round of ANN training withholding 10% of the available data as a cross validation set which was distinct from the data used in early stopping of the ANN training session. The top 250 genes were used to train 20 or more ANNs. The design was balanced by comparing each location

pairwise to the others and taking 90% of the smaller of the two sample sizes and an equal number of the larger set for training the ANN's. The remaining samples were allocated to the CV set. Each round of training produces a model that can be used to predict the state of the cross validation set (which is known) and thus generate a correlation between observed and predicted values. This is useful in examining the predictive value of any ANN model to data that has not been used in the training session using standard correlation coefficients comparing the observed value and that predicted by the ANN.

To compare the precision of the classifications derived from the ANN's we used receiver operating characteristic curves (ROC) and computed the area under the curve (AUC) as well as the standard error (SE) using only the CV data. For justifications of this method for comparing various classifiers see [259,260] . Statistical differences between two comparisons can then be assessed using standard z-scores [261]. When comparing two diagnostic or classificatory procedures, the calculation of the SE should include a measure of the correlation between the two AUC's, due to sampling of the same set of cases. The sampling procedure outlined above does not exclude the possibility that some ROC's include some of the same individuals, but it is not clear how the correlations should be estimated when some, but not all, cases are common to both analyses. We assume that the correlations are sufficiently small to be ignored, but have adjusted the significance level ($\alpha=0.01$) to compensate for this potential bias.

4.6 REAL-TIME PCR (*qRT-PCR*)

4.6.1 *qRT-PCR* PROTOCOL

qRT-PCR to quantify IL-8 and GAPDH message was performed on *pre* and *post* samples from 8 animals, four animals from each location (Table 4). The cDNA was originated from 2 µg of the same RNA used for microarray hybridizations, with M-MLV Reverse Transcriptase (Promega, Madison, WI). The cDNA resulting was purified with QIAquick[®] Purification kit (Qiagen, Valencia, CA). The PCR was performed with 50 ng of cDNA and SYBR QuantiTect[™] SYBR[®] Green (Qiagen, Valencia, CA), with primer concentration of 2.5 µM using a PCR profile as follow: 50°C for 20 s, 95°C for 15 min and 40 cycles with 95°C for 15 s, 58°C for 30 s and 72°C for 42 s. A single product was confirmed by dissociation analysis. Data were obtained by independent duplicate measurements.

Primers were designed on the sequences deposited at ncbi with Acc.nos DV467973 and DT660217 for GAPDH and IL-8, respectively.

The sequence of the primers used for IL-8 (1) and GAPDH (2) was:

(1)G-3281 forward 5' TGTCACTGCAAGCCTTATTATGC 3'

G-3282 reverse 5' GTGAATTTTTGCTGTTTTGAGAAAGA 3'

(2)G-3269 forward 5' GGGAGTCCTTGCCCCAACT 3'

G-3270 reverse 5' GGATGGAAACCGCATGGA 3'

4.6.2 *qRT-PCR* DATA ANALYSIS

Assessing the changes in message levels using *qRT-PCR* is often carried out by comparing a Ct value for the gene of interest (in this case IL-8) to the Ct value of an appropriate standard or reference gene (in this case GAPDH) using ratios or proportions. Such data (i.e. ratios or

proportions) have poor statistical properties in that they are not normally distributed and must be subjected to some transformation (e.g. arc-sin) before valid tests can be performed. In the present case, an alternative to transformation of the raw values was employed. Here, for statistical analysis, the *pre* GAPDH Ct values were subtracted from the *pre* IL-8 values and the resulting values were compared to those derived from subtracting *post* GAPDH values from *post* IL-8-values, using a paired t-test. The null expectation is that the differences will not be significant regardless of whether or not the veterinary examination suppresses (or enhances) overall transcription. Using this simple arithmetic scalar correction does not violate the assumption of normality and permitted the use of both one- and two-tailed tests to examine significant up or downregulation of IL-8 in comparison to GAPDH.

4.7 DOLPHIN GENOME SEQUENCING PROJECT

4.7.1 GENERATION OF cDNA LIBRARIES

Six cDNA libraries were generated from RNA extracted from liver, spleen, kidney, muscle, skin, buffy coat of different dolphins. Kidney and liver were obtained from the same animal, a captive dolphin female; spleen and buffy coat were obtained from 2 captive dolphins females; muscle was obtained from a captive dolphin male; skin was obtained from a wild dolphin female. Tissues were snap-frozen in liquid nitrogen during necropsy and stored at -80°C prior to RNA extraction. RNA was obtained using the QuickPrep™ Total RNA Extraction kit (Amersham Biosciences, UK). 1 µg of RNA was used to generate cDNA libraries using the SMART™ cDNA library Construction Kit (Clontech Laboratories, Inc., Mountain View, CA) following manufacturer's instructions.

The cDNA libraries were sequenced with both Sanger and 454 sequencing methods at the Human Genome Sequencing Center at Baylor College of Medicine. The ESTs and the 454 short sequence readings, together with the dolphin genome trace files, have been uploaded and are publicly available at the *T. truncatus* page at ncbi (<http://www.ncbi.nlm.nih.gov/Taxonomy/>).

PART II. DOLPHIN CELL BIOLOGY

4.8 CELL CULTURE, FIXING AND STAINING

4.8.1 CELLS AND CULTURE CONDITIONS

Dolphin lung cells TuTruL (kindly provided by Dr. B. Middlebrooks, University of Southern Mississippi) originated from a lung biopsy (parenchymal tissue) from a stillborn bottlenose dolphin calf (Marine Life Aquarium, Gulfport, MI). TuTruL were previously described and characterized by Garrick et al. [152]. TuTruL were single-cell cloned and cultured in RPMI 1640 medium supplemented with insulin-transferrin-selenium -G supplement (ITS; Invitrogen, Carlsbad, CA), 5 µg/ml bovine transferrin (Sigma, St. Louis, MO), 10 nM hydrocortisone (Sigma, St. Louis, MO), 10 nM beta-estradiol (Sigma, St. Louis, MO), 10 mM HEPES (Invitrogen, Carlsbad, CA), Glutamax™, penicillin (100 U/ml), streptomycin (100 µg/ml) and 2% (v/v) FBS (Invitrogen, Carlsbad, CA).

Human umbilical vein endothelial cells HUVECs (ATCC, Manassas, VA), were maintained in F-12K medium (ATCC, Manassas, VA), supplemented with 0.1 mg/ml heparin (Sigma, St. Louis, MO), 0.03 mg/ml endothelial cell growth supplement (ECGS; Sigma, St. Louis, MO), 10% (v/v) fetal bovine serum (FBS; Invitrogen, Carlsbad, CA), penicillin (100 U/ml), streptomycin (100 µg/ml).

Bovine lung microvessel endothelial cells BLMVEC (VEC technologies, Rensselaer, NY) were maintained in MCDB-131 medium as supplied by the manufacturer (VEC technologies, Rensselaer, NY).

NIH 3T3 mouse embryo fibroblasts cell line (ATCC, Manassas, VA) were maintained in Dulbecco's Modified Eagles Medium (DMEM; Mediatech, Herndon, VA) supplemented

with nonessential amino acids, Glutamax™ (Invitrogen, Carlsbad, CA), penicillin (100 U/ml), streptomycin (100 µg/ml), and 10% (v/v) FBS (Invitrogen, Carlsbad, CA).

All cell lines were maintained in a humidified 5% (v/v) CO₂ balanced-air atmosphere at 37°C. Subconfluent cultures were harvested by trypsinization and counted with a Beckman Coulter Multisizer III particle counter (Beckman Coulter, Fullerton, CA). Cell sizing data were analyzed and used to generate volume distribution plots.

4.8.2 CELLS FIXING AND STAINING

Cells (TuTruL, HUVECs, BLMVEC and NIH 3T3) were seeded at a density of 1000 cells/cm² in tissue culture polystyrene (TCPS) 6-well plates and incubated at 37°C, 5% CO₂. After 24 or 48 hours cells were fixed in 4% formaldehyde in DPBS (Dulbecco's Phosphate Buffered Saline) at room temperature for 20 min and stained by incubating with a solution containing 1 µM Texas-Red-C₂-Maleimide (Molecular Probes, Eugene, OR), 1 µg/ml 4',6-diamidino-2-phenylindole (DAPI) (Sigma, St. Louis, MO) and 0.05% Triton-X-100 (Sigma, St. Louis, MO) in DPBS for 2 h [208].

4.9 MORPHOLOGY ANALYSIS

Quantitative morphology analysis was carried out for TuTruL (passage no. 4), HUVECs (passage no. 6), BLMVEC (passage no. 3) and NIH 3T3 (passage no. 12) following the protocol previously described by Elliott et al. [208]. Cells were fixed and stained with Texas-Red-Maleimide which stains the whole cell by forming conjugates with cell proteins, thus allowing the spread areas of individual cells to be quantified. Cells were also stained with DAPI which provides good staining of the cell nuclei by binding strongly to the DNA.

Stained cells were examined by phase contrast and fluorescence microscopy using an inverted microscope (Zeiss Axiovert S100TV, Thornwood, NJ) outfitted with a computer-controlled stage (LEP, Hawthorne, NY), an excitation filter wheel (LEP), and a CCD camera (CoolSnap fx, Roper Scientific Photometrics, Tucson, AZ). Images were collected from 100 fields of cells per well using automated movement of the stage and autofocusing under IPlab software control (BD Biosciences, Rockville, MD) (10× objective). At each field, cellular fluorescence from Texas Red, and then DAPI, was collected by automated switching of the appropriate excitation filters and passing the emitted light through a multipass beam splitter (set no. 84000; Chroma Technology Inc, Brattleboro, VT). Exposure times were determined by comparing the ratio of pixel intensities within the cell areas with the intensities in non-cell areas (e.g., background). For each cell type images were collected in 100 fields for 6 replicate wells. ImageJ software was used for quantitative analysis: a single threshold was determined manually and applied to all images in a dataset (100 images) to determine areas of the images that were associated with cells to be distinguished from the non-fluorescent non-cell areas. The number of nuclei (or number of cell objects) was determined from the corresponding images collected with the DAPI filter. Every Texas Red fluorescent area that was associated with DAPI staining was identified as a cell object. The average area per cell was calculated by dividing the area corresponding to Texas Red fluorescence by the number of nuclei as determined by DAPI staining. Axial ratio was determined using the ratio of cell major axis/cell minor axis and the roundness was calculated as $(4*\pi*area)/perimeter^2$ [208,262].

Cluster analysis was calculated comparing the percentage of cell objects with more than one nucleus at 24h and 48h.

Each histogram and average area reported reflects the combined data from cells in 100 fields in 6 replicate wells.

4.10 CELL VOLUME DISTRIBUTION MEASUREMENTS

Cell volume distributions and cell number (cells/ml) for TuTruL, HUVECs, BLMVEC and NIH 3T3 were determined using a Coulter counter (Multisizer 3; Beckman Coulter, Fullerton, CA). A cell suspension was obtained by trypsinization, 100 μ L of the cell suspension were added to 9.9 ml of isotonic solution (Isoton II, Beckman Coulter, Fullerton, CA) and 1 ml of this solution was analyzed by the Coulter counter instrument. Approximately 1×10^5 to 2×10^5 cells were counted for each measurement. The volume measurements were calibrated against standard beads (Size Standard L20, Beckman Coulter, Fullerton, CA) for each measurement. Volume versus frequency data was obtained by rescaling the diameter versus frequency data within each of the Multisizer 3 files using Excel (Microsoft Corp., Redmond, WA). In the growth rate analysis, the population doubling time was calculated from Equation 1.

$$t_d = \frac{\log(2) \cdot T}{\log\left(\frac{N_f}{N_o}\right)} \quad (1)$$

where, t_d , is the population doubling time, N_o is the number of cells seeded, and N_f is the and the number of cells after time, T . N_o and N_f are determined using the Coulter counter at the same time the volume distribution measurement is made. Growth rates (mean and variation) for cells are determined by fitting the measured volume distribution to an analytical expression described in Halter et al. [212]. In this expression, population doubling times are estimated with Eq. (1) and a 30% variation in cell cycle times is assumed.

Grubb's test for outliers, two-sided with $P > 0.05$ and $Z\text{-value} = 1.89$ was used for statistical analysis of cell volume distribution measurements [211].

4.11 DOLPHIN CELLS LIVE-IMAGING

TuTruL cells (at passage no. 20 and at passage no. 30, temporally spaced) were seeded at a starting density of 2800 cells/cm² on TCPS 6 well-plate and placed on an inverted Axiovert 200 M microscope (Zeiss, Thornwood, NJ) equipped with an automated stage (Ludl, Hawthorne, NY) and a CoolSNAP HQ CCD camera (Roper Scientific, Tucson, AZ). The cells were maintained at 37°C in a microscope incubator (In Vivo Scientific, Gray Summit, MO) throughout the experiment. The culture headspace was maintained with humidified 5% CO₂ in balanced air and maintained at 37 °C. Phase contrast images were captured under the control of ISee software (ISee Imaging Systems, Raleigh, NC) every 15 min using a 5x/0.16 NA objective. A 0.63x demagnifying lens was positioned in front of the CCD, which acquired images using 2x2 binning and an integration time 0.05 s. The TuTruL cells at passage n. 20 were imaged for 7 days at 16 different fields and a total of 11000 images were used to generate a time lapse image sequence. The TuTruL cells passage n. 30 cells were imaged for 3 days at 16 different fields and a total of 3000 images were used to generate a time lapse image sequence.

4.12 ANALYSIS OF ENDOTHELIAL AND EPITHELIAL CELL MARKERS

4.12.1 IMMUNOCYTOCHEMISTRY

TuTruL, HUVECs, BLMVEC and NIH 3T3 were seeded at a high density (~50% confluence) in TCPS 48-well plates and/or in chamber slides and incubated at 37°C, 5% (v/v) CO₂. At confluence, cells were fixed in 4% formaldehyde (FA) in DPBS (Dulbecco's Phosphate Buffered Saline) at room temperature for 20 min.

Cells were washed 5x with a solution of DPBS and 0.05% Triton-X-100 (DPBS-T), and blocked with blocking solution (BS, 3% BSA in DPBS-T with 1% serum (rabbit or goat)) for 30 min. Primary antibodies used for immunocytostaining were:

- 1) rabbit polyclonal anti-human VE-Cadherin (160840, Cayman Chemical Company, Michigan, MI);
- 2) goat polyclonal anti-mouse PECAM-1 (SC-1506, Santa Cruz Biotechnology Inc, California, CA);
- 3) mouse monoclonal anti α -SMA (CP47, Calbiochem®, EMD Chemicals Inc, Merck, Darmstadt, Germany);
- 4) goat polyclonal anti-dolphin SP-B (manufactured by GenScript, Piscataway, NJ, against a synthetic peptide of 16aa of the dolphin mature SP-B).

For 1), 2) and 3), cells were cultured and fixed on in TCPS 48-well plates, primary antibodies were diluted 1:100 in BS containing 1 μ M Texas-Red-C₂-maleimide and 1 μ g/ml DAPI and incubated for 45 at room temperature, on a rocking platform. Secondary antibody, Alexa-488 goat anti-rabbit (Molecular Probes, Eugene, OR) was diluted 1:100 in BS containing 1 μ M

Texas-Red-C₂-maleimide and 1 µg/ml DAPI and incubated for 45 min, at room temperature, on a rocking platform, in the dark.

After secondary antibody incubation, cells were washed 5x with DPBS-T, fixed in 4% FA for 10 min and stored in DPBS-T at 4°C prior to imaging.

Stained cells were examined by phase contrast and fluorescence microscopy using an inverted microscope (Zeiss Axiovert S100TV, Thornwood, NJ) outfitted with a computer-controlled stage (LEP, Hawthorne, NY), an excitation filter wheel (LEP), and a CCD camera (CoolSnap fx, Roper Scientific Photometrics, Tucson, AZ). Images were collected from 49 fields of cells per well, using automated movement of the stage and autofocusing under IPlab software control (BD Biosciences, Rockville, MD) (10× objective). At each field, cellular fluorescence from Texas Red, DAPI and Alexa 488 was collected by automated switching of the appropriate excitation filters. Exposure times were determined by comparing the ratio of pixel intensities within the cell areas with the intensities in non-cell areas (e.g., background). For each cell type images were collected in 49 fields for 3 replicate wells. ImageJ software was used for quantitative analysis. Cell area and number of nuclei was determined by Texas Red and DAPI staining as previously described in section 4.9 of the Methods. The intensity/cell of the Alexa 488 staining was calculated for all the images collected and normalized to the total number of cells and area per each field.

For **4**), TuTruL cells were cultured on Small Airway Epithelial Cell (SAEC, PromoCell, Heidelberg, Germany) medium for up to 3 weeks in T25 TCPS flasks, prior the experiment. TuTruL at passage no. 33 (cultured separately in HITES and SAEC media) were seeded on 4 well chamber slides (Lab-Tek® Chamber Slide™ System, Nucnc, Inc, Naperville, IL) and fixed with 4% FA at ~ 80% confluence. Primary antibody (**4**) was diluted 1:100 in BS and

incubated for 16 hrs at room temperature, on a rocking platform. Secondary antibody, Alexa-488 goat anti-rabbit (Molecular Probes, Eugene, OR) was diluted 1:100 in BS and incubated for 2 hrs, at room temperature, on a rocking platform, in the dark. Cells were then washed with DPBS-T and incubated for 20 min with 1mM Topro-3 Iodide (Molecular Probes, Eugene, OR) in DPBS-T for nuclei staining. Cells were then washed 3x with DPBS-T. Chambers were removed and the slide was sealed with glass cover slips in 0.5% glycerol in DPBS-T at room temperature. Slides stained sections were examined under fluorescence microscope using an Olympus IX70 (Olympus, Tokyo, Japan) equipped with Fluoview 300 confocal capability. Digital images were processed using ImageJ software without biased manipulations. For each cell type images (bright field, Alexa-488 and Topro-3) were collected in 4 fields for 2 replicate chambers comprising ≥ 200 cells. ImageJ software was used for quantitative analysis. The number of nuclei (or number of cell objects) was determined from the corresponding images collected with the Topro-3 filter. Immunofluorescence intensity analyses were conducted based upon the mean pixel intensity of positively staining pixels of 4 random images (≥ 200 cells/sample) acquired for each culturing condition under fixed acquisition settings. Intensities were normalized to the mean pixel intensity of Topro-3 stained nuclei.

4.12.2 IMMUNOHISTOCHEMISTRY

Thin sections of alveolar tissue were prepared from dolphin lungs that were perfused with saline to clear blood after removal from the animal during necropsy. Thin sections were paraformaldehyde-fixed and co-stained with goat polyclonal anti-dolphin SP-B (manufactured by GenScript, Piscataway, NJ) followed by Alexa Fluor 488-conjugated

secondary antibodies (Molecular Probes, Eugene, OR). Cell nuclei were stained with Topro-3 (Molecular Probes, Eugene, OR). Slides stained sections were examined under fluorescence microscope using an Olympus IX70 (Olympus, Tokyo, Japan) equipped with Fluoview 300 confocal capability.

4.12.3 ACETILATED LOW-DENSITY LIPOPROTEIN ASSAY

Cells (TuTruL round and spindly, HUVECs, BLMVEC, and NIH 3T3) were seeded in 35 mm dishes in order to have 3×10^4 - 5×10^4 cells/dish when flow experiment was performed.

For each cell type, duplicate samples were either treated with 5 $\mu\text{g/ml}$ fluorescently labeled acetylated low density lipoprotein (DiI-Ac-LDL, Biomedical Technologies, Inc, Stoughton, MA) in the appropriate growth medium or exposed to growth medium only (controls) for 24 hours. Flow cytometry analysis was performed with a Cell Lab Quanta SC, (Beckman Coulter Inc, Miami, FL) equipped with a 488 nm laser. DiI-Ac-LDL fluorescence was recovered through a 575 BP filter. 1×10^4 cells were acquired per sample. Briefly, for each cell type, cells were washed once with complete medium, harvested by trypsinization, quenched with growth medium and analyzed. The efficiency of the Ac-LDL uptake for each cell type was expressed as difference in fluorescence intensity mean values of untreated vs. DiI-Ac-LDL treated cells.

4.12.4 WESTERN BLOT ANALYSIS

Western blot for PECAM-1 was carried out with cell lysates from a total of 4.6×10^4 cells for HUVECs, NIH 3T3, TuTruL round and TuTruL spindly. Dishes with cells were placed on ice and gently rinsed with ice-cold PBS, directly lysed into chilled SDS-PAGE sample buffer

and immediately boiled for 5 minutes. Lysates were separated on 4–20% (w/v) gradient polyacrylamide gels (ReadyGels™, Biorad, Hercules, CA) and separated proteins were transferred onto PVDF membrane (Biorad, Hercules, CA). The PVDF membranes were then blocked with 3% BSA in PBS containing 0.1% Tween. Blots were probed with 1:100 dilution of rabbit anti-mouse anti PECAM-1 (Santa Cruz Biotechnology Inc, California, CA) for 16 hrs at 4°C, followed by 1 hr incubation with 1:1000 of horse radish peroxidase (HRP) goat anti-rabbit (Pierce, Rockford, IL). Bands were detected using horse radish peroxidase-labeled secondary antibody and chemiluminescence detection (Pierce, Rockford, IL), on a Fuji LAS-3000 (Fujifilm, Edison, NJ).

Western blot for SP-B was carried out on 5 µl of dolphin airway fluid, 5 µg of dolphin whole lung lysate, 200 ng of purified bovine SP-B, and 200 ng purified dolphin SP-B antigenic peptide. The whole lung tissue was lysate with 1% SDS in RIPA buffer; the 5 µg was an estimate, since the bloodiness of the sample made standard quantification difficult. Samples were run on 4-12% SDS PAGE (Invitrogen, Carlsbad, CA), non-reducing, on MES SDS buffer (Invitrogen, Carlsbad, CA) for 35 min at 200V on the NuPAGE assembly (Invitrogen, Carlsbad, CA) and transferred on nitrocellulose membrane (Invitrogen, Carlsbad, CA) on 20% MeOH in tri-glycine buffer, according to manufacturer instructions. The membrane was blocked with 5% non-fat dry milk in TBS for 1 hr and then incubated for 1 hr with primary antibody, goat anti-dolphin SP-B (manufactured by GenScript), 1:2000 dilution in 0.5% non-fat dry milk in TBST. Secondary antibody, rabbit anti-goat, HRP-labeled (Thermo Fisher Scientific Inc, Waltham, MA) was added in 1:25000 dilution in 0.5% non-fat dry milk in TBST for 45 min. Before imaging, Supersignal west dura substrate (Thermo Fisher Scientific

Inc, Waltham, MA) was added for visualization. Chemiluminescent images were captured using Fluorchem™ 8900 (Alpha Innotech, Santa Clara, CA).

4.13 DEVELOPMENT OF PRIMARY CULTURES

The lung tissue sample (~2 cm³) was excised during necropsy from the left lung of a pygmy sperm whale (no. SC0934) stranded on July 9th, 2009, in Myrtle Beach, SC. The lung tissue was expanded in DMEM/F12 (Dulbecco's Modified Eagle Medium: Nutrient Mixture F-12, Invitrogen, Carlsbad, CA), and 10% DMSO (Dimethyl Sulfoxide, Sigma, St. Louis, MI) using a 20 ml syringe. The sample was then fractioned in 6 small pieces, added to DMEM/F12-10% DMSO medium, subject to slow freezing and stored in the -80°C.

4.13.1 DEVELOPMENT OF PYGMY SPERM WHALE ALVEOLAR TYPE II

One of the 6 square pieces was towed a month after, fractioned in RPMI-1640 (Invitrogen, Carlsbad, CA) and 2% FBS (Invitrogen, Carlsbad, CA) in 8 smaller pieces and washed 3x in the same medium. The fractions were subject to enzymatic digestion with 1 part Collagenase/Hyaluronidase (StemCell Technologies Inc, Vancouver, BC) and 9 parts of DMEM/F12 for 5 hrs at 37°C with gentle rock. After dissociation cells were triturate with a P1000 pipette, centrifuged and resuspended in a 1:4 mixture of HBSS (Hank's balanced Salt Solution, Invitrogen, Carlsbad, CA) modified with 2% FBS (HF) and ammonium chloride, NH₄Cl (StemCell Technologies Inc, Vancouver, BC). Cells were then mixed by pipetting in 0.25% Trypsin-EDTA (Invitrogen, Carlsbad, CA) then a solution with 5mg/ml Dispase and 1 mg/ml DNase I (StemCell Technologies Inc, Vancouver, BC) was used to generate a single cell suspensions. The suspension was diluted 5x in HF and filtered through a 40 µm cell

strainer. Filtered cells were plated in HITES medium on a T75 flask coated with 5% FBS and incubated at 37°C for 1 hr. Cells not attached were then collected and plated in Small Airway Epithelial Cell (SAEC, PromoCell, Heidelberg, Germany) medium to select for lung epithelial cells. Cells (KobreL1) were maintained in SAEC medium at 37°C, 5%CO₂. RNA was extracted using the RNeasy kit (Qiagen, Valencia, CA) according to manufacturer instruction and the cDNA was generated using the Omniscript RT Kit (Qiagen, Valencia, CA). The primers used for SP-B and actin amplification were designed to specifically amplify a 330bp fragment of dolphin actin and a 480bp fragment of dolphin SP-B, with the following sequences:

(3) Actin forward 5' GCACCACACCTTCTACAACGAGCTG 3'

Actin reverse 5' AGCCAGGTCCAGACGCAGGATGG 3'

(4) SP-B forward 5' CCGAGTTCTGGTGCCAAAGCCTG 3'

SP-B reverse 5' GCATGGGAATGGATAACTGCTGCTC 3'

The PCR was performed with 100ng of cDNA and Advantage cDNA PCR Kit (Clontech, Mountain View, CA), following manufacturer instruction with primer concentration of 2.5 µM using a touchdown PCR profile as follow: 95°C for 4 min, 2 cycles with 95°C for 20 s, 56°C for 30 s and 68°C for 1 min, 2 cycles with 95°C for 20 s, 54°C for 30 s and 68°C for 1 min, 2 cycles with 95°C for 20 s, 52°C for 30 s and 68°C for 1 min and 30 cycles with 95°C for 20 s, 50°C for 30 s and 68°C for 1 min. The molecular weight of the PCR products was analyzed by electrophoresis on 1% agarose gel and visualized using Fluorchem™ 8900 imager and software (Alpha Innotech, Santa Clara, CA). The PCR products were quantified using ImageJ software and SP-B relative expression was calculated after normalization to the expression of the housekeeping gene actin.

4.13.2 DEVELOPMENT OF PYGMY SPERM WHALE FIBROBLASTS

One of the 6 square pieces was towed six months after, fractioned in RPMI-1640 (Invitrogen, Carlsbad, CA) and 2% FBS (Invitrogen, Carlsbad, CA) in 8 smaller pieces and washed 3x in the same medium. The fractions were subject to enzymatic digestion for 6 hrs in 1:10 Liberase DL (Roche Applied Science, Mannheim, Germany) in DMEM-F12 (Invitrogen, Carlsbad, CA) cold. After dissociation cells were triturate with a P1000 pipette, centrifuged and resuspended in a 1:4 mixture of HBSS (Hank's balanced Salt Solution, Invitrogen, Carlsbad, CA) modified with 2% FBS (HF) and ammonium chloride, NH₄Cl (StemCell Technologies Inc, Vancouver, BC). Cells were then mixed by pipetting in 0.25% Trypsin-EDTA (Invitrogen, Carlsbad, CA) then a solution with 5mg/ml Dispase and 1 mg/ml DNase I (StemCell Technologies Inc, Vancouver, BC) was used to generate a single cell suspensions. The suspension was diluted 5x in HF and filtered through a 40 µm cell strainer. Filtered cells were plated (Kobref1) were plated 0.1% Gelatin (Sigma, St. Louis, MO) coated TCPS 24-well plate in conditioning medium DMEM-F12 supplemented with GlutaMAX™ (Invitrogen, Carlsbad, CA) and 10% FBS and plated on at 37°C, 5%CO₂.

4.14 MARINE MAMMAL INDUCED PLURIPOTENT STEM CELLS

2.4×10^5 TuTruL and Kobref were seeded on TCPS 6-well plates and the lentivirus infection to generate induced pluripotent stem (iPS) cells was performed when cells reached 80% confluence. The supernatant from 293T cells (Cell Biolabs Inc, San Diego, CA) trasfected with pLentG-KOSM lentiviral vector (Cell Biolabs Inc, San Diego, CA) (Figure 4.1) was diluted 1:1 in complete culture medium specific for each cell type and used for infection. Viraductin™ Lentivirus Transduction Reagent A 100x (Cell Biolabs Inc, San Diego, CA)

was added to the pLentG-KOSM solution for 5 min prior adding Viraductin™ Lentivirus Transduction Reagent B 100x (Cell Biolabs Inc, San Diego, CA) and incubate at 37°C for 30 min. Cells were infected with the lentivirus/ViraDuctin mix for 30 hrs at 37°C, 5%CO₂.

The medium was removed and replenished with Viraductin™ Lentivirus Transduction Reagent C 8x (Cell Biolabs Inc, San Diego, CA) in complete culture medium for 30-60 sec. Cells were then washed 2-3 times with Embrionic Stem (ES) complete culture medium (20ng/μl fibroblast growth factor FGF (Sigma, St. Louis, MO), 20ng/μl epidermal growth factor EGF (Stemgent, Cambridge, MA), 4μg/ml heparin (Sigma, St. Louis, MO), B-27 Supplement 50x (Invitrogen, Carlsbad, CA) in DMEM-F12 HAM (Invitrogen, Carlsbad, CA)) and incubated at 37°C, 5%CO₂. After 48 hrs, cell sorting was performed to separate potenital iPS cells, selecting green fluorescence protein (GFP) positive cells. Cells were washed twice with 0.5% BSA in 1X Solution A (10X Solution A: 0.3M HEPES, 40mM Glucose, 30mM KCl, 1.22M NaCl, 10mM Na₂HPO₄, 10ml of Phenol Red Solution in H₂O; pH 7,5) trypsinized and resuspended in 0.5% BSA in Solution A with 1μg/ml of propidium iodide (Invitrogen, Carlsbad, CA) then passed through a cell strainer and loaded on the BD FACS Aria™llu (BD Bioscience Inc, Bedford, MA) for sorting.

GFP positive cells were then plated in ES complete medium on 1) Matrigel (BD Biosciences, Bedford, MA) coated 6-well plate (1:3 in H₂O) and 2) 2x10⁵ mitotically inactivated mouse embrionic fibroblasts (MEFs) coated 6-well plate.

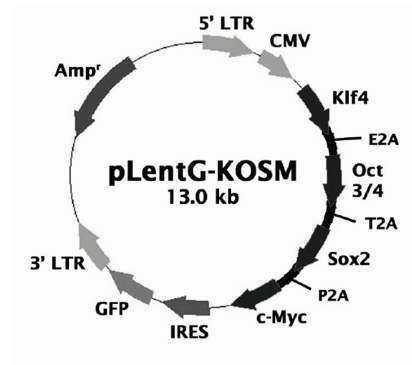


FIGURE 4.1 Schematic representation of pLentG-KOSM lentiviral vector (13 kb).

In the lentiviral vector the transcription factors Oct3/4, Sox2, c-Myc, and Klf4 are in-frame fused into a single open reading frame (ORF) via self-cleaving 2A peptides and are controlled by a CMV promoter. The transcription factor ORF is followed by IRES-GFP as a reporter for viral transduction.

5. APPENDIX

APPENDIX

Table A1. Dolphins sampled in the stress-induced study and their correlated microarray records.

SAMPLES				MICROARRAYS		
LOCATION	DOLPHIN ID	SEX	YEAR	HYB ID	BARCODE NO.	NCBI ACC.NO.
CHS	FB8180803 pre	M	2003	1A	13218794	GSM186669
CHS	FB8180803 post	M		1B	13222814	GSM186670
CHS	FB8210803 pre	F	2003	2A	13218837	GSM186671
CHS	FB8210803 post	F		2B	13222839	GSM186672
CHS	FB8250803 pre	F	2003	3A	13218836	GSM186673
CHS	FB8250803 post	F		3B	13222816	GSM186674
CHS	FB8330804 pre	F	2004	4A	13218869	GSM186677
CHS	FB8330804 post	F		4B	13218864	GSM186678
CHS	FB8450804 pre	F	2004	5A	13222805	GSM186675
CHS	FB8450804 post	F		5B	13222815	GSM186676
CHS	FB8530804 pre	F	2004	6A	13218830	GSM186679
CHS	FB8530804 post	F		6B	13218831	GSM186680
CHS	FB8740804 pre	M	2004	7A	13222850	GSM186681
CHS	FB8740804 post	M		7B	13222848	GSM186682
CHS	FB8760804 pre	M	2004	8A	13218834	GSM186683
CHS	FB8760804 post	M		8B	13218833	GSM186684
CHS	FB8900804 pre	M	2004	9A	13218866	GSM186685
CHS	FB8900804 post	M		9B	13218865	GSM186686
CHS	FB8940804 pre	M	2004	10A	13218842	GSM186687
CHS	FB8940804 post	M		10B	13219006	GSM186688
IRL	FB9190603 pre	F	2003	11A	13219005	GSM186689
IRL	FB9190603 post	F		11B	13219005	GSM186690
IRL	FB9360604 pre	M	2004	12A	13218878	GSM186691
IRL	FB9360604 post	M		12B	13218876	GSM186692
IRL	FB9390604 pre	F	2004	13A	13218878	GSM186693
IRL	FB9390604 post	F		13B	13222804	GSM186694
IRL	FB9410604 pre	F	2004	14A	13222807	GSM186695
IRL	FB9410604 post	F		14B	13222809	GSM186696
IRL	FB9470604 pre	F	2004	15A	13222808	GSM186697
IRL	FB9470604 post	F		15B	13218972	GSM186698
IRL	FB9490604 pre	F	2004	16A	13218995	GSM186699
IRL	FB9490604 post	F		16B	13218993	GSM186700
IRL	FB9520604 pre	M	2003	17A	13222856	GSM186701

Appendix

IRL	FB9520604 post	M		17B	13218986	GSM186702
IRL	FB9540604 pre	M	2004	18A	13218997	GSM186703
IRL	FB9540604 post	M		18B	13222806	GSM186704
IRL	FB9660604 pre	M	2004	19A	13222854	GSM186705
IRL	FB9660604 post	M		19B	13222857	GSM186706
IRL	FB9720604 pre	M	2004	20A	13222817	GSM186707
IRL	FB9720604 post	M		20B	13218828	GSM186708

Table A2. Genes showing significant regulation in *pre* versus *post* blood samples.

FREQUENCY*	ACCESSION NOS.†	df VALUE ‡	IDENTITY§	P VALUE¶
20	DT660209	0.577	Cytochrome c oxidase subunit I	1.00E-60
19	DV467853	0.596	ATP synthase F0 subunit 6	2.00E-56
19	DT660866	0.567	Pre-B-cell colony-enhancing factor 1	2.00E-56
19	DT661110	0.556	Bos taurus coronin, actin binding protein	2.00E-56
19	DV468132	0.553	ATP synthase F0 subunit 8	2.00E-56
18	DT661135	0.574	Thioredoxin	1.90E-52
18	DT660254	0.569	Hemoglobin beta chain	1.90E-52
18	DV468456	0.567	Cytochrome c oxidase subunit II	1.90E-52
18	DV467862	0.562	ATP synthase F0 subunit 6	1.90E-52
18	DT660860	0.56	Proteasome activator complex subunit 2	1.90E-52
18	DV468136	0.557	Tropomyosin 3, gamma	1.90E-52
18	DT660310	0.502	Cytochrome c oxidase subunit III	1.90E-52
17	DT660217	0.713	Bos taurus interleukin 8 mRNA	1.14E-48
17	DV468013	0.551	Ubiquinol-cytochrome-c reductase	1.14E-48
17	DV468042	0.54	Cytochrome c oxidase subunit I	1.14E-48
16	DV467863	0.535	CDC10 protein	4.83E-45
16	DT660252	0.535	Beta-2-microglobulin precursor	4.83E-45
16	DT661078	0.522	CD3G gamma precursor: T cell receptor	4.83E-45
16	DT660863	0.52	Homo sapiens guanylate binding protein 3	4.83E-45
16	DV468110	0.518	Ubiquinol-cytochrome-c reductase	4.83E-45
15	DT660214	0.566	Elongation factor 1a	1.54E-41
15	DT661089	0.537	P50	1.54E-41
13	DT660824	0.522	NADH dehydrogenase subunit 3	7.70E-35
12	DT661036	0.668	Similar to microfibrillar-associated protein	1.25E-31
12	DV467752	0.531	Ubiquinol-cytochrome-c reductase	1.25E-31
11	DT661056	0.75	UDP-N-Acetylglucosamine transporter	1.66E-28
11	DV468134	0.513	Cytochrome b	1.66E-28
10	DV468484	0.548	Homo sapiens ribosomal protein S11,	1.83E-25
10	DT660226	0.52	Proteoglycan 1, secretory granule precursor	1.83E-25
10	DV467837	0.698	Putative nuclear protein	1.83E-25
10	DV799584	0.747	Interleukin-1 beta	1.83E-25
10	DV468037	0.69	Similar to ribosomal protein L35a	1.83E-25
10	DT660214	0.566	Elongation factor 1a	1.83E-25
9	DV468218	0.636	Annexin A11 (Annexin XI)	1.66E-22
9	DV467899	0.661	3-isopropylmalate dehydratase large subunit	1.66E-22
9	DV468173	0.659	Similar to ganglioside-induced	1.66E-22
9	DT661382	0.526	ATP synthase F0 subunit 8	1.66E-22
9	DV467848	0.528	EF1a-like protein	1.66E-22
9	DV467810	0.615	Ferritin, light polypeptide	1.66E-22

8	DT660206	0.716	Acyl-CoA synthetase long-chain family	1.24E-19
8	DV468434	0.632	Homo sapiens zinc finger, FYVE domain	1.24E-19
8	DT660180	0.761	Bos taurus interleukin 1, alpha (IL1A)	1.24E-19
8	DV468613	0.63	Homo sapiens nucleophosmin	1.24E-19
8	DT660223	0.521	Ferritin, light polypeptide	1.24E-19
8	DT660134	0.624	Fc receptor gamma-chain	1.24E-19
8	DV468333	0.706	Protein synthesis initiation factor 4 A	1.24E-19
8	DV469409	0.688	Zinc finger protein 514	1.24E-19
8	DT660215	0.512	Ribosomal protein S4	1.24E-19
8	DV799560	-0.634	Toll-like receptor 3	1.24E-19
8	DT660299	-0.614	16S ribosomal RNA	1.24E-19
8	DT660331	-0.581	Bos taurus thymosin beta-10	1.24E-19
8	DT660825	0.645	NADH dehydrogenase (ubiquinone) 1 alpha	1.24E-19
8	DV468382	0.602	Dynein-associated protein RKM23	1.24E-19
8	DV468185	0.6	Chaperonin containing TCP1, subunit	1.24E-19
8	DV468069	0.654	Chain A, Small G Protein Arf6-Gdp	1.24E-19
8	DV468141	0.671	Serpentine Receptor, class D (delta)	1.24E-19
8	DV467994	0.682	HSPC297	1.24E-19
8	DV467947	0.841	H2A histone family, member Z	1.24E-19
10	DV468542	-0.620	Similar to zinc finger protein 219	1.83E-25
9	DV468544	-0.631	Bos taurus prp gene for prion protein	1.66E-22
9	DV799561	-0.623	Toll-like receptor 2	1.66E-22
9	DV468045	-0.581	Hypothetical protein	1.66E-22
9	DV468540	-0.561	DNA-binding storekeeper protein-related	1.66E-22
8	DV799586	-0.682	T cell receptor gamma	1.24E-19

*Number of dolphins (out of 20) in which significant regulation was observed; †highest value match from blastX search; ‡mean df value [120,263]. Negative values indicate down-regulation. §P value for the sample group of 20 dolphins, calculated as described in [249].

Table A3. Dolphins sampled in the ANN study and their correlated microarray records.

SAMPLES				MICROARRAYS		
LOCATION	DOLPHIN ID	SEX	YEAR	HYB ID	BARCODE NO.	NCBI ACC.NO.
CHS	001	male	2004	003	13541740	GSM267587
CHS	002	female	2004	011	13539521	GSM267590
CHS	003	female	2004	013	13541744	GSM267591
CHS	004	female	2003	015	13541765	GSM267592
CHS	005	female	2003	017	13539219	GSM267593
CHS	006	female	2003	019	13541764	GSM267594
CHS	007	female	2003	021	13539262	GSM267595
CHS	008	male	2004	023	13541703	GSM267596
CHS	009	male	2004	025	13541791	GSM267597
CHS	010	male	2004	027	13541784	GSM267598
CHS	011	male	2003	029	13539240	GSM267599
CHS	012	male	2003	031	13539466	GSM267600
CHS	013	male	2003	033	13539019	GSM267601
CHS	014	male	2003	035	13538994	GSM267602
CHS	015	female	2003	182	13539360	GSM267680
CHS	016	female	2003	186	13541713	GSM267681
CHS	017	female	2003	189	13541715	GSM267682
CHS	018	male	2003	190	13541721	GSM267683
CHS	019	female	2003	192	13539054	GSM267684
CHS	020	female	2003	194	13541810	GSM267685
CHS	021	female	2003	195	13541714	GSM267686
CHS	022	male	2003	196	13539055	GSM267687
CHS	023	male	2003	200	13541719	GSM267688
CHS	024	female	2003	201	13541720	GSM267689
CHS	025	male	2003	203	13539404	GSM267690
CHS	026	female	2003	205	13541732	GSM267691
CHS	027	male	2003	208	13541800	GSM267692
CHS	028	male	2003	210	13541811	GSM267693
CHS	029	male	2003	211	13539361	GSM267694
CHS	030	male	2003	214	13538810	GSM267695
CHS	031	male	2003	216	13539362	GSM267696
CHS	032	male	2003	218	13538893	GSM267697
CHS	033	male	2003	220	13538818	GSM267698
CHS	034	male	2003	222	13538817	GSM267699
CHS	035	male	2003	223	13539359	GSM267700
CHS	036	male	2004	239	13539417	GSM267707
CHS	037	female	2004	241	13539443	GSM267708
CHS	038	female	2004	243	13539448	GSM267709
CHS	039	female	2004	244	13539415	GSM267710
CHS	040	male	2004	245	13541802	GSM267711
CHS	041	male	2005	258	13539394	GSM267719
CHS	042	female	2005	261	13538745	GSM267720
CHS	043	male	2005	262	13539399	GSM267721
CHS	044	male	2005	264	13538746	GSM267722
CHS	045	female	2005	266	13539398	GSM267723

CHS	046	female	2005	269	13538736	GSM267724
CHS	047	male	2005	272	13539393	GSM267725
CHS	048	female	2005	273	13539421	GSM267726
CHS	049	female	2005	275	13538739	GSM267727
CHS	050	female	2005	279	13538769	GSM267728
CHS	051	female	2005	281	13538749	GSM267729
CHS	052	female	2005	284	13539386	GSM267730
CHS	053	male	2005	285	13538770	GSM267731
CHS	054	male	2005	288	13539383	GSM267732
CHS	055	male	2005	290	13538901	GSM267733
CHS	056	male	2005	291	13538900	GSM267734
CHS	057	male	2005	294	13538743	GSM267735
CHS	058	male	2005	296	13538742	GSM267736
CHS	059	male	2005	298	13538867	GSM267737
IRL	060	male	2004	005	13541743	GSM267588
IRL	061	female	2004	007	13541767	GSM267589
IRL	062	female	2004	037	13538734	GSM267603
IRL	063	female	2004	039	13539736	GSM267604
IRL	064	female	2004	041	13541704	GSM267605
IRL	065	female	2004	043	13541747	GSM267606
IRL	066	female	2003	045	13539260	GSM267607
IRL	067	female	2003	047	13539022	GSM267608
IRL	068	female	2004	049	13541819	GSM267609
IRL	069	male	2004	051	13538993	GSM267610
IRL	070	male	2004	053	13538995	GSM267611
IRL	071	male	2004	055	13539269	GSM267612
IRL	072	male	2004	057	13538990	GSM267613
IRL	073	male	2003	059	13541748	GSM267614
IRL	074	male	2003	061	13541736	GSM267615
IRL	075	male	2004	063	13539471	GSM267616
IRL	076	female	2003	171	13539156	GSM267674
IRL	077	female	2003	173	13539155	GSM267675
IRL	078	male	2003	176	13539631	GSM267676
IRL	079	male	2003	178	13539127	GSM267677
IRL	080	male	2003	179	13539157	GSM267678
IRL	081	male	2003	181	13541728	GSM267679
IRL	082	female	2004	224	13538777	GSM267701
IRL	083	female	2004	225	13538809	GSM267702
IRL	084	female	2004	231	13541730	GSM267703
IRL	085	male	2004	232	13257319	GSM267704
IRL	086	male	2004	234	13541733	GSM267705
IRL	087	male	2004	235	13541815	GSM267706
IRL	088	female	2005	247	13539446	GSM267712
IRL	089	male	2005	249	13538869	GSM267713
IRL	090	female	2005	251	13539164	GSM267714
IRL	091	male	2005	253	13539172	GSM267715
IRL	092	male	2005	254	13539173	GSM267716
IRL	093	male	2005	255	13539445	GSM267717
IRL	094	male	2005	256	13539419	GSM267718
SAR	095	female	2004	081	13539462	GSM267617

SAR	096	male	2004	083	13541701	GSM267618
SAR	097	female	2004	087	13541787	GSM267619
SAR	098	female	2004	089	13541792	GSM267620
SAR	099	male	2004	091	13541783	GSM267621
SAR	100	male	2004	093	13539735	GSM267622
SAR	101	female	2005	095	13539427	GSM267623
SAR	102	female	2005	097	13539734	GSM267624
SAR	103	male	2005	099	13539742	GSM267625
SAR	104	female	2005	102	13539737	GSM267626
SAR	105	female	2005	103	13539741	GSM267627
SAR	106	male	2005	104	13539429	GSM267628
SAR	107	male	2005	105	13539151	GSM267629
SAR	108	male	2005	107	13541794	GSM267630
SAR	109	male	2005	110	13539739	GSM267631
SAR	110	male	2005	112	13539153	GSM267632
SAR	111	female	2005	114	13539438	GSM267633
SAR	112	female	2005	116	13539149	GSM267634
SAR	113	male	2005	118	13539144	GSM267635
SAR	114	female	2006	119	13538772	GSM267636
SAR	115	male	2006	120	13539390	GSM267637
SAR	116	female	2006	121	13539146	GSM267638
SAR	117	female	2006	122	13539385	GSM267639
SAR	118	male	2006	123	13538774	GSM267640
SAR	119	female	2006	124	13539437	GSM267641
SAR	120	male	2006	125	13539435	GSM267642
SAR	121	female	2006	126	13539145	GSM267643
SAR	122	male	2006	127	13539384	GSM267644
SAR	123	male	2006	128	13538775	GSM267645
SAR	124	male	2006	129	13539436	GSM267646
SAR	125	male	2006	130	13539147	GSM267647
SAR	126	male	2006	132	13539148	GSM267648
SJB	127	female	2006	133	13539216	GSM267649
SJB	128	female	2006	134	13539746	GSM267650
SJB	129	male	2006	135	13539751	GSM267651
SJB	130	male	2006	136	13539444	GSM267652
SJB	131	male	2006	137	13538812	GSM267653
SJB	132	female	2006	138	13541804	GSM267654
SJB	133	female	2006	139	13539418	GSM267655
SJB	134	male	2006	140	13539743	GSM267656
SJB	135	female	2006	141	13539748	GSM267657
SJB	136	male	2006	142	13539715	GSM267658
SJB	137	male	2006	143	13539714	GSM267659
SJB	138	male	2006	144	13539161	GSM267660
SJB	139	female	2006	145	13539754	GSM267661
SJB	140	female	2006	146	13539124	GSM267662
SJB	141	male	2006	147	13539752	GSM267663
SJB	142	female	2006	148	13539163	GSM267664
SJB	143	male	2006	149	13539717	GSM267665
SJB	144	male	2005	150	13539716	GSM267666
SJB	145	male	2005	151	13539749	GSM267667

SJB	146	female	2005	152	13539162	GSM267668
SJB	147	male	2005	153	13539744	GSM267669
SJB	148	male	2005	154	13539713	GSM267670
SJB	149	female	2005	155	13539747	GSM267671
SJB	150	female	2005	156	13539123	GSM267672
SJB	151	female	2005	157	13539753	GSM267673

Column 1: sampling geographical location (CHS: Charleston, SC; IRL: Indian River Lagoon, FL; SJB: Saint Joseph Bay, FL; SAR: Sarasta Bay, Florida). Column 2: Dolphin ID. Column 3: dolphin sex. Column 4: year of sampling. Column 5: microarray hybridization ID. Column 6: microarray barcode ID. Column 7: microarray ncbi accession numbers. Dolphins from CHS have been sampled in the month of August in 2003, 2004 and 2005. Dolphins from IRL have been sampled in the month of June in 2004 and July in 2003 and in 2005. Dolphins from SAR have been sampled in June in 2004, February and June in 2005 and June and July in 2006. Dolphins in SJB have been sampled in April in 2005 and July in 2006. Dolphin samples from the same collection event (year-month) have been sampled during 2 weeks of capture-release health assessment studies in the specified location.

Table A4. List of most significantly differentially regulated genes selected from ANNs for the determination of sex in dolphins from 4 geographic locations.

ESTS NCBI ACC.NO.	IDENTITY	SEQUENCE LENGTH	# HITS	MIN. EVALUE	MEAN SIMILARITY	#GOs
Contig23 (DV468056, DV468606)	beta-2-microglobulin precursor	615	20	3.113E-50	0.8995	5
Contig8 (DT661121, DT661130)	endonuclease reverse transcriptase	757	20	9.245E-25	0.5075	0
Contig9 (DT661146, DV468349)	endonuclease reverse transcriptase	655	20	6.793E-41	0.8995	0
Contig16 (DV467822, DV468030, DT661250)	endonuclease reverse transcriptase	1021	20	1.295E-54	0.414	0
Contig17 (DV467848, DV468052, DT660342, DT660214)	eukaryotic translation elongation factor 1 alpha 1	1128	20	2.87E-147	0.99	8
Contig13 (DT661332, DV468062)	eukaryotic translation elongation factor 1 epsilon 1	801	20	5.033E-72	0.963	11
Contig18 (DV467901, DV468515)	h+ lysosomal v0 subunit e1	798	20	3.158E-42	0.924	9
Contig21 (DV467972, DV468548)	heat shock factor binding protein 1	536	20	3.485E-21	0.958	6
Contig27 (DV468285, DV468404)	histone	751	20	2.354E-75	0.9865	10
Contig30 (DV468523, DV468543)	line-1 reverse transcriptase homolog	622	20	5.259E-15	0.56	3
Contig15 (DV467784, DT661404)	nucleophosmin 1 isoform 1	628	20	7.359E-79	0.9915	2
Contig19 (DV467909, DT661152)	prothymosin alpha	820	2	4.944E-14	0.79	0
Contig12 (DT661197, DT661410)	ribosomal protein l27	492	20	6.929E-65	0.987	4
Contig3 (DT660346, DV467881, DV468107)	ribosomal protein s3a	800	20	6.84E-138	0.985	8

Contig22 (DV467994, DT660290)	selenoprotein k	703	20	3.828E-19	0.934	2
Contig5 (DT660891, DT661019, DV468123, DT661205)	thymosin beta 4	622	19	1.228E-09	0.9347368	10
Contig14 (DT661382, DV468102, DT660273, DV468009, DV468341, DV467843, DV468605, DT660962, DV468076, DT660994, DT661003)	cytochrome c oxidase subunit iii	1570	20	2.25E-122	0.938	4
Contig20 (DV467950, DT660370, DV467982, DV468000)	cytochrome c oxidase subunit i	1154	20	1.76E-107	0.96	9
Contig25 (DV468145, DV467924, DV467772)	cytochrome c oxidase subunit i	812	20	2E-116	0.935	9
Contig4 (DT660358, DV468456)	cytochrome c oxidase subunit ii	577	20	3.64E-76	0.959	7
DT660143	beta globin	558	20	4.289E-47	0.9205	6
DT660146	heavy polypeptide 1	534	20	8.524E-44	0.9825	8
DT660169	c-c chemokine receptor-like 2	458	20	2.73E-29	0.7425	4
DT660171	ribosomal protein l36a	219	20	2.73E-16	1	4
DT660178	elongation factor 1-alpha	711	20	7.493E-55	0.9335	5
DT660181	endonuclease reverse transcriptase	370	20	3.296E-38	0.8355	0
DT660202	s100 calcium binding protein a8	385	12	1.121E-06	0.875	6
DT660206	acyl- synthetase long-chain family member 5	769	20	3.082E-84	0.9075	9
DT660222	endonuclease reverse transcriptase	390	20	2.795E-50	0.8285	0
DT660226	proteoglycan 1 precursor-like	778	20	5.425E-60	0.748	10
DT660231	slam family member 7	597	20	6.878E-72	0.576	1
DT660247	hypothetical protein PC101070.00.0	622	1	2.832E-06	0.81	0
DT660265	nop16 nucleolar protein homolog	687	20	7.96E-83	0.813	1
DT660268	endonuclease reverse transcriptase	301	20	4.443E-12	0.6075	0
DT660276	endonuclease reverse transcriptase	463	20	2.895E-18	0.8695	0
DT660327	wd repeat domain 12	173	20	5.35E-25	0.9345	3
DT660336	hCG2038477 [Homo sapiens]	411	1	2.938E-07	0.64	0
DT660347	endonuclease reverse transcriptase	507	20	1.088E-16	0.3095	0

DT660351	endonuclease reverse transcriptase	507	20	1.039E-35	0.479	0
DT660352	wd repeat domain 26	808	20	6.734E-40	0.98	1
DT660353	ribosomal protein l12	567	20	7.795E-44	0.9865	7
DT660379	transposase	824	20	3.676E-25	0.63	0
DT660794	cytochrome c oxidase subunit VIIb	466	20	5.781E-35	0.855	4
DT660808	polymerase II (dna directed) polypeptide h	544	20	7.915E-40	0.9635	6
DT660825	nadh dehydrogenase 1 alpha 2	416	20	1.94E-43	0.8825	5
DT660836	beta lysosomal-like	719	1	8.84E-11	0.57	0
DT660847	breast cancer early isoform cra_g	707	20	4.91E-115	0.9335	18
DT660851	dead (asp-glu-ala-asp) box polypeptide 39	789	20	5.67E-129	0.9665	7
DT660857	nicotinamide phosphoribosyltransferase	725	20	3.81E-102	0.9755	13
DT660858	endonuclease reverse transcriptase	515	20	1.535E-14	0.6315	0
DT660860	proteasome (macropain) activator subunit 2 (pa28 beta)	756	20	4.18E-118	0.952	5
DT660862	endonuclease reverse transcriptase	374	13	3.783E-10	0.7438462	10
DT660863	guanylate binding protein 3	732	20	2E-114	0.9375	4
DT660880	ribosomal protein l32	494	20	9.668E-67	0.974	5
DT660902	endonuclease reverse transcriptase	718	20	7.785E-08	0.344	0
DT660913	p40	776	20	1.932E-25	0.5185	3
DT660931	14 kd	510	1	8.802E-05	0.47	0
DT660972	nkg2a	672	20	2.128E-77	0.748	3
DT660985	endonuclease reverse transcriptase	261	20	6.62E-31	0.824	0
DT660987	cytochrome c oxidase subunit vib polypeptide 1	457	20	3.792E-47	0.965	4
DT660988	mitochondrial ribosomal protein l22	456	20	2.238E-23	0.81	4
DT661002	peroxiredoxin 1	541	20	8.468E-87	0.9645	7
DT661013	endonuclease reverse transcriptase	659	20	3.287E-51	0.8735	0
DT661036	microfibrillar-associated protein 1	248	20	1.897E-14	0.999	2
DT661042	mitochondrial ribosomal protein s33	595	20	1.833E-41	0.9045	3
DT661064	orf2	393	19	6.026E-11	0.6415789	2
DT661081	endonuclease reverse transcriptase	636	20	5.647E-13	0.2565	13
DT661112	endonuclease reverse transcriptase	715	20	3.148E-28	0.506	0
DT661142	poly (adp-ribose) glycohydrolase	762	20	8.76E-108	0.986	6
DT661165	signal sequence alpha	718	20	9.16E-117	0.984	7
DT661199	yme1-like 1 (cerevisiae)	679	20	9.451E-73	0.9895	8
DT661260	transposase [Lipotes vexillifer]	609	2	3.389E-09	0.63	0
DT661289	signal peptidase complex subunit 1 homolog (cerevisiae)	531	20	3.137E-54	0.9705	6
DT661361	endonuclease reverse transcriptase	784	20	1.04E-79	0.4285	0
DT661378	endonuclease reverse transcriptase	737	20	2.862E-83	0.383	0

DT661388	beta-2-microglobulin precursor	627	20	3.222E-50	0.8995	5
DT661394	leucyl-trna synthetase	804	20	4.494E-28	0.979	4
DT661395	bub3 budding uninhibited by benzimidazoles 3 homolog	473	20	1.549E-56	0.9695	5
DT661401	atp h+ mitochondrial f0 subunit isoform 2	380	20	5.072E-07	0.9285	11
DV467742	son dna binding isoform f	380	20	2.482E-54	0.999	3
DV467751	endonuclease reverse transcriptase	406	20	2.604E-07	0.539	0
DV467752	cytochrome b	765	20	7.74E-104	0.96	6
DV467753	endonuclease reverse transcriptase	681	20	3.932E-26	0.57	0
DV467758	endonuclease reverse transcriptase	429	20	3.682E-58	0.88	0
DV467780	nhp2 non-histone chromosome protein 2-like 1 (cerevisiae)	526	20	4.976E-49	0.9845	8
DV467805	atp h+ mitochondrial f1 epsilon subunit	322	17	9.929E-11	0.9	7
DV467813	chromobox homolog 3 (hp1 gamma drosophila)	269	20	7.284E-22	0.8605	20
DV467833	nadh dehydrogenase 1 alpha subcomplex 4	257	20	5.657E-22	0.9215	5
DV467837	splicing factor subunit 1	683	20	1.992E-70	1	7
DV467845	ribosomal p0	564	20	7.841E-81	0.99	6
DV467863	septin 7	774	20	5.09E-135	0.9875	10
DV467871	protein kinase c inhibitor aswz variant 5	537	20	9.246E-62	0.974	6
DV467928	calmodulin	699	20	1.581E-41	0.99	13
DV467942	tetratricopeptide repeat domain 13	675	20	1.466E-17	1	1
DV467957	isoform cra_a	662	20	1.325E-54	0.622	3
DV467962	beta-2-microglobulin precursor	649	20	1.862E-51	0.907	5
DV467963	p40	788	20	4.217E-60	0.642	3
DV467978	thymosin beta 4	614	20	5.859E-09	0.961	10
DV467985	p150	662	20	3.473E-16	0.7235	11
DV467999	ribosomal protein l14	636	20	2.651E-47	0.976	3
DV468014	endonuclease reverse transcriptase	541	20	2.013E-39	0.6725	0
DV468034	cyclin i	398	20	5.643E-14	0.9265	2
DV468041	cell division cycle 42	785	20	6.495E-69	0.9965	22
DV468044	ribosomal protein l9	425	20	7.466E-67	0.983	10
DV468051	isoform cra_b	557	20	1.767E-53	0.85	2
DV468053	cornichon homolog 4	497	20	8.035E-61	0.712	4
DV468075	eukaryotic translation elongation factor 1 epsilon 1	140	9	0.0003033	0.7755556	8
DV468085	h2a histone member v	638	20	4.988E-54	0.9995	5
DV468098	nadh dehydrogenase subunit 1	873	20	2.36E-105	0.9495	4
DV468101	guanine nucleotide exchange factor p532	416	19	6.518E-07	0.9936842	4
DV468104	mediator complex subunit 4	259	20	8.676E-31	0.885	9
DV468115	anaphase promoting complex subunit 13	748	20	1.026E-36	0.917	4
DV468152	regulator of g-protein signalling 1	383	20	5.36E-33	0.872	8
DV468171	nuclear receptor binding set domain protein 1	323	20	3.638E-21	0.938	14

DV468180	imap family member 7	391	20	1.591E-37	0.9015	1
DV468184	ribosomal protein s25	455	20	9.085E-41	0.9915	5
DV468187	endonuclease reverse transcriptase	621	20	5.614E-63	0.8675	0
DV468206	ribosomal protein s15a	258	20	1.339E-31	0.9695	5
DV468217	endonuclease reverse transcriptase	413	20	4.38E-11	0.7275	0
DV468232	p40	511	20	4.06E-26	0.7625	2
DV468239	translocated promoter region (to activated met oncogene)	595	20	5.151E-78	0.6235	8
DV468247	nascent polypeptide-associated complex subunit alpha	746	20	4.64E-98	0.9675	8
DV468268	malate dehydrogenase nad	283	20	8.745E-31	0.998	11
DV468297	fucosyltransferase 8	564	20	1.378E-93	0.975	12
DV468298	endonuclease reverse transcriptase	359	20	2.172E-34	0.7715	0
DV468323	c-type lectin-like protein	553	20	2.428E-47	0.732	4
DV468336	light chain smooth muscle and non-muscle	421	20	1.81E-20	0.9795	7
DV468348	endonuclease reverse transcriptase	609	12	5.193E-10	0.5625	0
DV468360	eukaryotic translation elongation factor 1 alpha 1 isoform 1	524	20	1.745E-22	0.98	5
DV468382	dynein light chain roadblock-type 1	530	20	1.53E-45	0.951	7
DV468405	light chain non-sarcomeric	668	20	2.453E-86	0.9775	6
DV468406	orf2	110	8	7.444E-06	0.82	3
DV468414	casps8 and fadd-like apoptosis regulator precursor (cellular fllice-like inhibitory protein) (c-flip) (caspase-eight-related protein) (caspase-like apoptosis regulatory protein) (mach-related inducer of toxicity) (iso	687	20	3.871E-37	0.86	4
DV468423	centrin 3	625	20	1.753E-32	0.9365	5
DV468443	ribosomal protein l23	505	20	1.708E-69	0.9755	5
DV468470	p40	731	20	1.074E-43	0.671	3
DV468484	ribosomal protein s11	429	20	7.01E-25	0.9895	6
DV468486	endonuclease reverse transcriptase	679	20	5.593E-53	0.6495	0
DV468492	ribosomal protein s26	451	20	2.248E-39	0.996	5
DV468530	ribosomal protein l38	328	20	1.017E-15	0.968	5
DV468569	eukaryotic translation initiation factor 3 subunit k	709	20	1.832E-45	0.954	7
DV468572	endonuclease reverse transcriptase	562	20	3.656E-06	0.7	18
DV468607	transmembrane protein 184c	743	20	4.267E-11	0.6875	2
DV468616	alpha 1b	630	20	3.699E-78	0.93	7
DV468626	subfamily member 14	596	20	9.767E-27	0.777	9
DV799543	toll-like receptor 7	434	20	5.372E-37	0.429	13
DV799549	t cell receptor alpha chain	279	10	0.0002321	0.74	0
DV799550	signal transducer and activator of transcription 6	295	15	1.773E-44	0.8273333	12

DV799557	aryl hydrocarbon receptor nuclear translocator	424	20	5.482E-56	0.56	5
DV799558	toll-like receptor 4	283	20	4.396E-29	0.55	1
DV799561	toll-like receptor 2	245	20	2.567E-19	0.6885	8
DV799563	protein kinase beta	280	20	1.705E-31	1	23
DV799566	interleukin 17a	324	20	2.043E-40	0.812	8
DV799568	interleukin 13	279	20	4.21E-22	0.906	9
DV799571	cytochrome family subfamily polypeptide 1	338	20	2.54E-43	0.943	8
DV799573	granulocyte-macrophage colony-stimulating factor	388	17	7.214E-08	0.8817647	3
DV799577	interleukin 2	287	20	5.12E-23	0.838	10
DV799583	interferon gamma	501	20	8.353E-37	0.935	19
DV799584	interleukin-1 beta	801	20	3.94E-109	0.8465	11
DV799590	interleukin 1 alpha	798	20	8.34E-144	0.8695	7
EG329066	heat shock protein 70	523	20	1.116E-58	0.6495	17

ESTs selected from ANNs were assembled into contigs using CAP3 analysis. The resulting contigs and ESTs were then blasted against the (nr) non-redundant protein sequences database (nr) at NCBI using Blast2go. (Blastx cutoff value 1.0E-3).

Table A5. List of genes showing highest sensitivity values selected from ANNs for the determination of the location in male (I) and female (II) dolphins.

I. MALE DOLPHINS

EST NCBI ACC.NO.	IDENTITY	SEQ. LENGTH	#HITS	MIN. EVALUE	SIMILARITY
DT661406	acidic (leucine-rich) nuclear phosphoprotein 32member b	308	20	3.14E-38	96.30%
DT660354	alpha peptide	295	20	5.44E-38	90.35%
DT661123	atp synthase f0 subunit 6	232	20	1.39E-17	89.55%
DT660757	cd47 antigen	772	20	2.03E-96	82.55%
DT661317 ^a	cytochrome b	595	20	1.74E-92	95.00%
DV468628 ^a	cytochrome b	709	20	2.33E-101	95.00%
DT660298	dna replication inhibitor	828	20	5.51E-90	82.70%
DT660989	dpy-30 homolog	655	20	1.13E-48	93.30%
DV468279	dynein light chain roadblock-type 1	383	20	3.08E-17	93.00%
DT660276	endonuclease reverse transcriptase	463	20	2.83E-18	86.95%
DT660828	endonuclease reverse transcriptase	815	20	3.68E-22	76.05%
DT660858	endonuclease reverse transcriptase	515	20	1.54E-14	66.40%
DT661112	endonuclease reverse transcriptase	715	20	3.12E-28	62.95%
DT661240	endonuclease reverse transcriptase	434	20	4.57E-20	84.50%
DV467958	endonuclease reverse transcriptase	768	20	2.20E-10	52.60%
DV468192	endonuclease reverse transcriptase	287	4	2.94E-07	56.00%
DV468356	endonuclease reverse transcriptase	355	20	1.53E-24	76.85%
DV468368	endonuclease reverse transcriptase	711	20	5.65E-47	85.00%
DV468589	endonuclease reverse transcriptase	672	20	1.64E-56	78.20%
DV468593	endonuclease reverse transcriptase	719	20	1.52E-51	75.75%
DT660381	fau	507	20	8.23E-56	96.70%
DV467972	heat shock factor binding protein 1	520	20	3.14E-21	95.80%
DT660904	isoform cra_a	436	1	1.12E-11	74.00%
DV468160	nadh dehydrogenase subunit 2	173	20	1.58E-13	93.10%
DV467908 ^b	normal mucosa of esophagus-specific gene 1 protein	661	19	8.60E-28	82.05%
DV467923 ^b	normal mucosa of esophagus-specific gene 1 protein	634	19	7.73E-28	82.05%
DT660244	novel protein	760	20	4.06E-49	71.45%
DT661221	novel protein	522	20	3.43E-23	98.65%
DV468535	nuclear dna-binding protein	468	20	2.99E-28	96.85%
DT660284	oncostatin m receptor	383	13	4.00E-41	69.15%
DV468406	orf2	110	8	7.27E-06	82.00%
DT661250	p150	543	20	6.82E-12	74.10%
DT661196	peptidylprolyl isomerase-like 1	549	20	1.49E-86	97.50%
DT661142	poly (adp-ribose) glycohydrolase	762	20	8.67E-108	98.60%
DT661405	proteasomebeta1	240	20	5.44E-06	98.20%
DV468234	protein tyrosinenon-receptor type 12	657	20	7.07E-91	82.40%
DT661120	reticulon 4	558	20	1.17E-57	97.00%

DV467845	ribosomal phosphoprotein large PO subunit	564	20	7.66E-81	99.00%
DT660353	ribosomal protein l12	567	20	7.61E-44	98.65%
DV467974	ribosomal protein l21	564	20	4.39E-44	99.45%
DV468450	ribosomal protein l35	236	20	1.94E-11	96.85%
DT660854	signal transducer and activator of transcription 1	745	20	9.36E-128	97.55%
DV468267	thymosin beta 4	471	19	6.23E-10	93.58%
DV799561	toll-like receptor 2	245	20	2.51E-19	68.85%
DV799545	toll-like receptor 6	396	20	4.18E-46	91.20%
DT660379	transposase	824	20	3.63E-25	63.00%
DV468136	tropomyosin 3	465	20	1.49E-35	98.00%
DV468003	upf0197 protein c11orf10 homolog	392	20	9.12E-30	95.85%
DT660255	Zinc cchc domain containing 17	726	20	3.18E-93	97.20%

The following ESTs didn't pass the Evalue cutoff for in the BlastX analysis:

DT660128, DT660132, DT660159, DT660211, DT660251, DT660279, DT660318, DT660321, DT660349, DT660359, DT660362, DT660369, DT660780, DT660787, DT660814, DT660844, DT660848, DT660849, DT660901, DT661031, DT661070, DT661095, DT661122, DT661125, DT661126, DT661138, DT661153, DT661203, DT661248, DT661249, DT661271, DT661280, DT661306, DT661309, DT661350, DT661354, DT661390, DT661391, DT661426, DT661427, DV467765, DV467791, DV467799, DV467810, DV467815, DV467841, DV467842, DV467852, DV467859, DV467864, DV467878, DV467886, DV467912, DV467919, DV467932, DV467939, DV467944, DV467973, DV467986, DV467988, DV467993, DV467998, DV468004, DV468006, DV468022, DV468032, DV468039, DV468061, DV468069, DV468096, DV468122, DV468154, DV468162, DV468170, DV468182, DV468183, DV468194, DV468196, DV468202, DV468227, DV468276, DV468281, DV468293, DV468300, DV468309, DV468311, DV468339, DV468340, DV468371, DV468377, DV468388, DV468400, DV468407, DV468413, DV468419, DV468439, DV468452, DV468459, DV468461, DV468467, DV468469, DV468475, DV468482, DV468489, DV468503, DV468504, DV468516, DV468519, DV468525, DV468526, DV468546, DV468588, DV468591, DV468609, DV468624, DV468625.

Additional 85 ESTs were unsequenced clones (data not shown).

^(a, b) ESTs belonging to the same contig.

II. FEMALE DOLPHINS

EST NCBI ACC.NO.	IDENTITY	SEQ. LENGTH	#HITS	MIN. EVALUE	SIMILARITY
DT661406	acidic (leucine-rich) nuclear phosphoprotein 32member b	308	20	3.14E-38	96.30%
DV468115	anaphase promoting complex subunit 13	748	20	1.00E-36	91.70%
DV467951	atg12 autophagy related 12 homolog	724	20	6.21E-57	92.85%
DT660847	breast cancer early isoform cra_g	707	20	4.79E-115	93.35%
DV468041	cell division cycle 42	785	20	6.34E-69	99.65%
DV467933	centrosome protein 4	700	20	1.54E-49	87.80%
DT661066	cytochrome c oxidase subunit viic	396	20	1.03E-28	94.00%
DT660222	endonuclease reverse transcriptase	390	20	2.73E-50	82.85%

DT660858	endonuclease reverse transcriptase	515	20	1.54E-14	66.40%
DT660862	endonuclease reverse transcriptase	374	13	3.69E-10	74.38%
DT660902	endonuclease reverse transcriptase	718	20	7.60E-08	47.00%
DT661013	endonuclease reverse transcriptase	659	20	3.21E-51	87.35%
DT661320	endonuclease reverse transcriptase	575	20	5.42E-21	81.25%
DV468286	endonuclease reverse transcriptase	547	20	2.55E-21	76.55%
DV468367	endonuclease reverse transcriptase	626	20	5.87E-50	82.35%
DT660293	ferritin I subunit	721	20	4.67E-89	90.15%
DV468264	general transcription factor polypeptide beta 34kda	675	20	8.74E-108	97.25%
DT660850	guanylate binding protein 1	634	20	2.13E-94	94.35%
DV468462	h+lysosomal v0 subunit e1	557	20	1.37E-42	92.40%
DT660816 ^c	h2a histone member v	780	20	1.96E-54	99.95%
DV468085 ^c	h2a histone member v	638	20	4.87E-54	99.95%
DT660235	heavy polypeptide 1	287	20	1.61E-13	90.10%
DV468180	imap family member 7	391	20	1.55E-37	90.15%
DV799547	mediator complex subunit 7	278	0	1.00E-08	100%
DT660825	nadh dehydrogenase 1 alpha 8kda	416	20	1.89E-43	90.40%
DT660265	nop16 nucleolar protein homolog	687	20	7.77E-83	90.55%
DT661250	p150	543	20	6.82E-12	74.10%
DT660160	p40	673	20	1.20E-52	53.00%
DV468470	p40	731	20	1.05E-43	67.10%
DT660328	pap associated domain containing 4	298	20	8.68E-28	95.50%
DV468040	phosphoglycerate mutase 1	718	20	1.77E-56	100.00%
DT661142	poly (adp-ribose) glycohydrolase	762	20	8.67E-108	98.60%
DT661405	proteasome beta 1	240	20	5.44E-06	98.20%
DV468234	protein tyrosine non-receptor type 12	657	20	7.07E-91	82.40%
DT661120	reticulon 4	558	20	1.17E-57	97.00%
DT660353	ribosomal protein l12	567	20	7.61E-44	98.65%
DV468443	ribosomal protein l23	505	20	1.67E-69	99.30%
DT660979	ribosomal protein l23a	149	20	7.27E-06	77.00%
DT661197	ribosomal protein l27	492	20	6.76E-65	98.70%
DV468450	ribosomal protein l35	236	20	1.94E-11	96.85%
DV468037	ribosomal protein l35a	419	20	2.81E-50	98.50%
DT660171	ribosomal protein l36a	219	20	2.66E-16	100.00%
DV468044	ribosomal protein l9	425	20	7.29E-67	98.30%
DV467845	ribosomal protein, large, P0	564	20	7.66E-81	99.00%
DT660202	s100 calcium binding protein a8	385	12	1.09E-06	87.50%
DT660931	similar to ATPase, vacuolar, 14 kD	510	1	9.00E-05	47.00%
DV468287	son dna binding isoform f	381	20	1.02E-36	99.85%
DV468358	sub1 homolog	478	20	7.46E-48	96.20%
DT661029	thymosin beta 4	599	19	1.07E-09	93.53%
DV468393	transmembrane protein 167 precursor	726	20	1.41E-24	98.70%
DV468517	vamp (vesicle-associated membrane protein)- associated protein 33kda	667	20	1.17E-88	94.45%

The following ESTs didn't pass the Evalue cutoff for in the BlastX analysis:

DT660179, DT660190, DT660210, DT660230, DT660237, DT660263, DT660266, DT660299, DT660309, DT660356, DT660377, DT660777, DT660784, DT660812, DT660814, DT660849, DT660901, DT660952, DT660960, DT660967, DT661034, DT661049, DT661054, DT661083, DT661122, DT661125, DT661153, DT661174, DT661188, DT661192, DT661193, DT661222, DT661242, DT661249, DT661251, DT661271, DT661279, DT661304, DT661327, DT661328, DT661333, DT661350, DT661356, DT661391, DT661413, DV467760, DV467767, DV467776, DV467781, DV467793, DV467798, DV467807, DV467842, DV467877, DV467903, DV467904, DV467907, DV467917, DV467939, DV467944, DV467965, DV467970, DV467986, DV468004, DV468022, DV468039, DV468063, DV468067, DV468070, DV468073, DV468109, DV468122, DV468151, DV468158, DV468204, DV468208, DV468249, DV468255, DV468259, DV468271, DV468290, DV468299, DV468307, DV468330, DV468361, DV468362, DV468380, DV468381, DV468388, DV468397, DV468400, DV468407, DV468408, DV468410, DV468428, DV468437, DV468439, DV468447, DV468464, DV468487, DV468489, DV468510, DV468511, DV468527, DV468562, DV468604, DV468625.

Additional 91 ESTs were unsequenced clones (data not shown).

(^c) ESTs belonging to the same contig.

Table A6. List of most significantly differentially regulated genes selected from linear statistical analysis (Bioconductor) for the determination of the location in male (I) and female (II) dolphins.

I. MALE DOLPHINS

EST NCBI ACC.NO.	IDENTITY	SEQ. LENGTH	#HITS	MIN. EVALUE	SIMILARITY
DV468102 ^d	atp synthase f0 subunit 6	755	20	1.84E-78	93.30%
DV468132 ^d	atp synthase f0 subunit 8	435	20	1.32E-28	92.30%
DT661032	atph+mitochondrial f0subunit e	290	20	5.71E-11	86.45%
DT660169	c-c chemokine receptor-like 2	458	20	2.67E-29	74.25%
DT660990	cd48 molecule	713	20	2.72E-57	69.25%
DY470720	cd79aimmunoglobulin-associated alpha	670	9	1.74E-15	75.56%
DV468387 ^f	c-type lectin domain familymember e	308	15	2.60E-08	62.53%
DV468323 ^f	c-type lectin-like protein	553	20	2.37E-47	73.20%
DV467752 ^b	cytochrome b	765	20	7.65E-104	96.00%
DV468013 ^b	cytochrome b	679	20	2.65E-112	96.00%
DV468110 ^b	cytochrome b	654	20	1.83E-99	96.00%
DV468134 ^b	cytochrome b	391	20	1.11E-59	96.00%
DV799537	cytochrome b	276	20	2.96E-12	95.90%
DV467982 ^c	cytochrome c oxidase subunit i	754	20	2.02E-93	97.00%
DV468262 ^c	cytochrome c oxidase subunit i	527	20	6.76E-59	96.00%
DV467789	cytochrome c oxidase subunit ii	442	20	2.00E-56	91.35%
DT660994	cytochrome c oxidase subunit iii	807	20	9.52E-31	95.70%
DT661408	dihydrofolate reductase	624	20	1.27E-83	95.70%
DT660181	endonuclease reverse transcriptase	370	20	3.22E-38	83.55%
DT660271	endonuclease reverse transcriptase	803	20	1.22E-07	55.40%
DT660872	endonuclease reverse transcriptase	833	20	4.91E-61	74.50%
DT660983	endonuclease reverse transcriptase	674	20	2.26E-57	71.35%
DT660984	endonuclease reverse transcriptase	725	20	4.06E-32	65.45%
DT661081	endonuclease reverse transcriptase	636	20	5.51E-13	55.75%
DT661121	endonuclease reverse transcriptase	757	20	9.03E-25	51.60%
DT661240	endonuclease reverse transcriptase	434	20	4.57E-20	84.50%
DV468014	endonuclease reverse transcriptase	541	20	1.97E-39	88.90%
DV468025	endonuclease reverse transcriptase	528	20	4.36E-29	85.10%
DV468138	endonuclease reverse transcriptase	236	20	7.10E-30	89.90%
DV468217	endonuclease reverse transcriptase	413	20	4.28E-11	74.10%
DV468282	endonuclease reverse transcriptase	710	20	1.96E-07	60.85%
DV468589	endonuclease reverse transcriptase	672	20	1.64E-56	78.20%
DT660342	eukaryotic translation elongation factor 1 alpha 1	709	20	1.86E-82	99.00%
DT660236	eukaryotic translation initiation factor 43	414	20	4.64E-58	99.35%
DV467775	eukaryotic translation initiation factorsubunit 236kda	508	20	1.28E-40	99.05%
DV468529	hbs1-like isoform 1	723	20	4.18E-45	97.70%

DV799590	interleukin 1 alpha	798	20	8.15E-144	86.95%
DV799568	interleukin 13	279	20	4.11E-22	94.50%
DV468389	jerky homolog-like	641	2	1.63E-22	69.00%
DV468491	light chainnon-sarcomeric	708	20	3.78E-89	99.10%
DV799542	lymphotoxin alpha precursor	350	0		
DV799541	metallothionein 1E isoform cra_b	172	1	1.34E-04	87.00%
DT661342	mhc class ii antigen	238	20	1.94E-11	79.20%
DT660302 ^a	nadh dehydrogenase subunit 4l	767	20	5.59E-38	95.75%
DV467860 ^a	nadh dehydrogenase subunit 4l	714	20	5.76E-39	97.80%
DV468406	orf2	110	8	7.27E-06	82.00%
DV467974	ribosomal protein l21	564	20	4.39E-44	99.45%
DV467794	ribosomal protein l9	415	20	1.54E-61	98.25%
DT660375	ribosomal proteinx-linked	294	20	1.30E-23	96.00%
DT661289	signal peptidase complex subunit 1 homolog	531	20	3.06E-54	97.05%
DT661135	thioredoxin domain containing 4 (endoplasmic reticulum)	581	20	5.05E-70	90.50%
DV468179 ^e	thymosin beta 4	345	19	5.53E-06	95.26%
DV468267 ^e	thymosin beta 4	471	19	6.23E-10	93.58%
DV799560	toll-like receptor 3	427	20	2.70E-45	86.05%
DV468622	trap mediator complex component trap25	513	1	4.63E-09	80.00%
DV468136	tropomyosin 3	465	20	1.49E-35	98.00%

The following ESTs didn't pass the Evalue cutoff for in the BlastX analysis:

DT660185, DT660296, DT660300, DT660309, DT660368, DT660780, DT660826, DT660849, DT660932, DT660935, DT660956, DT660995, DT661015, DT661028, DT661068, DT661071, DT661110, DT661185, DT661249, DT661275, DT661276, DT661302, DT661353, DT661376, DT661380, DV467765, DV467773, DV467778, DV467799, DV467887, DV467919, DV467926, DV467932, DV467981, DV467983, DV467988, DV468094, DV468135, DV468154, DV468386, DV468407, DV468408, DV468413, DV468476, DV468549, DV468562, DV468599, DV468610, DV799539.

Additional 63 ESTs were unsequenced clones (data not shown).

(^{a, b, c, d, e}) ESTs belonging to the same contig.

II. FEMALE DOLPHINS

EST NCBI ACC.NO.	IDENTITY	SEQ. LENGTH	#HITS	MIN. EVALUE	SIMILARITY
DT661032	atph+mitochondrial f0subunit e	290	20	5.71E-11	86.45%
DT660165 ^f	beta-2-microglobulin precursor	621	20	3.12E-50	89.95%
DT660252 ^f	beta-2-microglobulin precursor	568	20	6.43E-51	89.75%
DV468606	beta-2-microglobulin precursor	402	20	7.87E-21	83.95%
DT660990	cd48 molecule	713	20	2.73E-57	69.25%
DV799572	conserved helix-loop-helix ubiquitous kinase	470	20	2.29E-72	97.10%
DV468387 ^h	c-type lectin domain familymember e	308	15	2.60E-08	62.53%

DV468323 ^h	c-type lectin-like protein	553	20	2.37E-47	73.20%
DV468034	cyclin i	398	20	5.51E-14	92.65%
DV467752	cytochrome b	765	20	7.65E-104	96.00%
DV799537	cytochrome b	276	20	2.96E-12	95.90%
DV467982	cytochrome c oxidase subunit i	754	20	2.02E-93	97.00%
DV468042	cytochrome c oxidase subunit i	412	20	1.96E-48	92.60%
DT660181	endonuclease reverse transcriptase	370	20	3.22E-38	83.55%
DT660222	endonuclease reverse transcriptase	390	20	2.73E-50	82.85%
DT660271	endonuclease reverse transcriptase	803	20	1.22E-07	55.40%
DT660872	endonuclease reverse transcriptase	833	20	4.91E-61	74.50%
DT660896	endonuclease reverse transcriptase	539	20	5.92E-21	84.05%
DT660983	endonuclease reverse transcriptase	674	20	2.26E-57	71.35%
DT661112	endonuclease reverse transcriptase	715	20	3.12E-28	62.95%
DT661146	endonuclease reverse transcriptase	655	20	4.17E-27	90.05%
DV467896	endonuclease reverse transcriptase	728	1	3.96E-04	70.00%
DV468282	endonuclease reverse transcriptase	710	20	1.96E-07	60.85%
DV468589	endonuclease reverse transcriptase	672	20	1.64E-56	78.20%
DV799556	endonuclease reverse transcriptase	140	0	7.00E-12	78.00%
DT660225	esterase d formylglutathione hydrolase	491	20	1.28E-71	97.70%
DV468557	eukaryotic translation elongation factor 1 alpha	818	20	1.33E-104	98.00%
DV467775	eukaryotic translation initiation factor subunit 236kda	508	20	1.28E-40	99.05%
DT660223	ferritin l subunit	685	20	3.34E-86	93.35%
DV468064	heterogeneous nuclear ribonucleoprotein u	550	20	2.19E-29	100.00%
DV799583	interferon gamma	501	20	8.16E-37	93.50%
DV468103	isoform cra_a	453	1	1.63E-10	70.00%
DV799542	lymphotoxin alpha precursor	350	0	1.00E-04	72.00%
DT661342 ^g	mhc class ii antigen	238	20	1.94E-11	79.20%
DV468048 ^g	mhc class ii antigen	644	20	4.78E-89	92.85%
DT660302	nadh dehydrogenase subunit 4l	767	20	5.59E-38	95.75%
DT661339	nefa-interacting nuclear protein nip30	390	20	6.35E-15	96.90%
DV467780	nhp2 non-histone chromosome protein 2-like 1	526	20	4.86E-49	98.45%
DV468613	nucleophosmin 1 isoform 1	689	20	1.47E-73	97.10%
DV468406	orf2	110	8	7.27E-06	82.00%
DV468512	rap1a member of ras oncogene family	659	0	1.00E-05	100%
DT660909	required for meiotic nuclear division 5 homolog	755	20	1.94E-120	92.15%
DT660353	ribosomal protein l12	567	20	7.61E-44	98.65%
DV467824	ribosomal protein l23	486	20	5.97E-69	99.45%
DT661412	ribosomal protein l27	492	20	6.76E-65	98.70%
DV467794	ribosomal protein l9	415	20	1.54E-61	98.25%
DV468563	ribosomal protein s3	743	20	6.28E-92	98.45%
DV467994	selenoprotein k	703	20	3.74E-19	93.40%
DV468123	thymosin beta 4	614	19	1.15E-09	93.47%
DV799564	toll-like receptor 1	473	20	5.75E-49	75.65%

DV799558	toll-like receptor 4	283	20	4.29E-29	100.00%
DV799543	toll-like receptor 7	434	20	5.24E-37	90.55%
DV799544	toll-like receptor 8	443	20	1.60E-29	86.60%
DV468622	trap mediator complex component trap25	513	1	4.63E-09	80.00%
DV467875	tsc1 protein	445	1	4.21E-06	64.00%
DT660315	ubiquitin c	548	20	4.63E-32	99.85%
DV468421	vimentin	639	20	9.00E-48	96.95%
DV468409	zinc finger protein 514	230	6	2.16E-10	73.67%

The following ESTs didn't pass the Evalue cutoff for in the BlastX analysis:

DT660266, DT660296, DT660309, DT660360, DT660780, DT660793, DT660826, DT660849, DT660887, DT660898, DT660932, DT661068, DT661069, DT661071, DT661092, DT661150, DT661158, DT661209, DT661212, DT661248, DT661259, DT661275, DT661276, DT661294, DT661309, DT661315, DT661316, DT661345, DT661346, DT66137, DT661380, DT661411, DV467773, DV467778, DV467799, DV467817, DV467826, DV467827, DV467882, DV467917, DV467921, DV467932, DV467983, DV467988, DV468015, DV468047, DV468095, DV468196, DV468274, DV468303, DV468407, DV468424, DV468468, DV468475, DV468476, DV468477, DV468547, DV468562, DV468608, DV468621, DV468624, DV468630, DV468636, DV468639, DV799580, DV799581.

Additional 68 ESTs were unsequenced clones (data not shown).

(*f,g,h*) ESTs belonging to the same contig.

6. REFERENCES

References

REFERENCES

1. Montagu G (1821) Description of a species of *Delphinus*, which appears to be new. *Memoirs of the Wernerian Natural History Society* 3: 75-82.
2. Caldwell DKaC, M.C. (1972) *The World of the Bottlenose Dolphin*. Philadelphia: Lippincott Williams & Wilkins. 157 p.
3. Shane SH (1988) *The Bottlenose Dolphin in the Wild*. CA: Felton.
4. Laetherwood SaR, R.R. (1990) *The Bottlenose Dolphin San Diego*: Academic Press.
5. Thompson PaW, B. (1994) *Bottlenose Dolphins*. Stillwater: Voyageur Press.
6. Reynolds JE, Wells, R.S., and Eide, S.D. (2000) *Biology and Conservation of the Bottlenose Dolphin*. Gainesville: University of Florida Press.
7. Rice DW (1998) *Marine mammals of the world: systematics and distribution*. Lawrence, KS, USA: Allen Press Inc.
8. Duffield DA, S. H. Ridgway, and L. H. Cornell (1983) Hematology distinguishes coastal and offshore forms of dolphins. *Canadian Journal of Zoology* 61: 930-933.
9. Wells RaS, M. (2002) Bottlenose Dolphins. In: Perrin WW, B. and Thewissen, J., editor. *Encyclopedia of Marine Mammals*: Academic Press. pp. 122-127.
10. Shirihai HaJ, B. (2006) *Whales Dolphins and Other Marine Mammals of the World*. Princeton: Princeton Univ. Press. pp. 155-161.
11. Reeves R, Stewart, B., Clapham, P., Powell, J. (2002) *Guide to Marine Mammals of the World*. New York: Knopf. 528 p.
12. Wells RS, Scott, M.D., Irvine, A.F. (1987) The social structure of free ranging bottlenose dolphins. In: Genoways H, ed, editor. *Current mammalogy*. New York: Plenum Press. pp. 247-305.
13. Zornetzer HR, Duffield D.A. (2003) Captive-born bottlenose dolphin × common dolphin (*Tursiops truncatus* × *Delphinus capensis*) intergeneric hybrids. *Canadian Journal of Zoology* 81: 1755-1762.
14. Herzog D, Moewe, K., & Brunnick, B. (2003) Interspecies interactions between Atlantic spotted dolphins, *Stenella frontalis* and bottlenose dolphins, *Tursiops truncatus*, on Great Bahama Bank, Bahamas. *Aquatic Mammals* 29: 335-341.
15. Pack AA, Herman LM (1995) Sensory integration in the bottlenosed dolphin: immediate recognition of complex shapes across the senses of echolocation and vision. *J Acoust Soc Am* 98: 722-733.
16. Janik VM, Slater PJB (1998) Context-specific use suggests that bottlenose dolphin signature whistles are cohesion calls. *Anim Behav* 56: 829-838.
17. LeDuc RG, Perrin WF, Dizon AE (1999) Phylogenetic relationships among the delphinid cetaceans based on full cytochrome b sequences. *Mar Mamm Sci* 15: 619-648.
18. Xiong Y, Brandley MC, Xu S, Zhou K, Yang G (2009) Seven new dolphin mitochondrial genomes and a time-calibrated phylogeny of whales. *BMC Evol Biol* 9: 20.
19. Graur D, Higgins, D. G. (1996) Molecular evidence for the inclusion of cetaceans within the order Artiodactyla. *Mol Biol Evol* 11: 357-364.

20. Hasegawa M, Adachi, J. (1996) Phylogenetic position of cetaceans relative to artiodactyls: reanalysis of mitochondrial and nuclear sequences. *Mol Biol Evol* 13: 710-717.
21. Berta A, Sumich, J.L., Kovacs, K.M (2006) *Marine Mammals Evolutionary Biology*, second edition: Academic Press. 547 p.
22. O'Leary MA, Geisler JH (1999) The position of Cetacea within mammalia: phylogenetic analysis of morphological data from extinct and extant taxa. *Syst Biol* 48: 455-490.
23. Irwin DM, Arnason U (1994) Cytochrome b gene of marine mammals: phylogeny and evolution. *Journal of Mammalian Evolution* 2: 37-55.
24. Gatesy J, Hayashi C, Cronin MA, Arctander P (1996) Evidence from milk casein genes that cetaceans are close relatives of hippopotamid artiodactyls. *Mol Biol Evol* 13: 954-963.
25. Gingerich PD, Haq M, Zalmout IS, Khan IH, Malkani MS (2001) Origin of whales from early artiodactyls: hands and feet of Eocene Protocetidae from Pakistan. *Science* 293: 2239-2242.
26. Price SA, Bininda-Emonds OR, Gittleman JL (2005) A complete phylogeny of the whales, dolphins and even-toed hoofed mammals (Cetartiodactyla). *Biol Rev Camb Philos Soc* 80: 445-473.
27. Uhen MD (1998) Middle to late Eocene basilosaurines and dorudontines. In: Thewissen JGM, editor. *The Emergence of Whales: Patterns in the Origin of Cetacea*. New York: Plenum Press. pp. 29-61.
28. Jefferson T, Webber, M., Pitman, R. (2008) *Marine Mammals of the World*. Burlington, MA: Academic Press.
29. Goforth HWJ (1990) Ergometry (Exercise Testing) of the Bottlenose Dolphin. In: Reeves SLaRR, editor. *The Bottlenose Dolphin*. San Diego: Academic Press. pp. 559-574.
30. Ridgway S (1972) *Mammals of the Sea. Biology and Medicine*. Springfield, Illinois: Charles C. Thomas.
31. Bryden MM, Harrison R (1986) *Research on Dolphins*. New York: Oxford University Press.
32. Ridgway SH (1990) The Central Nervous System of the Bottlenose Dolphin. In: Leatherwood S RR, editor. *The Bottlenose Dolphin*. San Diego: Academic Press. pp. 69-97.
33. Noren SR, Williams TM, Pabst DA, McLellan WA, Dearolf JL (2001) The development of diving in marine endotherms: preparing the skeletal muscles of dolphins, penguins, and seals for activity during submergence. *J Comp Physiol B* 171: 127-134.
34. Noren SR, Lacave, G., Wells, R.S., Williams, T.M. (2002) The development of blood oxygen stores in bottlenose dolphins (*Tursiops truncatus*): implications for diving capacity. *J Zool* 258: 105-113.
35. Noren SR, Cuccurullo V, Williams TM (2004) The development of diving bradycardia in bottlenose dolphins (*Tursiops truncatus*). *J Comp Physiol B* 174: 139-147.
36. Scott MD, Wells, R.S., Irvine, A.B. (1990) A long-term study of bottlenose dolphins on the west coast of Florida. In: Leatherwood S RR, editor. *The bottlenose dolphin*. San Diego: Academic Press. pp. 235-244.
37. Mukhametov LM, Oleksenko AI, Polyakova IG (1987) Quantification of ECoG stages of sleep in the bottlenose dolphin *Neurophysiology* 20: 398-403.

38. Houde M, Pacepavicius G, Wells RS, Fair PA, Letcher RJ, et al. (2006) Polychlorinated biphenyls and hydroxylated polychlorinated biphenyls in plasma of bottlenose dolphins (*Tursiops truncatus*) from the Western Atlantic and the Gulf of Mexico. *Environ Sci Technol* 40: 5860-5866.
39. Fair PA, Mitchum G, Hulsey TC, Adams J, Zolman E, et al. (2007) Polybrominated diphenyl ethers (PBDEs) in blubber of free-ranging bottlenose dolphins (*Tursiops truncatus*) from two southeast Atlantic estuarine areas. *Arch Environ Contam Toxicol* 53: 483-494.
40. Stavros HC, Bossart GD, Hulsey TC, Fair PA (2008) Trace element concentrations in blood of free-ranging bottlenose dolphins (*Tursiops truncatus*): influence of age, sex and location. *Mar Pollut Bull* 56: 371-379.
41. Wells DE, Campbell LA, Ross HM, Thompson PM, Lockyer CH (1994) Organochlorine residues in harbour porpoise and bottlenose dolphins stranded on the coast of Scotland, 1988-1991. *Sci Total Environ* 151: 77-99.
42. Scholin CA, Gulland F, Doucette GJ, Benson S, Busman M, et al. (2000) Mortality of sea lions along the central California coast linked to a toxic diatom bloom. *Nature* 403: 80-84.
43. Vos JG, Bossart, G.D., Fournier, T.J., O'Shea, T.J. (2003) *Toxicology of marine mammals*: CRC Press, 2003. 643 p.
44. Flewelling LJ, Naar JP, Abbott JP, Baden DG, Barros NB, et al. (2005) Brevetoxicosis: red tides and marine mammal mortalities. *Nature* 435: 755-756.
45. Van Dolah FM (2005) Effects of Harmful Algal Blooms. In: Reynolds JE, Perrin, W.F., Reeves, R.R., Montgomery, S., Ragen, T.J., editor. *Marine Mammal Research Conservation beyond Crisis*. Baltimore: The John Hopkins University press.
46. Wells RS (1991) The role of long-term study in understanding the social structure of a bottlenose dolphin community. In: Norris KP, S., editor. *Dolphin Societies: Discoveries and Puzzles*. Berkeley: Univ. of California Press. pp. 199-225.
47. Owen ECG, Hofmann, S., Wells, R.S. (2002) Ranging and social association patterns of paired and unpaired adult male bottlenose dolphins, *Tursiops truncatus*, in Sarasota, Florida, provide no evidence for alternative male strategies. *Canadian Journal of Zoology* 80: 2072-2089.
48. Hansen LJ, Schwacke LH, Mitchum GB, Hohn AA, Wells RS, et al. (2004) Geographic variation in polychlorinated biphenyl and organochlorine pesticide concentrations in the blubber of bottlenose dolphins from the US Atlantic coast. *Sci Total Environ* 319: 147-172.
49. Montie EW, Garvin SR, Fair PA, Bossart GD, Mitchum GB, et al. (2007) Blubber morphology in wild bottlenose dolphins (*Tursiops truncatus*) from the Southeastern United States: Influence of geographic location, age class, and reproductive state. *J Morphol* 269: 496-511.
50. Montie EW, Fair PA, Bossart GD, Mitchum GB, Houde M, et al. (2008) Cytochrome P4501A1 expression, polychlorinated biphenyls and hydroxylated metabolites, and adipocyte size of bottlenose dolphins from the Southeast United States. *Aquat Toxicol* 86: 397-412.
51. Wilson J, Wells RS, Aguilar A, Borrell A, Tornero V, et al. (2007) Correlates of cytochrome P450 1A1 expression in bottlenose dolphin (*Tursiops truncatus*) integument biopsies. *Toxicol Sci* 97: 111-119.

52. Wells RS, Tornero V, Borrell A, Aguilar A, Rowles TK, et al. (2005) Integrating life-history and reproductive success data to examine potential relationships with organochlorine compounds for bottlenose dolphins (*Tursiops truncatus*) in Sarasota Bay, Florida. *Sci Total Environ* 349.
53. Rehtanz M, Ghim SJ, Rector A, Van Ranst M, Fair PA, et al. (2006) Isolation and characterization of the first American bottlenose dolphin papillomavirus: *Tursiops truncatus* papillomavirus type 2. *J Gen Virol* 87: 3559-3565.
54. Bracht AJ, Brudek RL, Ewing RY, Manire CA, Burek KA, et al. (2006) Genetic identification of novel poxviruses of cetaceans and pinnipeds. *Arch Virol* 151: 423-438.
55. Van Bresse MF, Van Waerebeek K, Raga JA (1999) A review of virus infections of cetaceans and the potential impact of morbilliviruses, poxviruses and papillomaviruses on host population dynamics. *Dis Aquat Organ* 38: 53-65.
56. Kiszka J, Van Bresse MF, Pusineri C (2009) Lobomycosis-like disease and other skin conditions in Indo-Pacific bottlenose dolphins *Tursiops aduncus* from the Indian Ocean. *Dis Aquat Organ* 84: 151-157.
57. Murdoch ME, Reif JS, Mazzoil M, McCulloch SD, Fair PA, et al. (2008) Lobomycosis in bottlenose dolphins (*Tursiops truncatus*) from the Indian River Lagoon, Florida: estimation of prevalence, temporal trends, and spatial distribution. *Ecohealth* 5: 289-297.
58. Dubey JP, Fair PA, Sundar N, Velmurugan G, Kwok OC, et al. (2008) Isolation of *Toxoplasma gondii* from bottlenose dolphins (*Tursiops truncatus*). *J Parasitol* 94: 821-823.
59. Dubey JP, Mergl J, Gehring E, Sundar N, Velmurugan GV, et al. (2009) Toxoplasmosis in captive dolphins (*Tursiops truncatus*) and walrus (*Odobenus rosmarus*). *J Parasitol* 95: 82-85.
60. Inskoop W, 2nd, Gardiner CH, Harris RK, Dubey JP, Goldston RT (1990) Toxoplasmosis in Atlantic bottle-nosed dolphins (*Tursiops truncatus*). *J Wildl Dis* 26: 377-382.
61. Jardine JE, Dubey JP (2002) Congenital toxoplasmosis in a Indo-Pacific bottlenose dolphin (*Tursiops aduncus*). *J Parasitol* 88: 197-199.
62. Ewing RY, Mignucci-Giannoni AA (2003) A poorly differentiated pulmonary squamous cell carcinoma in a free-ranging Atlantic bottlenose dolphin (*Tursiops truncatus*). *J Vet Diagn Invest* 15: 162-165.
63. Renner MS, Ewing R, Bossart GD, Harris D (1999) Sublingual squamous cell carcinoma in an Atlantic bottlenose dolphin (*Tursiops truncatus*). *J Zoo Wildl Med* 30: 573-576.
64. Sanchez J, Kuba L, Beron-Vera B, Dans SL, Crespo EA, et al. (2002) Uterine adenocarcinoma with generalised metastasis in a bottlenose dolphin *Tursiops truncatus* from northern Patagonia, Argentina. *Dis Aquat Organ* 48: 155-159.
65. Rotstein DS, Burdett LG, McLellan W, Schwacke L, Rowles T, et al. (2009) Lobomycosis in offshore bottlenose dolphins (*Tursiops truncatus*), North Carolina. *Emerg Infect Dis* 15: 588-590.
66. Bossart GD (2006) Marine Mammals as Sentinel Species for Oceans and Human Health. *Oceanography* 19: 134-137.
67. McKenzie C, Rogan E, Reid RJ, Wells DE (1997) Concentrations and patterns of organic contaminants in Atlantic white-sided dolphins (*Lagenorhynchus acutus*) from Irish and Scottish coastal waters. *Environ Pollut* 98: 15-27.

68. Kastelein RA, Vaughan N, Walton S, Wiepkema PR (2002) Food intake and body measurements of Atlantic bottlenose dolphins (*Tursiops truncatus*) in captivity. *Mar Environ Res* 53: 199-218.
69. Camara Pellisso S, Munoz MJ, Carballo M, Sanchez-Vizcaino JM (2008) Determination of the immunotoxic potential of heavy metals on the functional activity of bottlenose dolphin leukocytes in vitro. *Vet Immunol Immunopathol* 121: 189-198.
70. Sitt T, Bowen L, Blanchard MT, Smith BR, Gershwin LJ, et al. (2008) Quantitation of leukocyte gene expression in cetaceans. *Dev Comp Immunol* 32: 1253-1259.
71. Shirai K, Sakai T, Fukuda M, Oike T (1998) A monoclonal antibody against dolphin lymphocytes (6E9) which recognizes bovine MHC class II antigens. *J Vet Med Sci* 60: 291-293.
72. Shirai K, Sakai T, Oike T (1998) Molecular cloning of bottle-nosed dolphin (*Tursiops truncatus*) MHC class I cDNA. *J Vet Med Sci* 60: 1093-1096.
73. Wiinschmann A, Armien A, Harris NB, Brown-Elliott BA, Wallace RJ, Jr., et al. (2008) Disseminated panniculitis in a bottlenose dolphin (*Tursiops truncatus*) due to *Mycobacterium chelonae* infection. *J Zoo Wildl Med* 39: 412-420.
74. Malakoff D (2001) Marine mammals. Scientists use strandings to bring species to life. *Science* 293: 1754-1757.
75. Miclard J, Mokhtari K, Jouvion G, Wyrzykowski B, Van Canneyt O, et al. (2006) Microcystic meningioma in a dolphin (*Delphinus delphis*): immunohistochemical and ultrastructural study. *J Comp Pathol* 135: 254-258.
76. Miller WG, Adams LG, Ficht TA, Cheville NF, Payeur JP, et al. (1999) Brucella-induced abortions and infection in bottlenose dolphins (*Tursiops truncatus*). *J Zoo Wildl Med* 30: 100-110.
77. Parsons EC, Jefferson TA (2000) Post-mortem investigations on stranded dolphins and porpoises from Hong Kong waters. *J Wildl Dis* 36: 342-356.
78. Reidarson TH, Griner LA, Pappagianis D, McBain J (1998) Coccidioidomycosis in a bottlenose dolphin. *J Wildl Dis* 34: 629-631.
79. Reidarson TH, Harrell JH, Rinaldi MG, McBain J (1998) Bronchoscopic and serologic diagnosis of *Aspergillus fumigatus* pulmonary infection in a bottlenose dolphin (*Tursiops truncatus*). *J Zoo Wildl Med* 29: 451-455.
80. Blanchard TW, Santiago NT, Lipscomb TP, Garber RL, McFee WE, et al. (2001) Two novel alphaherpesviruses associated with fatal disseminated infections in Atlantic bottlenose dolphins. *J Wildl Dis* 37: 297-305.
81. McFee WE, Carl AO (2004) Struvite calculus in the vagina of a bottlenose dolphin (*Tursiops truncatus*). *J Wildl Dis* 40: 125-128.
82. Bearzi M, Rapoport S, Chau J, Saylan C (2009) Skin lesions and physical deformities of coastal and offshore common bottlenose dolphins (*Tursiops truncatus*) in Santa Monica Bay and adjacent areas, California. *Ambio* 38: 66-71.
83. Mazzoil M, Reif JS, Youngbluth M, Murdoch ME, Bechdel SE, et al. (2008) Home ranges of bottlenose dolphins (*Tursiops truncatus*) in the Indian River Lagoon, Florida: environmental correlates and implications for management strategies. *Ecohealth* 5: 278-288.
84. Mazzoil MS, McCulloch SD, Youngbluth M, Kilpatrick DS, Murdoch ME, et al. (2008) Radio-Tracking and Survivorship of Two Rehabilitated Bottlenose Dolphins

- (*Tursiops truncatus*) in the Indian River Lagoon, Florida. *Aquatic Mammals* 34: 54-64.
85. Van Bresselem MF, Santos MC, Oshima JE (2009) Skin diseases in Guiana dolphins (*Sotalia guianensis*) from the Paranagua estuary, Brazil: a possible indicator of a compromised marine environment. *Mar Environ Res* 67: 63-68.
 86. Fossi MC, Casini S, Bucalossi D, Marsili L (2008) First detection of CYP1A1 and CYP2B induction in Mediterranean cetacean skin biopsies and cultured fibroblasts by Western blot analysis. *Mar Environ Res* 66: 3-6.
 87. Wilson JY, Wells R, Aguilar A, Borrell A, Tornero V, et al. (2007) Correlates of cytochrome P450 1A1 expression in bottlenose dolphin (*Tursiops truncatus*) integument biopsies. *Toxicol Sci* 97: 111-119.
 88. Goldstein JD, Reese E, Reif JS, Varela RA, McCulloch SD, et al. (2006) Hematologic, biochemical, and cytologic findings from apparently healthy atlantic bottlenose dolphins (*Tursiops truncatus*) inhabiting the Indian River Lagoon, Florida, USA. *J Wildl Dis* 42: 447-454.
 89. Dubey JR, Fair PA, Bossartt GD, Hill D, Fayer R, et al. (2005) A comparison of several serologic tests to detect antibodies to *Toxoplasma gondii* in naturally exposed bottlenose dolphins (*Tursiops truncatus*). *J Parasitol* 91: 1074-1081.
 90. Colgrove GS (1978) Stimulation of lymphocytes from a dolphin (*Tursiops truncatus*) by phytomitogens. *Am J Vet Res* 39: 141-144.
 91. Mumford DM, Stockman GD, Barsales PB, Whitman T, Wilbur JR (1975) Lymphocyte transformation studies of sea mammal blood. *Experientia* 31: 498-500.
 92. Erickson KL, DiMolfetto-Landon L, Wells RS, Reidarson T, Stott JL, et al. (1995) Development of an interleukin-2 receptor expression assay and its use in evaluation of cellular immune responses in bottlenose dolphin (*Tursiops truncatus*). *J Wildl Dis* 31: 142-149.
 93. Lahvis GP, Wells RS, Kuehl DW, Stewart JL, Rhinehart HL, et al. (1995) Decreased lymphocyte responses in free-ranging bottlenose dolphins (*Tursiops truncatus*) are associated with increased concentrations of PCBs and DDT in peripheral blood. *Environ Health Perspect* 103 Suppl 4: 67-72.
 94. Nakata H, Sakakibara A, Kanoh M, Kudo S, Watanabe H, et al. (2002) Evaluation of mitogen-induced responses in marine mammal and human lymphocytes by in-vitro exposure of butyltins and non-ortho coplanar PCBs. *Environ Pollut* 120: 245-253.
 95. Inoue Y, Ito T, Oike T, Sakai T (1999) Cloning and sequencing of the bottle-nosed dolphin (*Tursiops truncatus*) interferon-gamma gene. *J Vet Med Sci* 61: 939-942.
 96. Inoue Y, Ito T, Sakai T, Oike T (1999) Cloning and sequencing of a bottle-nosed dolphin (*Tursiops truncatus*) interleukin-4-encoding cDNA. *J Vet Med Sci* 61: 693-696.
 97. Inoue Y, Ito T, Ueda K, Oike T, Sakai T (1999) Cloning and sequencing of a bottle-nosed dolphin (*Tursiops truncatus*) interleukin-1alpha and -1beta complementary DNAs. *J Vet Med Sci* 61: 1317-1321.
 98. Inoue Y, Ito T, Jimbo T, Syouji Y, Ueda K, et al. (2001) Molecular cloning and functional expression of bottle-nosed dolphin (*Tursiops truncatus*) interleukin-1 receptor antagonist. *Vet Immunol Immunopathol* 78: 131-141.

99. Itou T, Yoshida Y, Shoji Y, Sugisawa H, Endo T, et al. (2003) Molecular cloning and expression of bottlenose dolphin (*Tursiops truncatus*) interleukin-8. *J Vet Med Sci* 65: 1351-1354.
100. Lundqvist ML, Kohlberg KE, Gefroh HA, Arnaud P, Middleton DL, et al. (2002) Cloning of the IgM heavy chain of the bottlenose dolphin (*Tursiops truncatus*), and initial analysis of VH gene usage. *Dev Comp Immunol* 26: 551-562.
101. Mancia A, Romano, T. A., Gefroh, H. A., Chapman, R. W., Middleton, D. L., Warr, G. W. and Lundqvist, M. L. (2006) The Immunoglobulin G Heavy Chain (IGHG) genes of the Atlantic bottlenose dolphin, *Tursiops truncatus*. *Comp Biochem Physiol B Biochem Mol Biol* 144: 38-46.
102. Mancia A, Romano TA, Gefroh HA, Chapman RW, Middleton DL, et al. (2007) Characterization of the immunoglobulin A heavy chain gene of the Atlantic bottlenose dolphin (*Tursiops truncatus*). *Vet Immunol Immunopathol* 118: 304-309.
103. Murray BW, White BN (1998) Sequence variation at the major histocompatibility complex DRB loci in beluga (*Delphinapterus leucas*) and narwhal (*Monodon monoceros*). *Immunogenetics* 48: 242-252.
104. Romano TA, Ridgway SH, Felten DL, Quaranta V (1999) Molecular cloning and characterization of CD4 in an aquatic mammal, the white whale *Delphinapterus leucas*. *Immunogenetics* 49: 376-383.
105. Shoji Y, Inoue Y, Sugisawa H, Itou T, Endo T, et al. (2001) Molecular cloning and functional characterization of bottlenose dolphin (*Tursiops truncatus*) tumor necrosis factor alpha. *Vet Immunol Immunopathol* 82: 183-192.
106. Spinsanti G, Panti C, Lazzeri E, Marsili L, Casini S, et al. (2006) Selection of reference genes for quantitative RT-PCR studies in striped dolphin (*Stenella coeruleoalba*) skin biopsies. *BMC Mol Biol* 7: 32.
107. Mollenhauer MA, Carter BJ, Peden-Adams MM, Bossart GD, Fair PA (2009) Gene expression changes in bottlenose dolphin, *Tursiops truncatus*, skin cells following exposure to methylmercury (MeHg) or perfluorooctane sulfonate (PFOS). *Aquat Toxicol* 91: 10-18.
108. De Guise S, Erickson K, Blanchard M, DiMolfetto L, Lepper H, et al. (1998) Characterization of a monoclonal antibody that recognizes a lymphocyte surface antigen for the cetacean homologue to CD45R. *Immunology* 94: 207-212.
109. De Guise S, Erickson K, Blanchard M, DiMolfetto L, Lepper HD, et al. (2004) Characterization of F21.A, a monoclonal antibody that recognize a leucocyte surface antigen for killer whale homologue to beta-2 integrin. *Vet Immunol Immunopathol* 97: 195-206.
110. De Guise S, Erickson K, Blanchard M, DiMolfetto L, Lepper HD, et al. (2002) Monoclonal antibodies to lymphocyte surface antigens for cetacean homologues to CD2, CD19 and CD21. *Vet Immunol Immunopathol* 84: 209-221.
111. St-Laurent G, Archambault D (2000) Molecular cloning, phylogenetic analysis and expression of beluga whale (*Delphinapterus leucas*) interleukin 6. *Vet Immunol Immunopathol* 73: 31-44.
112. St-Laurent G, Beliveau C, Archambault D (1999) Molecular cloning and phylogenetic analysis of beluga whale (*Delphinapterus leucas*) and grey seal (*Halichoerus grypus*) interleukin 2. *Vet Immunol Immunopathol* 67: 385-394.

113. Halic M, Becker T, Pool MR, Spahn CM, Grassucci RA, et al. (2004) Structure of the signal recognition particle interacting with the elongation-arrested ribosome. *Nature* 427: 808-814.
114. Zabka TS, Romano TA (2003) Distribution of MHC II (+) cells in skin of the Atlantic bottlenose dolphin (*Tursiops truncatus*): an initial investigation of dolphin dendritic cells. *Anat Rec A Discov Mol Cell Evol Biol* 273: 636-647.
115. Beck BM, Rice CD (2003) Serum antibody levels against select bacterial pathogens in Atlantic bottlenose dolphins, *Tursiops truncatus*, from Beaufort NC USA and Charleston Harbor, Charleston, SC, USA. *Mar Environ Res* 55: 161-179.
116. Nielsen O, Stewart RE, Nielsen K, Measures L, Duignan P (2001) Serologic survey of *Brucella* spp. antibodies in some marine mammals of North America. *J Wildl Dis* 37: 89-100.
117. Nollens HH, Ruiz C, Walsh MT, Gulland FM, Bossart G, et al. (2008) Cross-reactivity between immunoglobulin G antibodies of whales and dolphins correlates with evolutionary distance. *Clin Vaccine Immunol* 15: 1547-1554.
118. Nollens HH, Green LG, Duke D, Walsh MT, Chittick B, et al. (2007) Development and validation of monoclonal and polyclonal antibodies for the detection of immunoglobulin G of bottlenose dolphins (*Tursiops truncatus*). *J Vet Diagn Invest* 19: 465-470.
119. Kato M, Itou T, Nagatsuka N, Sakai T (2009) Production of monoclonal antibody specific for bottlenose dolphin neutrophils and its application to cell separation. *Dev Comp Immunol* 33: 14-17.
120. Mancia A, Lundqvist ML, Romano TA, Peden-Adams MM, Fair PA, et al. (2007) A dolphin peripheral blood leukocyte cDNA microarray for studies of immune function and stress reactions. *Dev Comp Immunol* 31: 520-529.
121. Almeida JS, McKillen DJ, Chen YA, Gross PS, Chapman RW, et al. (2005) Design and calibration of microarrays as universal transcriptomic environmental biosensors. *Comp Funct Genomics* 6: 132-137.
122. Gracey AY, Cossins AR (2003) Application of microarray technology in environmental and comparative physiology. *Annu Rev Physiol* 65: 231-259.
123. Gracey AY, Fraser EJ, Li W, Fang Y, Taylor RR, et al. (2004) Coping with cold: An integrative, multitissue analysis of the transcriptome of a poikilothermic vertebrate. *Proc Natl Acad Sci U S A* 101: 16970-16975.
124. Scherf U, Ross DT, Waltham M, Smith LH, Lee JK, et al. (2000) A gene expression database for the molecular pharmacology of cancer. *Nat Genet* 24: 236-244.
125. Staunton JE, Slonim DK, Collier HA, Tamayo P, Angelo MJ, et al. (2001) Chemosensitivity prediction by transcriptional profiling. *Proc Natl Acad Sci U S A* 98: 10787-10792.
126. Weinstein JN (1998) Fishing expeditions. *Science* 282: 628-629.
127. Weinstein JN (2000) Pharmacogenomics--teaching old drugs new tricks. *N Engl J Med* 343: 1408-1409.
128. Chapman RW (2001) EcoGenomics--a consilience for comparative immunology? *Dev Comp Immunol* 25: 549-551.
129. De Ceuninck F, Berenbaum F (2009) Proteomics: addressing the challenges of osteoarthritis. *Drug Discov Today*.

130. Freeman WM, Hemby SE (2004) Proteomics for protein expression profiling in neuroscience. *Neurochem Res* 29: 1065-1081.
131. Graham DR, Elliott ST, Van Eyk JE (2005) Broad-based proteomic strategies: a practical guide to proteomics and functional screening. *J Physiol* 563: 1-9.
132. Nordon I, Brar R, Hinchliffe R, Cockerill G, Loftus I, et al. (2009) The role of proteomic research in vascular disease. *J Vasc Surg* 49: 1602-1612.
133. Taylor AD, Hancock WS, Hincapie M, Taniguchi N, Hanash SM (2009) Towards an integrated proteomic and glycomic approach to finding cancer biomarkers. *Genome Med* 1: 57.
134. Weiss LM, Fiser A, Angeletti RH, Kim K (2009) *Toxoplasma gondii* proteomics. *Expert Rev Proteomics* 6: 303-313.
135. Alberts B, Johnson A, Julian L, Raff M, Roberts K, et al. (2007) *Molecular Biology of the Cell*: Garland Science.
136. Houde M, Bujas TA, Small J, Wells RS, Fair PA, et al. (2006) Biomagnification of perfluoroalkyl compounds in the bottlenose dolphin (*Tursiops truncatus*) food web. *Environ Sci Technol* 40: 4138-4144.
137. Cardellicchio N, Decataldo A, Di Leo A, Giandomenico S (2002) Trace elements in organs and tissues of striped dolphins (*Stenella coeruleoalba*) from the Mediterranean sea (Southern Italy). *Chemosphere* 49: 85-90.
138. Cardellicchio N, Giandomenico S, Ragone P, Di Leo A (2000) Tissue distribution of metals in striped dolphins (*Stenella coeruleoalba*) from the Apulian coasts, southern Italy. *Mar Environ Res* 49: 55-66.
139. Cardellicchio N, Decataldo A, Di LA, Misino A (2002) Accumulation and tissue distribution of mercury and selenium in striped dolphins (*Stenella coeruleoalba*) from the Mediterranean Sea (southern Italy). *Environ Pollut* 116: 265-271.
140. Parsons EC, Chan HM (2001) Organochlorine and trace element contamination in bottlenose dolphins (*Tursiops truncatus*) from the South China Sea. *Mar Pollut Bull* 42: 780-786.
141. Roditi-Elasar M, Kerem D, Hornung H, Kress N, Shoham-Frider E, et al. (2003) Heavy metal levels in bottlenose and striped dolphins off the Mediterranean coast of Israel. *Mar Pollut Bull* 46: 503-512.
142. Carvan M, Millar S, Busbee DL (2002) Cellular and molecular investigation utilizing a bottlenose dolphin epithelial cell line. In: Pfeiffer CJ, editor. *Molecular and cell biology of marine mammals*. Melabar, Florida: Krieger. pp. 313-327.
143. Carvan M, Santostefano M, Safe S, Busbee DL (1994) Characterization of a bottlenose dolphin (*Tursiops truncatus*) kidney epithelial cell line. *Mar Mammal Sci* 10: 52-69.
144. Cecil JT, Nigrelli RF (1970) Cell cultures from marine mammals. *J Wildl Dis* 6: 494-495.
145. Dotzauer A, Feinstone SM, Kaplan G (1994) Susceptibility of nonprimate cell lines to hepatitis A virus infection. *J Virol* 68: 6064-6068.
146. Kadoi K, Mochizuki A, Ikeda T, Kamata H, Yukawa M, et al. (1992) Susceptibility of a line of dolphin kidney cell culture to several herpesviruses. *J Basic Microbiol* 32: 227-232.
147. Hu W, Jones PD, Upham BL, Trosko JE, Lau C, et al. (2002) Inhibition of gap junctional intercellular communication by perfluorinated compounds in rat liver and

- dolphin kidney epithelial cell lines in vitro and Sprague-Dawley rats in vivo. *Toxicol Sci* 68: 429-436.
148. Pfeiffer CJ, Sharova LV, Gray L (2000) Functional and ultrastructural cell pathology induced by fuel oil in cultured dolphin renal cells. *Ecotoxicol Environ Saf* 47: 210-217.
 149. Wang A, Barber D, Pfeiffer CJ (2001) Protective effects of selenium against mercury toxicity in cultured Atlantic spotted dolphin (*Stenella plagiodon*) renal cells. *Arch Environ Contam Toxicol* 41: 403-409.
 150. Wang A, Pfeiffer CJ (2001) Cytopathology induced by mercuric chloride and methylmercury in cultured renal cells of the Atlantic spotted dolphin (*Stenella plagiodon*). *J Submicrosc Cytol Pathol* 33: 7-16.
 151. Rawson AJ, Bradley JP, Teetsov A, Rice SB, Haller EM, et al. (1995) A role for airborne particulates in high mercury levels of some cetaceans. *Ecotoxicol Environ Saf* 30: 309-314.
 152. Garrick RA, Woodin BR, Wilson JY, Middlebrooks BL, Stegeman JJ (2006) Cytochrome P4501A is induced in endothelial cell lines from the kidney and lung of the bottlenose dolphin, *Tursiops truncatus*. *Aquat Toxicol* 76: 295-305.
 153. Yu J, Kindy MS, Ellis BC, Baatz JE, Peden-Adams M, et al. (2005) Establishment of epidermal cell lines derived from the skin of the Atlantic bottlenose dolphin (*Tursiops truncatus*). *Anat Rec A Discov Mol Cell Evol Biol* 287: 1246-1255.
 154. Ellis BC, Gattoni-Celli S, Mancina A, Kindy MS (2009) The vitamin D3 transcriptomic response in skin cells derived from the Atlantic bottlenose dolphin. *Dev Comp Immunol* 33: 901-912.
 155. Marsili L, Casini S, Bucalossi D, Porcelloni S, Maltese S, et al. (2008) Use of immunofluorescence technique in cultured fibroblasts from Mediterranean cetaceans as new "in vitro" tool to investigate effects of environmental contaminants. *Mar Environ Res* 66: 151-153.
 156. Marsili L, Fossi MC, Neri G, Casini S, Gardi C, et al. (2000) Skin biopsies for cell cultures from Mediterranean free-ranging cetaceans. *Mar Environ Res* 50: 523-526.
 157. Dix DJ, Houck KA, Martin MT, Richard AM, Setzer RW, et al. (2007) The ToxCast program for prioritizing toxicity testing of environmental chemicals. *Toxicol Sci* 95: 5-12.
 158. Ortiz RM, Worthy GA (2000) Effects of capture on adrenal steroid and vasopressin concentrations in free-ranging bottlenose dolphins (*Tursiops truncatus*). *Comp Biochem Physiol A Mol Integr Physiol* 125: 317-324.
 159. Demonacos CV, Karayanni N, Hatzoglou E, Tsiriyiotis C, Spandidos DA, et al. (1996) Mitochondrial genes as sites of primary action of steroid hormones. *Steroids* 61: 226-232.
 160. Psarra AM, Solakidi S, Sekeris CE (2006) The mitochondrion as a primary site of action of regulatory agents involved in neuroimmunomodulation. *Ann N Y Acad Sci* 1088: 12-22.
 161. Ognjanovic S, Bao S, Yamamoto SY, Garibay-Tupas J, Samal B, et al. (2001) Genomic organization of the gene coding for human pre-B-cell colony enhancing factor and expression in human fetal membranes. *J Mol Endocrinol* 26: 107-117.

162. Higgins MA, Berridge BR, Mills BJ, Schultze AE, Gao H, et al. (2003) Gene expression analysis of the acute phase response using a canine microarray. *Toxicol Sci* 74: 470-484.
163. Yoo JY, Desiderio S (2003) Innate and acquired immunity intersect in a global view of the acute-phase response. *Proc Natl Acad Sci U S A* 100: 1157-1162.
164. Talwar S, Munson PJ, Barb J, Fiuza C, Cintron AP, et al. (2006) Gene expression profiles of peripheral blood leukocytes after endotoxin challenge in humans. *Physiol Genomics* 25: 203-215.
165. Remick DG (2005) Interleukin-8. *Crit Care Med* 33: S466-467.
166. Hack CE, Hart M, van Schijndel RJ, Eerenberg AJ, Nuijens JH, et al. (1992) Interleukin-8 in sepsis: relation to shock and inflammatory mediators. *Infect Immun* 60: 2835-2842.
167. Standiford TJ, Kunkel SL, Rolfe MW, Evanoff HL, Allen RM, et al. (1992) Regulation of human alveolar macrophage- and blood monocyte-derived interleukin-8 by prostaglandin E2 and dexamethasone. *Am J Respir Cell Mol Biol* 6: 75-81.
168. Chollet-Martin S, Montravers P, Gibert C, Elbim C, Desmonts JM, et al. (1993) High levels of interleukin-8 in the blood and alveolar spaces of patients with pneumonia and adult respiratory distress syndrome. *Infect Immun* 61: 4553-4559.
169. DeForge LE, Preston AM, Takeuchi E, Kenney J, Boxer LA, et al. (1993) Regulation of interleukin 8 gene expression by oxidant stress. *J Biol Chem* 268: 25568-25576.
170. Strieter RM, Kunkel SL (1994) Acute lung injury: the role of cytokines in the elicitation of neutrophils. *J Investig Med* 42: 640-651.
171. Strieter RM, Koch AE, Antony VB, Fick RB, Jr., Standiford TJ, et al. (1994) The immunopathology of chemotactic cytokines: the role of interleukin-8 and monocyte chemoattractant protein-1. *J Lab Clin Med* 123: 183-197.
172. Baggiolini M (1998) Chemokines and leukocyte traffic. *Nature* 392: 565-568.
173. Ajuebor MN, Swain MG, Perretti M (2002) Chemokines as novel therapeutic targets in inflammatory diseases. *Biochem Pharmacol* 63: 1191-1196.
174. Cassatella MA, Gasperini S, Calzetti F, McDonald PP, Trinchieri G (1995) Lipopolysaccharide-induced interleukin-8 gene expression in human granulocytes: transcriptional inhibition by interferon-gamma. *Biochem J* 310 (Pt 3): 751-755.
175. Gruys E, Toussaint MJ, Niewold TA, Koopmans SJ (2005) Acute phase reaction and acute phase proteins. *J Zhejiang Univ Sci B* 6: 1045-1056.
176. Almeida JS, Stanislaus R, Krug E, Arthur JM (2005) Normalization and analysis of residual variation in two-dimensional gel electrophoresis for quantitative differential proteomics. *Proteomics* 5: 1242-1249.
177. Weigend AS, Mangeas M, Srivastava AN (1995) Nonlinear gated experts for time series: discovering regimes and avoiding overfitting. *Int J Neural Syst* 6: 373-399.
178. Voit EO, Almeida J (2004) Decoupling dynamical systems for pathway identification from metabolic profiles. *Bioinformatics* 20: 1670-1681.
179. Khan J, Wei JS, Ringner M, Saal LH, Ladanyi M, et al. (2001) Classification and diagnostic prediction of cancers using gene expression profiling and artificial neural networks. *Nat Med* 7: 673-679.
180. Wei JS, Greer BT, Westermann F, Steinberg SM, Son CG, et al. (2004) Prediction of clinical outcome using gene expression profiling and artificial neural networks for patients with neuroblastoma. *Cancer Res* 64: 6883-6891.

181. Linder R, Dew D, Sudhoff H, Theegarten D, Remberger K, et al. (2004) The 'subsequent artificial neural network' (SANN) approach might bring more classificatory power to ANN-based DNA microarray analyses. *Bioinformatics* 20: 3544-3552.
182. Dankbar DM, Dawson ED, Mehlmann M, Moore CL, Smagala JA, et al. (2007) Diagnostic microarray for influenza B viruses. *Anal Chem* 79: 2084-2090.
183. Jiang ZF, Machado CA (2009) Evolution of sex-dependent gene expression in three recently diverged species of *Drosophila*. *Genetics* 183: 1175-1185.
184. Waters MD, Olden K, Tennant RW (2003) Toxicogenomic approach for assessing toxicant-related disease. *Mutat Res* 544: 415-424.
185. Whitehead A, Crawford DL (2006) Variation within and among species in gene expression: raw material for evolution. *Mol Ecol* 15: 1197-1211.
186. Lander ES, Linton LM, Birren B, Nusbaum C, Zody MC, et al. (2001) Initial sequencing and analysis of the human genome. *Nature* 409: 860-921.
187. Deininger PL, Moran JV, Batzer MA, Kazazian HH, Jr. (2003) Mobile elements and mammalian genome evolution. *Curr Opin Genet Dev* 13: 651-658.
188. Itoh K, Ishii T, Wakabayashi N, Yamamoto M (1999) Regulatory mechanisms of cellular response to oxidative stress. *Free Radic Res* 31: 319-324.
189. Borghesi LA, Lynes MA (1996) Stress proteins as agents of immunological change: some lessons from metallothionein. *Cell Stress Chaperones* 1: 99-108.
190. Baird SK, Kurz T, Brunk UT (2006) Metallothionein protects against oxidative stress-induced lysosomal destabilization. *Biochem J* 394: 275-283.
191. Small-Howard AL, Berry MJ (2005) Unique features of selenocysteine incorporation function within the context of general eukaryotic translational processes. *Biochem Soc Trans* 33: 1493-1497.
192. Anelli T, Alessio M, Mezghrani A, Simmen T, Talamo F, et al. (2002) ERp44, a novel endoplasmic reticulum folding assistant of the thioredoxin family. *EMBO J* 21: 835-844.
193. Kryukov GV, Castellano S, Novoselov SV, Lobanov AV, Zehtab O, et al. (2003) Characterization of mammalian selenoproteomes. *Science* 300: 1439-1443.
194. Richardson DR (2005) More roles for selenoprotein P: local selenium storage and recycling protein in the brain. *Biochem J* 386: e5-7.
195. Lu C, Qiu F, Zhou H, Peng Y, Hao W, et al. (2006) Identification and characterization of selenoprotein K: an antioxidant in cardiomyocytes. *FEBS Lett* 580: 5189-5197.
196. Bellinger FP, Raman AV, Reeves MA, Berry MJ (2009) Regulation and function of selenoproteins in human disease. *Biochem J* 422: 11-22.
197. Alberts B, Johnson, A., Julian, L., Raff, M., Roberts, K., Walter, P. (2007) *Molecular Biology of the Cell*: Garland Science.
198. Chatterjee R (2007) Cell biology. Cases of mistaken identity. *Science* 315: 928-931.
199. Drexler HG, Dirks WG, MacLeod RA (1999) False human hematopoietic cell lines: cross-contaminations and misinterpretations. *Leukemia* 13: 1601-1607.
200. Drexler HG, MacLeod RA, Dirks WG (2001) Cross-contamination: HS-Sultan is not a myeloma but a Burkitt lymphoma cell line. *Blood* 98: 3495-3496.
201. Liscovitch M, Ravid D (2007) A case study in misidentification of cancer cell lines: MCF-7/AdrR cells (re-designated NCI/ADR-RES) are derived from OVCAR-8 human ovarian carcinoma cells. *Cancer Lett* 245: 350-352.

202. Masters JR (2002) HeLa cells 50 years on: the good, the bad and the ugly. *Nat Rev Cancer* 2: 315-319.
203. Masters JR (2002) False cell lines: The problem and a solution. *Cytotechnology* 39: 69-74.
204. Nelson-Rees WA, Daniels DW, Flandermeyer RR (1981) Cross-contamination of cells in culture. *Science* 212: 446-452.
205. Nelson-Rees WA, Daniels DW, Flandermeyer RR (1981) Human embryonic lung cells (HEL-R66) are of monkey origin. *Arch Virol* 67: 101-104.
206. Kumar D, Cowan DF (2006) Cross-reactivity of antibodies to human antigens with tissues of the bottlenose dolphin, *Tursiops truncatus*, using immunoperoxidase techniques. *Marine Mammal Science* 10: 188-194.
207. Tibbs RF, Elghetany MT, Tran LT, Van Bonn W, Romano T, et al. (2005) Characterization of the coagulation system in healthy dolphins: the coagulation factors, natural anticoagulants, and fibrinolytic products. *Comp Clin Path* 14: 95-98.
208. Elliott JT, Tona A, Plant AL (2003) Comparison of reagents for shape analysis of fixed cells by automated fluorescence microscopy. *Cytometry A* 52: 90-100.
209. Bicknell RJ (1996) Endothelial cell culture *Handbooks in practical animal cell biology*. Cambridge University Press. 136 p.
210. De Groot CJ, Chao VA, Roberts JM, Taylor RN (1995) Human endothelial cell morphology and autacid expression. *Am J Physiol* 268: H1613-1620.
211. Grubbs FE (1969) Procedures for Detecting Outlying Observations in Samples. *Technometrics* 11: 1-21.
212. Halter M, Elliott JT, Hubbard JB, Tona A, Plant AL (2008) Cell volume distributions reveal cell growth rates and division times. *J Theor Biol*.
213. Nosedá M, Chang L, McLean G, Grim JE, Clurman BE, et al. (2004) Notch activation induces endothelial cell cycle arrest and participates in contact inhibition: role of p21^{Cip1} repression. *Mol Cell Biol* 24: 8813-8822.
214. Nosedá M, McLean G, Niessen K, Chang L, Pollet I, et al. (2004) Notch activation results in phenotypic and functional changes consistent with endothelial-to-mesenchymal transformation. *Circ Res* 94: 910-917.
215. Sommer M, Gerth J, Stein G, Wolf G (2005) Transdifferentiation of endothelial and renal tubular epithelial cells into myofibroblast-like cells under in vitro conditions: a morphological analysis. *Cells Tissues Organs* 180: 204-214.
216. Zhu P, Huang L, Ge X, Yan F, Wu R, et al. (2006) Transdifferentiation of pulmonary arteriolar endothelial cells into smooth muscle-like cells regulated by myocardin involved in hypoxia-induced pulmonary vascular remodeling. *Int J Exp Pathol* 87: 463-474.
217. Mani SA, Guo W, Liao MJ, Eaton EN, Ayyanan A, et al. (2008) The epithelial-mesenchymal transition generates cells with properties of stem cells. *Cell* 133: 704-715.
218. Katoh Y, Katoh M (2008) Hedgehog signaling, epithelial-to-mesenchymal transition and miRNA (review). *Int J Mol Med* 22: 271-275.
219. Arciniegas E, Frid MG, Douglas IS, Stenmark KR (2007) Perspectives on endothelial-to-mesenchymal transition: potential contribution to vascular remodeling in chronic pulmonary hypertension. *Am J Physiol Lung Cell Mol Physiol* 293: L1-8.

220. DeRuiter MC, Poelmann RE, VanMunsteren JC, Mironov V, Markwald RR, et al. (1997) Embryonic endothelial cells transdifferentiate into mesenchymal cells expressing smooth muscle actins in vivo and in vitro. *Circ Res* 80: 444-451.
221. Voyta JC, Via DP, Butterfield CE, Zetter BR (1984) Identification and isolation of endothelial cells based on their increased uptake of acetylated-low density lipoprotein. *J Cell Biol* 99: 2034-2040.
222. West J (1999) *Respiratory Physiology: The essentials*; Kelly P, editor. New York: Lippincott Williams & Wilkins.
223. Crapo JD, Barry BE, Gehr P, Bachofen M, Weibel ER (1982) Cell number and cell characteristics of the normal human lung. *Am Rev Respir Dis* 126: 332-337.
224. Wright JR, Dobbs LG (1991) Regulation of pulmonary surfactant secretion and clearance. *Annu Rev Physiol* 53: 395-414.
225. Wright JR (2004) Host defense functions of pulmonary surfactant. *Biol Neonate* 85: 326-332.
226. Wright JR (2005) Immunoregulatory functions of surfactant proteins. *Nat Rev Immunol* 5: 58-68.
227. Crouch E, Wright JR (2001) Surfactant proteins a and d and pulmonary host defense. *Annu Rev Physiol* 63: 521-554.
228. Haagsman HP, Diemel RV (2001) Surfactant-associated proteins: functions and structural variation. *Comp Biochem Physiol A Mol Integr Physiol* 129: 91-108.
229. Johansson J, Curstedt T, Robertson B (1994) The proteins of the surfactant system. *Eur Respir J* 7: 372-391.
230. Takahashi K, Tanabe K, Ohnuki M, Narita M, Ichisaka T, et al. (2007) Induction of pluripotent stem cells from adult human fibroblasts by defined factors. *Cell* 131: 861-872.
231. Takahashi K, Yamanaka S (2006) Induction of pluripotent stem cells from mouse embryonic and adult fibroblast cultures by defined factors. *Cell* 126: 663-676.
232. Yu J, Vodyanik MA, Smuga-Otto K, Antosiewicz-Bourget J, Frane JL, et al. (2007) Induced pluripotent stem cell lines derived from human somatic cells. *Science* 318: 1917-1920.
233. Okita K, Ichisaka T, Yamanaka S (2007) Generation of germline-competent induced pluripotent stem cells. *Nature* 448: 313-317.
234. Liu H, Zhu F, Yong J, Zhang P, Hou P, et al. (2008) Generation of induced pluripotent stem cells from adult rhesus monkey fibroblasts. *Cell Stem Cell* 3: 587-590.
235. Liao J, Cui C, Chen S, Ren J, Chen J, et al. (2009) Generation of induced pluripotent stem cell lines from adult rat cells. *Cell Stem Cell* 4: 11-15.
236. Esteban MA, Xu J, Yang J, Peng M, Qin D, et al. (2009) Generation of induced pluripotent stem cell lines from Tibetan miniature pig. *J Biol Chem* 284: 17634-17640.
237. Ezashi T, Telugu BP, Alexenko AP, Sachdev S, Sinha S, et al. (2009) Derivation of induced pluripotent stem cells from pig somatic cells. *Proc Natl Acad Sci U S A* 106: 10993-10998.
238. Luo Y, Kuang SY, Hoffer B (2009) How useful are stem cells in PD therapy? *Parkinsonism Relat Disord* 15 Suppl 3: S171-175.

239. Raya A, Rodriguez-Piza I, Guenechea G, Vassena R, Navarro S, et al. (2009) Disease-corrected haematopoietic progenitors from Fanconi anaemia induced pluripotent stem cells. *Nature* 460: 53-59.
240. Hanna J, Wernig M, Markoulaki S, Sun CW, Meissner A, et al. (2007) Treatment of sickle cell anemia mouse model with iPS cells generated from autologous skin. *Science* 318: 1920-1923.
241. Ebert AD, Yu J, Rose FF, Jr., Mattis VB, Lorson CL, et al. (2009) Induced pluripotent stem cells from a spinal muscular atrophy patient. *Nature* 457: 277-280.
242. Rubin LL (2008) Stem cells and drug discovery: the beginning of a new era? *Cell* 132: 549-552.
243. Van Haute L, De Block G, Liebaers I, Sermon K, De Rycke M (2009) Generation of lung epithelial-like tissue from human embryonic stem cells. *Respir Res* 10: 105.
244. Consortium GO (2004) The Gene Ontology (GO) database and informatics resource. *Nucleic Acids Res* 32: D258-261.
245. Chen YA, McKillen DJ, Wu S, Jenny MJ, Chapman R, et al. (2004) Optimal cDNA microarray design using expressed sequence tags for organisms with limited genomic information. *BMC Bioinformatics* 5: 191.
246. Fair PA, Adams, J.D., Zolman, E. et al. (2006a) Protocols for conducting dolphin capture-release health assessment studies. NOAA Technical Memorandum NOS/NCCOS 40: 1-83.
247. McKillen DJ, Chen YA, Chen C, Jenny MJ, Trent HF, 3rd, et al. (2005) Marine genomics: a clearing-house for genomic and transcriptomic data of marine organisms. *BMC Genomics* 6: 34.
248. Parzen E (1962) On estimation of a probability density function and mode. *Ann Math Stat* 33: 1065-1076.
249. Chapman RW, Sedberry GR, Koenig CC, Eleby BM (1999) Stock Identification of Gag, *Mycteroperca microlepis*, Along the Southeast Coast of the United States. *Mar Biotechnol (NY)* 1: 137-146.
250. Gentleman RC, Carey VJ, Bates DM, Bolstad B, Dettling M, et al. (2004) Bioconductor: open software development for computational biology and bioinformatics. *Genome Biol* 5: R80.
251. Smyth GK, Michaud J, Scott HS (2005) Use of within-array replicate spots for assessing differential expression in microarray experiments. *Bioinformatics* 21: 2067-2075.
252. Smyth GK (2005) Limma: linear models for microarray data. In: Gentleman R C, V., Dudoit, S., Irizarry, R., Huber W., eds., editor. *Bioinformatics and Computational Biology Solutions using R and Bioconductor*. New York: Springer. pp. 397-420.
253. Ritchie ME, Silver J, Oshlack A, Holmes M, Diyagama D, et al. (2007) A comparison of background correction methods for two-colour microarrays. *Bioinformatics* 23: 2700-2707.
254. Smyth GK, Speed T (2003) Normalization of cDNA microarray data. *Methods* 31: 265-273.
255. Huber W, von Heydebreck A, Sultmann H, Poustka A, Vingron M (2002) Variance stabilization applied to microarray data calibration and to the quantification of differential expression. *Bioinformatics* 18 Suppl 1: S96-104.
256. Smyth GK (2004) Linear models and empirical bayes methods for assessing differential expression in microarray experiments. *Stat Appl Genet Mol Biol* 3: Article3.

257. Benjamini YaH, Y (1995) Controlling the False Discovery Rate - a Practical and Powerful Approach to Multiple Testing. *Journal of the Royal Statistical Society Series B-Methodological* 57: 289-300.
258. Haykin S (1999) *Neural Networks: A Comprehensive Foundation*. New Jersey: Prentice Hall.
259. Bradley AP (1997) The Use of the Area Under the ROC Curve in the Evaluation of Machine Learning Algorithms. *Pattern Recognition*: 1145-1159.
260. Stephan C, Wesseling S, Schink T, Jung K (2003) Comparison of eight computer programs for receiver-operating characteristic analysis. *Clin Chem* 49: 433-439.
261. Hanley JA, McNeil BJ (1982) The meaning and use of the area under a receiver operating characteristic (ROC) curve. *Radiology* 143: 29-36.
262. Warren KS, Shutt DC, McDermott JP, Lin JL, Soll DR, et al. (1996) Overexpression of microfilament-stabilizing human caldesmon fragment, CaD39, affects cell attachment, spreading, and cytokinesis. *Cell Motil Cytoskeleton* 34: 215-229.
263. Robalino J, Almeida JS, McKillen D, Colglazier J, Trent HF, 3rd, et al. (2007) Insights into the immune transcriptome of the shrimp *Litopenaeus vannamei*: tissue-specific expression profiles and transcriptomic responses to immune challenge. *Physiol Genomics* 29: 44-56.

7. ACKNOWLEDGEMENTS

Acknowledgements

ACKNOWLEDGEMENTS

*And Here It Comes,
My Favorite Part,
Which It All Really Sums,
Oh, Where Should I Start?*

*So Many People Will Make This List
From Far and from Close They Indeed Assist
With The Scientific World Then, I Shall Begin
Then Friends, Family And Everyone Within!*

First of all I would like to thank Gregory W. Warr for his support, for his valuable advice and for his mentoring over all these years. For teaching me the science and the love for it. This work would not have been possible without him. Thanks, **Greg**.

I owe my deepest gratitude to my Italian thesis advisor, Marialuisa Melli, for her help in getting started, going through and finishing these PhD years, for being there every time I needed her, even if I was so far away. And for her friendship. Thanks, **Lulla**.

I am heartily thankful to my American advisor John E. Baatz for all his help, advice, for his being there, for all the extra-work I know I have been lately. Thanks so much, **John**.

I am deeply grateful to **Anne L. Plant** at the National Institute of Standard and Technologies (NIST) up in Maryland, and to her group (**John, Kiran, Mike, Ale, Tighe, Alex**) for their patience in teaching me everything I know about cell culture, for their enthusiasm about the dolphin cells and their always positive attitude. Thanks so much guys, it was a great year. Bit cold up there, but still, great.

Thanks to Robert W. Chapman and his help with the data analysis (and we know how much he likes dolphins!!!); thanks for his excitement every time it's about crunching data, doing statistics and playing with numbers... Thanks to **Bob** and his "beautiful mind", where, I am afraid, I still get totally lost.

Thanks to **Danny** and **Demetri**, for all their help in this last year, and for the extremely fascinating projects we are working on right now. Amazing fantascience! *Divide and Conquer...*

I am very grateful to Eric. R. Lacy at the MUSC Marine Biomedicine Program, for letting me be part of this group (for so long!) and for the attention he pays to every issue. Thanks, **Eric**.

I would like to thank all my former and present colleagues at HML which have also been good friends, for all their help and support during these years. Thanks to **Nuala** and **Javier, Mats, Yannick, Darlene, Jessalyn, Marion, James, Tash, Blake, and Guillaume**. Thanks for the science discussions but also for all the fun, for the coffee, for the art walks, for the beach days, and for everything we shared in Charleston and Folly... thanks.

I would like to show my gratitude to **James Powell** and **Wayne McFee** for their help with the samples (and for kindly providing some pictures) at the Coastal Strandings Assessment Project at NOAA's Center for Coastal

Acknowledgements

Environmental Health and Biomolecular Research. Thanks also to **Lori** Schwacke and **Fran** Van Dolah (NOAA) for the intro info and pictures.

Thanks for the patience. For the teaching. For the listening and the non-listening. For lowering my salt intake. For doubling my sugar intake. Thanks for a million things, **Jimmy** (namely JR, read as GEIAR).

Thanks to the best friend, great scientist and great athlete, **Lara**. Thanks Lara because all these years have been so much more fun with you. For all the 5Ks, the 10Ks, the half-marathons, the marathons, for all the sprints, Olympics, half-Iroman, Ironman. For all the complaining. For all the running in the rain, the riding in the heat, and the swims at 5am under the rising sun. Crazy. And, of course, thanks **Clint**, my baby's Doctor, my Sherpa, my Coach. Thanks **Ben**, for the happiness you brought. And, of course, thanks **Cole**.

Thanks to all my other friends here in Charleston (especially **Tanner**, **Michelle**, **Mike** and of course **Guillaume** and that's the second time kiddo!) and to the tri world, to the underwater hockey team, thanks to all my friends in Italy (especially **Sandro**, **Simo**, **Lida**, **Andrea**, **Ile e Jack**, **Anto**, **Alessandra**, **Nadia**, **Marilu'**, **Valeria**) that are still there when I need them, every time I come back...thanks to Skype, msn, Facebook, Gmail, Yahoo, AT&T, Tim...everything that helped to keep in touch. Thanks ya'll. Special thanks to **Luca**. A good friend, a great person.

Thanks to all the Natale's, **Angela**, **Ale**, **Luca**, **Luigi**, **Marinella** e **Flaviano**.

But, most of all, thanks **Carlo**. Ca', none of this would have been possible without you. *"...niente a che vedere col circo, nè acrobati nè mangiatori di fuoco, piuttosto un santo a piedi nudi, quando vedi che non si taglia, già lo sai..."*

And finally, thanks to my Family. First of all, thanks to the new addition, **Lorenzo**. The masterpiece, the perfection, my beautiful nephew. Thanks to **Roberta**, sis, to whom this thesis is dedicated (as "history repeats itself"), because she has been and is the best sister and everything else really, including a good, wise, friend. Thanks to **Alfredo** for taking care of everything. For being so good at it. For his patience. For being the best daddy. Thanks to **Giovannina** and **Pippo**, for how nice they welcome me home, all the time. For the food I dream all year around, for the good wine, and "Oh, the Anisetta" I dream all year around, thank you so much. Thanks to my aunt **Paola**, because she always cares even with the million things she has to think about. And to my cousin **Daniela**, so far, but so close.

And at least, but not at last, thanks to those without with this work would definitively have not been possible, this work is from them and for them, the smartest animals, cutest smiles, sweetest eyes, the **dolphins**.

Grazie.

This research was supported by awards from the National Ocean Services/NOAA (NCNS4000-4-0054), the Office of Naval Research (N000140610296) and by the National Institute of Standards and Technology (NIST). The construction and characterization of the dolphin microarrays was supported by the Hollings Marine Laboratory (National Ocean Service, National Center for Coastal Ocean Science) and the Center of Excellence in Oceans and Human Health in the Hollings Marine Laboratory. Samples from Sarasota Bay dolphins were collected through the support of Dolphin Quest, NOAA Fisheries Service, the Chicago Zoological Society, and Mote Marine Laboratory. The samples were collected under National Marine Fisheries Service (NMFS) Permits # 998-1678-01, 522-1785, 932-1489-09 to Gregory Bossart, Randall Wells and Teri Rowles respectively.

